Universidade do Minho
Escola de Medicina

Miguel Leal Quintas Neves

Magnetic resonance imaging brain atrophy assessment in primary age-related tauopathy

abril de 2025

Uminho | 2025 Miguel Leal Quintas Neves **Magnetic resonance imaging brain atrophy assessment in primary age-related tauopathy**

Universidade do Minho
Escola de Medicina

Miguel Leal Quintas Neves

Magnetic resonance imaging brain atrophy assessment in primary age-related tauopathy

Tese de Doutoramento em Medicina

Trabalho efetuado sob a orientação do
Professor Doutor Tiago Gil Oliveira

abril de 2025

DIREITOS DE AUTOR E CONDIÇÕES DE UTILIZAÇÃO DO TRABALHO POR TERCEIROS

Este é um trabalho académico que pode ser utilizado por terceiros desde que respeitadas as regras e boas práticas internacionalmente aceites, no que concerne aos direitos de autor e direitos conexos.

Assim, o presente trabalho pode ser utilizado nos termos previstos na licença abaixo indicada.

Caso o utilizador necessite de permissão para poder fazer um uso do trabalho em condições não previstas no licenciamento indicado, deverá contactar o autor, através do RepositóriUM da Universidade do Minho.



Atribuição-NãoComercial-SemDerivações
CC BY-NC-ND
https://creativecommons.org/licenses/by/4.0/

Acknowledgments

I would like to start by deeply thanking Professor Tiago Gil Oliveira for giving me the opportunity to perform this thesis, for tirelessly providing me the mental strength and willingness needed to successfully achieve its aims, and, mostly, for being a supportive friend and excellent working colleague. His immense knowledge on neurodegenerative conditions was (and still is, of course) a constant source of inspiration.

To my close collaborators and friends, Dr. Francisco Almeida and Dr. Rafaela Morais Ribeiro, for their constant support, friendship and belief in this project; without them, this thesis would be almost impossible to achieve.

To our excellent collaborators from the US, Dr. Merilee Teylan, Dr. Kathryn Gauthreaux, Professor Charles Mock, Professor Walter Kukull and Professor John Crary, for giving me the opportunity to work with the National Alzheimer's disease Coordinating Centers database and, of course, for the paramount and constant feedback given regarding this project.

To the members of the PhD thesis Commission, that besides my mentor were composed by Professor Torcato Meira, Professor Patrício Costa and Professor Sofia Reimão, for the valuable feedback and support regarding this project.

To my dear colleague and friend, Dr. João Saraiva, for the interest always shown on this project and for the refreshing talks on the statistics involved.

To the European Society of Neuroradiology and, specially, to Professor Sven Haller, for believing in the value of this project, namely by awarding me the "ESNR Scientific Award" in 2023. Regarding this prize, I would also like to thank Dr. Sérgio Humberto (ex-president of the Trofa City Council and currently European Deputy) and Dr. Marques Mendes for congratulating me regionally and nationally, respectively.

To all my other colleagues from the Department of Neuroradiology of Unidade Local de Saúde de Braga, for the interest shown in this project and for the valuable support.

And finally, but definitely not least, to my closest family, namely my mother, father, godmother, grandmother, brother, sister-in-law and, of course, wife and daughter, without which it would be impossible to perform this project.

STATEMENT OF INTEGRITY

I hereby declare having conducted this academic work with integrity. I confirm that I have not used plagiarism or any form of undue use of information or falsification of results along the process leading to its elaboration.

I further declare that I have fully acknowledged the Code of Ethical Conduct of the University of Minho.

Resumo

A tauopatia primária relacionada à idade (PART) é uma condição cujo diagnóstico é realizado exclusivamente *post mortem*, pela deteção de tranças neurofibrilares cerebrais com estadio Braak ≤ 4 e ausência de placas neuríticas (*Consortium to Establish a Registry for Alzheimer Disease* – CERAD – de 0) ou com pouca ou nenhuma deposição de β-amilóide (fase Thal ≤ 2). Por outro lado, o diagnóstico de doença de Alzheimer (AD), a tauopatia mais estudada e frequente na população mundial, caracteriza-se por depósitos cerebrais de emaranhados neurofibrilares e de β-amilóide, *in vivo* (pelos biomarcadores AT(N) propostos pelo National Institute on Aging and Alzheimer's Association – NIA-AA) ou *post mortem* (utilizando o score "ABC", que avalia deposição de β-amilóide com fases Thal (A), de emaranhados neurofibrilares pelo estadiamento Braak (B) e de placas neuríticas pelo CERAD (C)). Tem existido intenso debate acerca da relação entre estas condições, pelo que o principal objetivo desta tese consistiu em avaliar esta relação, utilizando ressonância magnética cerebral *in vivo* e testes neuropsicológicos em doentes com diagnóstico por autópsia. Primeiro, comparámos aspetos neuropatológicos com padrões de atrofia cerebral entre estes dois grupos, e avaliámos a relação entre esses padrões e eventuais défices cognitivos. Enquanto na AD há aumento progressivo da atrofia temporal medial corrigida para a idade com o aumento do CERAD, na PART há atrofia regional intermédia. Adicionalmente, enquanto na AD observámos correlações difusas entre atrofia cerebral e défices cognitivos, na PART apenas há correlação entre atrofia temporal anterior e défices de linguagem. Em segundo lugar, comparámos estigmas microangiopáticos cerebrais com aspetos neuropatológicos entre esses grupos, e avaliámos a relação entre os primeiros e os padrões de atrofia. Encontrámos correlações significativas entre estigmas microangiopáticos e padrões de atrofia em ambos os grupos, com correlações mais fortes na PART, sobretudo na região fronto-insular. Finalmente, avaliámos potenciais diferenças na atrofia do córtex entorrinal entre estes dois grupos, e estudámos qual o seu impacto na cognição. Encontrámos diferenças significativas na atrofia do córtex entorrinal entre PART e AD severa, e entre estadios ligeiro e severo da AD. Também encontramos correlações significativas entre défices cognitivos e atrofia entorrinal nos dois grupos.

Globalmente, estes resultados apoiam a noção de que a PART e a AD poderão ser processos patológicos distintos, com diferentes relações entre atrofia cerebral, microangiopatia e performance cognitiva.

Palavras-chave: Doença de Alzheimer, Ressonância magnética, Tauopatia primária relacionada à idade.

Abstract

Primary Age-Related Tauopathy (PART) is a neuropathological condition whose diagnosis is performed exclusively *post mortem*, by detecting cerebral neurofibrillary tangles with a Braak stage ≤ 4 and absence of neuritic plaques (Consortium to Establish a Registry for Alzheimer's Disease – CERAD – score of 0) or with sparse to no β-amyloid deposition (Thal phase ≤ 2). On the other hand, the diagnosis of Alzheimer's disease (AD), the most studied and prevalent primary tauopathy worldwide, is characterized by brain deposits of neurofibrillary tangles and β-amyloid, *in vivo* (by the AT(N) biomarkers proposed by the National Institute on Aging and Alzheimer's Association – NIA-AA) or *post mortem* (using the "ABC" score, which assesses β-amyloid deposition with Thal phases (A), neurofibrillary tangles distribution with Braak staging (B), and neuritic plaques with CERAD (C)). As there has been intense debate regarding the relationship between these conditions, the main objective of this thesis was to investigate this relationship using *in vivo* brain magnetic resonance imaging and neuropsychological testing in patients with autopsy-confirmed diagnoses. First, we compared neuropathological aspects with brain atrophy patterns between these groups, while evaluating the relationship between these patterns and potential cognitive deficits. While AD exhibits a stepwise increase in age-corrected medial temporal atrophy with increasing CERAD scores, PART presents intermediate regional atrophy. Additionally, while AD is associated with widespread correlations between brain atrophy and cognitive deficits, PART only shows correlation between anterior temporal atrophy and language deficits. Second, we compared cerebral microangiopathic burden with neuropathological aspects between these groups, while assessing the relationship between the former and atrophy patterns. We found significant correlations between microangiopathic burden and atrophy patterns in both groups, with stronger correlations in PART, particularly in the fronto-insular region. Finally, we assessed potential differences in the entorhinal cortex atrophy between the two groups, while studying its impact on cognition. We found significant differences in entorhinal cortex atrophy between PART and severe AD, and between mild and severe AD. We also found significant correlations between cognitive deficits and entorhinal atrophy in both groups.

Overall, these findings support the notion that PART and AD may represent distinct neuropathological processes, with different interconnections between brain atrophy, microangiopathy, and cognitive performance.

Keywords: Alzheimer's disease, Magnetic resonance imaging, Primary age-related tauopathy.

Table of Contents

1. Introduction 1
   a. Alzheimer's disease 2
      i. Biological definition 2
      ii. Genetics – Familial vs sporadic forms 3
      iii. Clinical presentation 4
      iv. Biomarkers 5
      v. Current and future treatments 7
   b. Primary age-related tauopathy & Alzheimer's disease 8
      i. Neuropathological definitions 8
      ii. Current state of the art of the clinical manifestations 11
   c. Magnetic resonance imaging in neurodegenerative conditions 12
      i. Atrophy assessment: visual rating scales versus quantitative evaluation 12
      ii. Microangiopathic burden assessment: the role of the Fazekas score 14
      iii. Magnetic resonance imaging in Alzheimer's disease 14
      iv. Magnetic resonance imaging in primary age-related tauopathy 18
   d. Aims 20
   e. References 21
2. Experimental work 28
   a. Divergent magnetic resonance imaging atrophy patterns in Alzheimer's disease and primary age-related tauopathy 29
   b. Fazekas scale magnetic resonance imaging assessment in Alzheimer's disease and primary age-related tauopathy 48
   c. ERICA scale magnetic resonance imaging assessment in Alzheimer's disease and primary age-related tauopathy 63
3. Discussion, conclusions & future perspectives 88
   a. References 94

Abbreviations List

AD - Alzheimer's disease

Aβ - amyloid-beta

APP - amyloid precursor protein

ARIA - amyloid-related imaging abnormalities

ARIA-E - ARIA with edema/effusion

ARIA-H - ARIA with hemorrhage

CSF - cerebrospinal fluid

CERAD - Consortium to Establish a Registry for AD

ERICA - entorhinal cortex atrophy

FLAIR - fluid-attenuated inversion recovery

MRI - magnetic resonance imaging

NIA-AA - National Institute on Aging and Alzheimer's Association

NFTs - neurofibrillary tangles

NMDA - N-methyl-D-aspartic acid

PET - positron emission tomography

PSEN1 - Presenilin-1

PSEN2 - Presenilin-2

PART - Primary age-related tauopathy

TDP-43 - TAR DNA-binding protein 43

Figures and tables

Chapter 1

Figure 1. Amyloid cascade hypothesis.

Figure 2. The AT(N) scheme.

Figure 3. Neuritic plaque density according to the CERAD score.

Figure 4. Spreading pattern of tau throughout the brain.

Figure 5. Six visual rating scales for semiquantitative assessment of brain atrophy.

Figure 6. Fazekas rating scale for the periventricular and deep white matter.

Figure 7. Magnetic resonance imaging across AD phenotypes.

Figure 8. Dynamic biomarkers of the Alzheimer's pathological cascade.

Figure 9. The ERICA score for the entorhinal cortex atrophy evaluation.

Figure 10. Medial temporal lobe atrophy significantly correlating with increasing Braak stage and age in "definite" PART participants, after correction for age and Braak, respectively.

Figure 11. Anterior and medial temporal lobe atrophy significantly correlating with decreased semantic memory/language tests performance in "definite" PART participants, after correction for age.

Table 1. Integrated biological and clinical staging.

Table 2. Primary age-related tauopathy neuropathological criteria.

Chapter 2.1

Table 1. Characterization of patients according to the density of neocortical neuritic plaques (CERAD score).

Figure 1. Age-c relative regional brain atrophy shows differential patterns in PART and Alzheimer's disease spectrum CERAD groups.

Figure 2. Braak-corrected relative regional brain atrophy shows no significant changes in PART and Alzheimer's disease spectrum CERAD groups.

Figure 3. Correlation analysis between relative regional brain atrophy and CDR shows differential patterns in Alzheimer's disease and PART.

Figure 4. Correlation analysis between relative regional brain atrophy and neuropsychological assessment shows differential patterns in Alzheimer's disease and PART.

Supplementary figure. Braak and age-corrected relative regional brain atrophy shows significant changes between CERAD groups with and without TDP-43, predominantly in the medial temporal region.

Supplementary Table 1. Post hoc analysis of variables significantly different between groups of patients according to the density of neocortical neuritic plaques - CERAD score.
Supplementary Table 2. Multiple Linear Regression Coefficient estimates and p values for regional brain atrophy dependent upon Group and CDR Sum Of Boxes.
Supplementary Table 3. Comparison of Neuropsychological Test z-scores between PART and Alzheimer's disease.
Supplementary Table 4. TDP-43 in PART and Alzheimer's disease.
Figure S1. Braak and age-corrected relative regional brain atrophy shows significant changes between CERAD groups with and without TDP-43, predominantly in the medial temporal region.
Figure S2. Pearson correlation analysis of relative brain atrophy per region after age correction versus neuropsychological test z-scores.

Chapter 2.2

Figure 1. Representative case of a 91 year-old male patient with AD.
Figure 2. No significant differences were found in the Fazekas grading between patients with PART and AD.
Figure 3. Correlation analysis between relative regional brain atrophy and Fazekas scores, corrected for age, shows differential patterns in AD and PART.
Table 1. Characterization of patients according to the density of neocortical neuritic plaques (CERAD score).
Table S1. Correlation analysis between CDR Sum Of Boxes and the Fazekas scores in patients with Alzheimer's disease and primary age-related tauopathy, before and after adjusting for age and Braak.
Table S2. Correlation analysis between relative regional brain atrophy and the Fazekas scores corrected for age in patients with Alzheimer's disease and primary age-related tauopathy.
Table S3. Intraclass correlation coefficients (ICC) between raters.
Table S4. Residuals corrected for age of relative regional brain atrophy differences among groups classified according to the density of neocortical neuritic plaques (CERAD score).
Figure S1. No statistically significant differences were found in the periventricular or deep Fazekas scores.

Chapter 2.3

Table 1. Characterization of patients according to the density of neocortical neuritic plaques (CERAD score).

Figure 1. Flow diagram resuming the inclusion and exclusion criteria used to obtain the final sample.
Figure 2. Representative case of a 95-year old male patient with primary age-related tauopathy (PART).
Figure 3. After correcting for age and sex, the entorhinal cortex atrophy (ERICA) score is significantly different between CERAD 0 and CERAD 3, and between CERAD 1 and CERAD 3. Significant differences are also found between PART and AD neuropathologic change, after correcting for age and sex.
Figure 4. After adjusting for Braak, age and sex, no significant differences are found between the entorhinal cortex atrophy (ERICA) score among the 4 groups of CERAD, and between PART and AD neuropathologic change.
Figure 5. Significant correlations are found between the entorhinal cortex atrophy (ERICA) score and the CDR® Sum of Boxes, for patients with PART and with AD neuropathologic change, after controlling for age and sex. There are no significant differences between the regression lines of both groups.

Chapter 1

Introduction

a. Alzheimer's disease

i. Biological definition

Alzheimer' disease (AD) is a neurodegenerative disorder characterized by global cognitive decline, involving memory, orientation, judgement and reasoning, with consequent progressive functional decline, firstly reported by Alois Alzheimer in 1906, a psychiatrist with expertise in neuropathology (Tanzi & Bertram, 2005). Its primary pathological hallmarks include amyloid-beta (Aβ) plaques, neurofibrillary tangles (NFTs), gliosis and neuronal loss, accompanied by cerebrovascular amyloidosis, inflammation and major synaptic changes (Guo et al., 2020). Aβ protein is the main component of AD-associated amyloid plaques, which are produced by protease cleavage of the type I transmembrane amyloid precursor protein (APP), which is comprised of 8 to 11 isoforms generated by alternative transcriptional splicing, with the most frequent being composed of 695, 751 and 770 amino acids (respectively, APP695, APP751 and APP770) (Guo et al., 2020). Gradual changes in the steady-state levels of Aβ are thought to initiate the so-called amyloid cascade (**Figure 1**), with elevated levels of Aβ potentially linked to increased production and/or decreased clearance (Haass & Selkoe, 2007; Karran et al., 2011). The relative increase in Aβ42 peptide, a 42 amino acid proteolytic product resulting from APP cleavage by γ-secretase (Guo et al., 2020) (i.e. increase in Aβ42/Aβ40 ratio), enhances oligomer formation, with progressive (and increasingly severe and permanent) changes in synaptic function (Haass & Selkoe, 2007; Karran et al., 2011). Simultaneously, Aβ42 forms microscopically visible deposits in the brain, first as relatively benign diffuse plaques (i.e. non-fibrillar), and later, as they acquire fibrils of Aβ, triggering inflammatory responses characterized by microglial and astrocytic activation, followed by synaptic spine loss and neuritic dystrophy (Haass & Selkoe, 2007). As these processes ensue, several biochemical changes take place, specially oxidative injury and altered neuronal ionic homeostasis, with subsequent aberrant oligomerization and hyperphosphorylation of tau proteins, due to altered kinase and phosphatase activities, leading to NFTs formation (Haass & Selkoe, 2007) in the form of paired helical filaments of tau aggregates and, ultimately, to neuronal loss and progressive dementia (Haass & Selkoe, 2007; Karran et al., 2011).

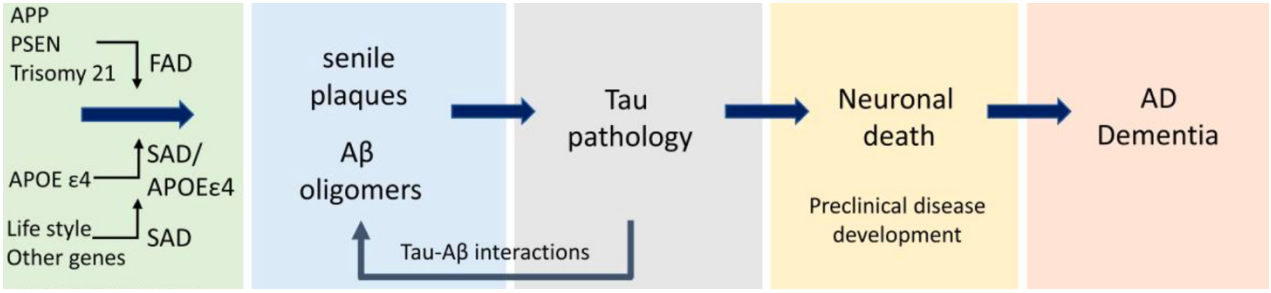


Figure 1. Amyloid cascade hypothesis; adapted from (Kepp et al., 2023).

Intracellular NFTs are composed of hyperphosphorylated tau proteins, which are encoded by the *MAPT* gene on chromosome 17 (Guo et al., 2020), that physiologically promote the polymerization and stability of microtubules; it comprises 16 exons, with alternative splice variation including exons 2, 3 and 10 generating up to six different tau isoform variants in the human brain (Guo et al., 2020). These can be distinguished from one another through compositional inclusion or exclusion of zero (0 N), one (1 N) or two (2 N) 29 amino acid inserts at the N-terminus, and three (3R) or four (4R) microtubule-binding repeats (Guo et al., 2020). Impaired 3R:4R tau ratios result from altered *MAPT* pre-mRNA splicing (Guo et al., 2020), with several studies supporting the notion that, in AD, there might be overexpression of 4R tau in vulnerable brain regions (Ginsberg et al., 2006).

ii. Genetics – Familial vs sporadic forms

AD can be broadly categorized as familial or sporadic, each with distinct genetic and molecular underpinnings (Schilling et al., 2023). Familial AD can be found in around 5% of cases, typically manifesting as early-onset AD due to autosomal-dominant mutations, while sporadic AD emerges later in life, influenced by a complex interplay of genetic, environmental, and lifestyle factors (Karran et al., 2011; Schilling et al., 2023).

Familial AD is predominantly associated with mutations in the *APP*, *PSEN1*, and *PSEN2* genes (Guo et al., 2020; Schilling et al., 2023), which drive abnormal production and consequent accumulation of Aβ. Regarding APP, mutations such as the Swedish one (KM670/671NL, according to numbering of APP695 or position – 1/ – 2, Aβ numbering) enhance cleavage of this protein by β-secretase, leading to excessive production of Aβ42 (Schilling et al., 2023). Moreover, the Arctic mutation (E693G) promotes Aβ fibril formation, intensifying plaque deposition (Schilling et al., 2023). Presenilin-1 (PSEN1) mutations, such as the E280A mutation in the Colombian Paisa population, alter the activity of γ-secretase, increasing the Aβ42/Aβ40 ratio and exacerbating amyloid aggregation (Guo et al., 2020; Karran et al., 2011; Schilling et al., 2023). Presenilin-2 (PSEN2) mutations, though less frequent, show comparable effects (Guo et al., 2020; Schilling et al., 2023).

In contrast, sporadic forms of AD are linked to a broader set of risk factors (Karran et al., 2011), with the *APOE* ε4 allele being the most significant genetic contributor, enhancing amyloid deposition and exacerbating neuroinflammation (Guo et al., 2020; Schilling et al., 2023). Moreover, this

form of AD is also highly linked to oxidate stress and mitochondrial dysfunction, processes which are less pronounced in the familial form (Schilling et al., 2023).

Therefore, although both forms of AD share the hallmarks of amyloid plaques and tau tangles, their molecular underpinnings diverge. In the familial form, genetic mutations directly drive amyloid pathology from an early age, while in the sporadic form there is a greater contribution from neuroinflammation, as well as from metabolic and lipid dysregulation (Schilling et al., 2023). It is also known that sporadic AD brains often experience greater loss of excitatory neurons, such as RORB-positive cells, driven by tau toxicity, while some familial AD brains demonstrate resilience mechanisms, such as protective astrocytic changes or altered tau clearance linked to *APOE* variants like Christchurch (M. C. Almeida et al., 2024).

iii. Clinical presentation

AD can clinically manifest as typical (i.e. memory predominant AD) or as a variant syndrome, such as early-onset AD, behavioral and/or dysexecutive, or logopenic (Haller & Barkhof, 2018). By far, the most common type of AD is its typical senile form, which is characterized by slowly progressive neurocognitive impairment, with short term memory loss (i.e. the ability to remember recent events) as the first clinical manifestation in most cases (Haller & Barkhof, 2018; Knopman et al., 2021). As the disease progresses, several additional symptoms may develop, such as language impairment, disorientation, mood disbalance, loss of motivation and self-care, and inappropriate behavior (sometimes characterized by aggressiveness towards relatives) (Haller & Barkhof, 2018). Mild cognitive impairment is frequently considered as a potential precursor state of progressive neurodegeneration and subsequent AD (Haller & Barkhof, 2018); however, it is important to keep in mind that this is a heterogeneous condition, with several subclassifications according to the clinical presentation, such as the amnestic, frontal or multidomain forms (Haller & Barkhof, 2018). The amnestic mild cognitive impairment cases have the highest likelihood of later progression to AD, in about 50% of patients (Haller & Barkhof, 2018). Moreover, it is also important to keep in mind that other types of neurodegenerative conditions, such as vascular dementia or dementia with Lewy bodies, can also present with initial progressive memory loss (Haller & Barkhof, 2018; Haller et al., 2019).

Early-onset or young-onset AD is the term reserved for cases diagnosed before the age of 65, corresponding to 5-10% of all cases of AD (Haller & Barkhof, 2018; Knopman et al., 2021), of which approximately 10-15% being the familial form, with mutations found, for example, in the *PSEN1*, *PSEN*2 or *APP* genes (Haller & Barkhof, 2018; Knopman et al., 2021). The main clinical presentation of young-

onset AD is a progressive decline in visuospatial or visuoperceptual skills, in literacy, and in praxis, symptoms that define the so-called posterior cortical atrophy (acronym PCA) syndrome (Haller & Barkhof, 2018; Haller et al., 2019), with less frequently reported memory loss. This syndrome is typically characterized by disruption of complex visual processing related to neurodegeneration in posterior brain areas (i.e. the parietal and occipital lobes); despite in most cases occurring in the setting of AD pathology, it can also be found in other neurodegenerative conditions, such as dementia with Lewy bodies or corticobasal degeneration (Haller & Barkhof, 2018). Moreover, in these younger patients (i.e. with less than 65 years), frontotemporal lobe degeneration variants are relatively more common, despite in absolute numbers AD being more frequent (Haller & Barkhof, 2018; Knopman et al., 2021).

The rarer behavioral and/or dysexecutive presentations are very important variants of AD to be aware of, given the potential differential diagnosis with other neurodegenerative conditions, such as frontotemporal lobe degeneration, that can also present with behavioral dysfunction (Haller & Barkhof, 2018). Despite the underlying pathology being equivalent to typical AD, the spatial distribution of abnormalities might differ, with, for example, pronounced frontal lobe involvement in the behavioral presentation of AD (Haller & Barkhof, 2018; Knopman et al., 2021).

Finally, the logopenic variant of primary progressive aphasia is another rare non-amnestic form of AD, characterized by nonfluent aphasia with prominent word-finding pauses, naming and repetition difficulties (Haller & Barkhof, 2018; Knopman et al., 2021). It is important to keep in mind that primary progressive aphasia is a clinical diagnosis that can be further divided into a nonfluent/agrammatic variant (also referred to as “progressive nonfluent aphasia”), a semantic variant (“semantic dementia”), and, as stated, a logopenic variant (“also referred to as “logopenic progressive aphasia”) (Haller & Barkhof, 2018); the first two belong to the group of frontotemporal lobe degeneration, while the latter is generally associated with AD.

iv. Biomarkers

Biomarkers play a critical role in diagnosing and staging AD, according to the National Institute on Aging and Alzheimer’s Association (Jack et al., 2018). The most recent update (Jack et al., 2024) to diagnostic frameworks emphasize a biology-based approach, incorporating advanced biomarkers with the objective of improving accuracy and filling the gap between research and clinical care; in this setting, the AT(N) diagnostic framework was proposed (**Figure 2**), with “A” representing Aβ pathology, “T” representing tau pathology (including hyperphosphorylated tau), and “(N)” representing neurodegeneration (i.e. neuronal damage) (Jack et al., 2018); the reason why “(N)” is placed in

parenthesis is due to its unspecific nature, not exclusive of AD, that can also be found in other comorbid conditions, most of which with no extant biomarker (Jack et al., 2018). These biomarkers can be assessed through cerebrospinal fluid (CSF), blood plasma assays, or neuroimaging techniques, such as positron emission tomography (PET) or magnetic resonance imaging (MRI) scans (Jack et al., 2024; Jack et al., 2018), and can be divided in two categories according to their diagnostic accuracy: core 1 and core 2. The former group is critical to the diagnosis of AD and include CSF assays (measurements of Aβ42/40 ratios and of phosphorylated tau – for example, p-tau181), imaging (amyloid PET scans to detect amyloid plaques), and, eventually, plasma biomarkers (which are emerging as reliable alternatives, testing, for instance, p-tau217) (Jack et al., 2024). An abnormal core 1 biomarker is sufficient to establish a diagnosis of AD and to inform clinical decision making throughout the disease continuum, potentially enabling the diagnosis in asymptomatic individuals (Jack et al., 2024; Jack et al., 2018). Core 2 biomarkers (biofluid and tau PET) provide additional information for disease staging and progression (i.e. disease severity), also providing important prognostic information and increasing confidence that AD is contributing to symptoms (Jack et al., 2024; Knopman et al., 2021).

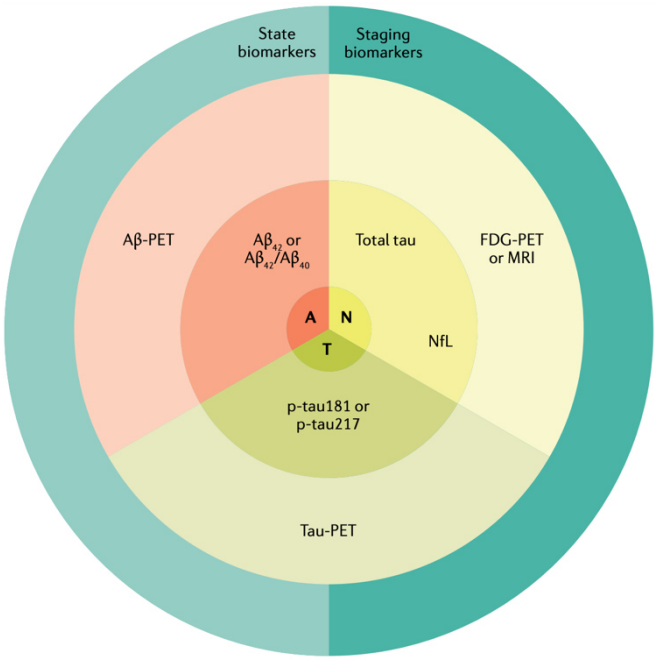


Figure 2. The AT(N) scheme, as presented by Knopman et al (Knopman et al., 2021); NfL stands for neurofilament light chain.

However, it is paramount to keep in mind that the biologically based diagnosis of AD is meant to assist rather than supplant the clinical evaluation of individuals with cognitive impairment (Jack et al.,

2024). Therefore, the clinical use of these biomarkers should be focused on the evaluation of symptomatic individuals (**Table 1**), not cognitively unimpaired ones (Jack et al., 2024).

Table 1. Integrated biological and clinical staging, as described by Jack et al (Jack et al., 2024).

	Stage 0	Clinical Stage 1	Clinical Stage 2	Clinical Stage 3	Clinical Stages 4–6
Initial biological stage (A)	X	1A	2A	3A	4-6A
Early biological stage (B)	X	1B	2B	3B	4-6B
Intermediate biological stage (C)	X	1C	2C	3C	4-6C
Advanced biological stage (D)	X	1D	2D	3D	4-6D

iv. Current and future treatments

AD has been shown to be associated with neurodegeneration of several cholinergic centers, such as the nucleus basalis of Meynert, whose neurons send efferents to the entire neocortex (Liu et al., 2015). This is the theoretical basis of using cholinesterase inhibitors for the symptomatic and unspecific treatment of AD for several years, such as donepezil, rivastigmine and galantamine, which can be used at early and moderate stages of the disease and are not approved for individuals with mild cognitive impairment (Knopman et al., 2021; Wu et al., 2023); however, they have shown only modest benefits in providing a delay in symptoms progression, and were associated with several potential adverse effects, such as nausea and vomiting (Knopman et al., 2021). Moreover, a non-competitive N-methyl-D-aspartic acid (NMDA) receptor antagonist, memantine, was also widely approved for the symptomatic treatment of moderate to severe dementia due to AD, with the advantage of having less adverse effects, but still, with no relevant effect in the underlying biology of the disease (Knopman et al., 2021; Wu et al., 2023). Moreover, unspecific treatments also included medications for managing behavioral and psychological symptoms of dementia, such as antipsychotics, antidepressants, and anxiolytics, with the caveat of more potential side effects (Knopman et al., 2021).

More recently, several disease modifying treatments emerged, specifically based on immunotherapy targeting the pathological hallmarks of AD, such as Aβ deposition (i.e. anti-Aβ immunotherapy) (Jack et al., 2024; Knopman et al., 2021; Wu et al., 2023). They were shown to dramatically reduce the load of amyloid plaques in a time- and dose-dependent manner, to normalize downstream biomarkers (such as CSF and plasma p-tau and total tau, and plasma glial fibrillary acid protein), and to slow accumulation of tau PET (Jack et al., 2024). Even more importantly, clinical trials have demonstrated that anti-Aβ immunotherapy, which substantially reduces fibrillar Aβ levels on PET, can also slow the rate of cognitive decline in early symptomatic AD (Jack et al., 2024; Wu et al., 2023). However, despite a dramatic reduction in Aβ deposits throughout the brain, small recurrent amyloid accumulation on PET and clinical progression similar to patients receiving placebo were found on follow-

up (Jack et al., 2024); this led to the conclusion that the pathophysiological process is still active on such cases. Another interesting remark is that these patients (i.e. on which there was plaque dose reduction) developed higher rates of whole-brain volume loss or ventricular enlargement, effects that were absent on the placebo group, with relative sparing of the hippocampus (Jack et al., 2024); possible theories included therapy-related fluid shifts or a reduction in volume of amyloid plaque and peri-plaque inflammation (Jack et al., 2024). The Food and Drug Administration approved in 2021, 2023 and 2024, respectively, the monoclonal antibodies Aducanumab®, Lecanemab®, and Donanemab® for the treatment of patients with mild forms of AD (i.e. with mild cognitive impairment or mild dementia and elevated Aβ in the brain) (Zhang et al., 2024). Another important remark regards the concept of amyloid-related imaging abnormalities (ARIA), which is an umbrella term that refers to MRI brain signal changes firstly observed, as adverse events, on clinical trials of anti-Aβ therapies, consisting of 2 types: ARIA with edema/effusion (ARIA-E) and ARIA with hemorrhage (ARIA-H) (Godi & Falini, 2019); both are seen as a consequence of altered vessel permeability induced by therapeutic mobilization and clearance of Aβ deposits (Godi & Falini, 2019). Most cases develop 6-8 weeks from the first infusion, with ARIA-E being characterized by reversible subcortical/sulcal fluid-attenuated inversion recovery (FLAIR) hyperintensities and gyral swelling, and ARIA-H characterized by parenchymal microhemorrhages and/or subarachnoid bleeding (Godi & Falini, 2019). They can be asymptomatic and only incidentally detected, however, there are rare cases in which seizures or focal neurological deficits might occur, which demands a tight follow-up (Godi & Falini, 2019).

Simultaneously, many other possible targets are under investigation, such as anti-tau therapy (with antibodies or vaccine-based) or even immunomodulation (which attempts to control neuroinflammation) (Zhang et al., 2024); an example of the latter is the targeting of microglia, which is a cell involved in the neuroimmune response and neuroinflammation, by Daratumumab®, an antibody already used for treating multiple myeloma that has also shown promising results in the treatment of mild to moderate AD (Zhang et al., 2024).

b. Primary age-related tauopathy & Alzheimer's disease

i. Neuropathological definitions

Degenerative dementias share the common feature of misfolded proteins deposited in the brain, specifically in a characteristic topographical distribution, both of which defining their type. An example of this is, as already stated, the accumulation of NFTs, composed of hyperphosphorylated tau protein, in a subset of neurodegenerative diseases known as tauopathies (Hyman et al., 2012). AD is the

most studied and well known tauopathy, which is also characterized by the deposition of amyloid-beta, whether *in vivo* [based on the AT(N) biomarkers proposed by the National Institute on Aging and Alzheimer's Association (NIA-AA) 2018 Research Framework (Jack et al., 2018)] or *postmortem* [using the "ABC score", which is based on grading amyloid plaques with Thal phases (A), NFTs with Braak staging (B) and neuritic plaques with the Consortium to Establish a Registry for AD (CERAD) assessment (C)] (Hyman et al., 2012).

The CERAD score (**Figure 3**), originally described in 1991 by Mirra et al (Mirra et al., 1991), assesses the density and distribution of neuritic plaques, which are composed of Aβ deposits surrounded by dystrophic neurites, and it is based on semiquantitative measures from histological brain sections stained for amyloid. According to it, the density of neuritic plaques is graded as none, sparse, moderate, or frequent (Mirra et al., 1991), with higher scores correlating with clinical dementia (Hyman et al., 2012).

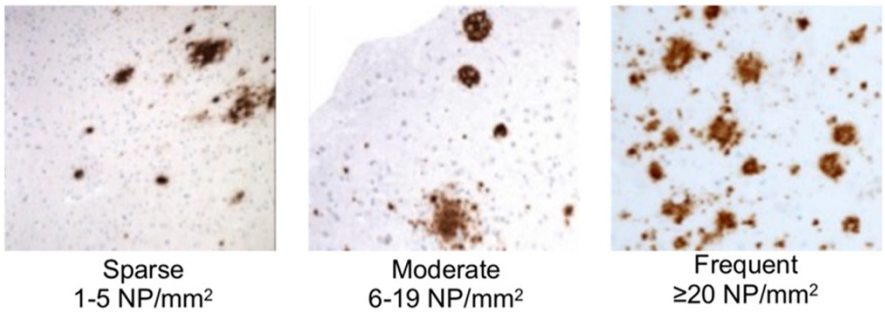


Figure 3. Neuritic plaque density according to the CERAD score, from the UCSF Neurodegenerative Disease Brain Bank, as presented by Chapleau et al (Chapleau et al., 2022).

On the other hand, the Braak staging system, which was originally described by Braak et al (Braak & Braak, 1991) in the early 90s, evaluates the NFTs composed of hyperphosphorylated tau protein, which can be found in specific brain regions as the disease progresses and is typically associated with neuronal loss; six stages were originally described (Braak & Braak, 1991), that were latter reduced to four (**Figure 4**) with improved inter-rater reliability (Nagy et al., 1998).

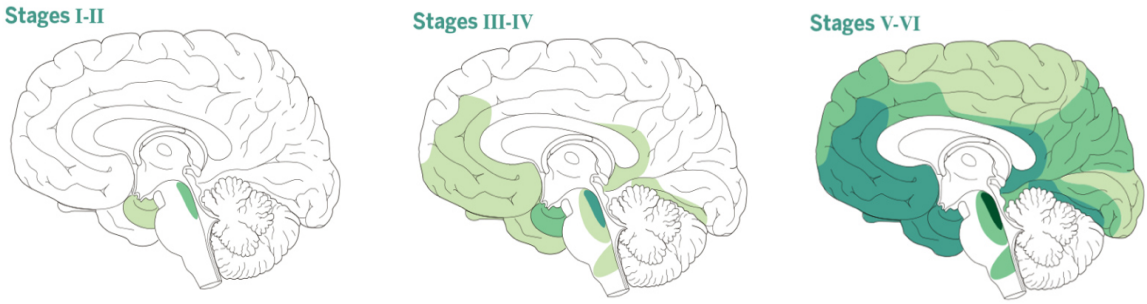


Figure 4. Spreading pattern of tau throughout the brain from Braak stage I-II (locus coeruleus, transentorhinal and entorhinal regions) to stage III-IV (hippocampus and some parts of the neocortex) and stage V-VI (large parts of the neocortex), as presented by (Goedert, 2015).

Primary age-related tauopathy (PART) is a term firstly proposed in 2014 by Crary et al (Crary et al., 2014), to describe a pathologic continuum ranging from focally-distributed NFTs observed in cognitively normal aged individuals, through the pathology observed in individuals with dementing illnesses that have been previously referred to as "tangle-predominant senile dementia", "tangle-only dementia", "preferential development of NFTs without senile plaques" and, among others, "senile dementia of the neurofibrillary tangle type". Interestingly, this condition has been reported as having deposited brain NFTs indistinguishable from those of AD, in the absence of neuritic plaques (Crary et al., 2014); therefore, no formal criteria for AD neuropathologic changes are met. Moreover, the NFTs deposition has been found to be mostly restricted to the medial temporal lobe, the basal forebrain, the brainstem, and the olfactory areas (Crary et al., 2014). As such, formal neuropathological criteria for PART were proposed by Crary et al (**Table 2**), consisting in the presence of tau-positive NFTs with a Braak stage ≤ 4 (minimal deposition beyond medial temporal lobes) and sparse ("possible PART") to absent ("definite PART") amyloid-beta deposition (ie Thal amyloid-beta phase ≤ 2 or a CERAD amyloid-beta stage of 0 to 1).

Table 2. Primary age-related tauopathy neuropathological criteria, as defined by Crary et al (Crary et al., 2014).

1. Requires:

NFT present with Braak stage ≤ IV (usua lly III or lower)

2. Then subclassify as follows:

Category	Thal Aβ Phase[a]	Other disease associated with NFT[b]
Definite	0	Absent
Possible	1-2	Absent

Examples:

"Primary age-related tauopathy (PART), Definite, Braak stage II"

"Primary age-related tauopathy (PART), Possible, Braak stage III, Thal Aβ phase 2"

3. Ancillary studies (not required):

- Immunohistochemistry: 3R and 4R tau-positive
- Electron microscopy: paired helical filaments present
- Genetics: absence of pathogenic FTLD-tau mutation

[a] See [116, 135]. Laboratories using the CERAD neuritic plaque density score [96, 97] may classify subjects with neuritic plaque frequency of "None" as "Definite" and "Sparse" as "Possible."

[b] For example, progressive supranuclear palsy, corticobasal degeneration, Pick's disease, frontotemporal lobar degeneration with *MAPT* mutation, and chronic traumatic encephalopathy.

ii. Current state of the art of the clinical manifestations

In accordance to the aforementioned concepts, PART is currently a neuropathological diagnosis (i.e. only diagnosed *postmortem*). However, by retrospective analysis of patients with the *postmortem* diagnosis of this condition, Besser et al (Besser et al., 2017) found they could be divided in 2 groups, according to the clinical presentation: "symptomatic" (when dementia or cognitive deterioration were present up to the time of death) or "asymptomatic" (with no cognitive deficits). Moreover, "definite PART" individuals presented sparing of semantic memory/language compared to AD, and, when stratified by global Clinical Dementia Rating (CDR), had sparing of memory (CDR of 0.5 or 1) or attention (CDR of 2 or 3) (Besser et al., 2019), and presented slower cognitive decline across multiple neuropsychological domains, such as memory, language and visuospatial performance (Bell et al., 2019; Teylan et al., 2020). Conversely, AD patients showed a significantly steeper decline after becoming symptomatic (Teylan et al., 2020). These characteristics added to the fact that individuals with PART were originally described as being older than the ones with AD (Crary et al., 2014), something supported by other studies that followed-up a higher number of cases (Besser et al., 2019; Teylan et al., 2020). Given that AD is diagnosed more than 50% of the time in PART individuals with mild cognitive impairment or dementia (Teylan et al., 2019),

there is a need for *in vivo* (i.e. clinical setting) diagnostic tools to differentiate PART from other dementias, mostly AD, such as cerebrospinal fluid or magnetic resonance imaging biomarkers.

c. Magnetic resonance imaging in neurodegenerative conditions

i. Atrophy assessment: visual rating scales versus quantitative evaluation

Neurodegenerative conditions encompass a wide spectrum of disorders, such as mild cognitive impairment/dementia and movement disorders, with frequent overlap between neuropathological changes (i.e. the so-called co-pathology) and, consequently, clinical and imaging manifestations (Haller et al., 2019). To complicate the matter even more, the same misfolded protein deposited in the brain may lead to different neurodegenerative conditions; for instance, the accumulation of Lewy bodies might lead to Parkinson's disease (movement disorder) or dementia with Lewy bodies (dementia) (Haller et al., 2019). This overall complexity was also what led, for example, to the development of the most recent revised criteria for the diagnosis and staging of AD (Jack et al., 2024), with a shift from a diagnosis based on clinical symptoms to a biological one (i.e. preferential use of biomarkers to establish the diagnosis of this condition).

Despite some neurodegenerative conditions having typical MRI manifestations that point to a more specific diagnosis, such as the case of progressive supranuclear palsy or multiple system atrophy (Haller et al., 2018), in most situations it has a first objective of excluding other brain pathologies that could be responsible for the cognitive dysfunction, such as subdural hematoma, normal pressure hydrocephalus, malignancy and other surgical pathology (exclusive approach), and a second objective of identifying findings suggestive or supportive of a specific condition (inclusive approach) (Haller et al., 2019), with a special emphasis on brain atrophy and microangiopathy. For this purpose, several clinically-applicable semiquantitative rating scales were developed to facilitate reporting; in the case of atrophy, enhancing the detection of regional or global preference, and being appropriate or not for the age of the patient (Haller et al., 2019). Six visual rating scales were validated in a large population study (Harper et al., 2016), as long as applied by previously trained raters and performed on a 3D T1-weighted sequence, that namely evaluate the anterior cingulate, the orbitofrontal, the anterior temporal, the frontoinsular, the medial temporal and the posterior regions (**Figure 5**). Specifically, the orbitofrontal and anterior cingulate regions were rated on the first anterior slice where the corpus callosum becomes visible; the frontoinsular was rated over three slices, starting on the first anterior slice where the anterior cingulate becomes visible and moving posteriorly; the anterior temporal was rated at the level of the temporal pole, just anterior to where the "temporal stem" connects the frontal and temporal lobes; the medial temporal was rated

according to the medial temporal lobe atrophy score, and was performed on the hippocampus at the level of the anterior pons; the posterior region was rated according to the four-point posterior atrophy scale described by Koedam (Koedam et al., 2011), with overall score based on the presence of atrophy in sagittal (widening of the posterior cingulate and parieto-occipital sulcus, and atrophy of the precuneus on left and right by considering paramedian sagittal images), axial (widening of the posterior cingulate sulcus and sulcal dilatation in parietal lobes on axial imagens) and coronal (widening of the posterior cingulate sulcus and parietal lobes on coronal images) sections, assessed for left and right separately.

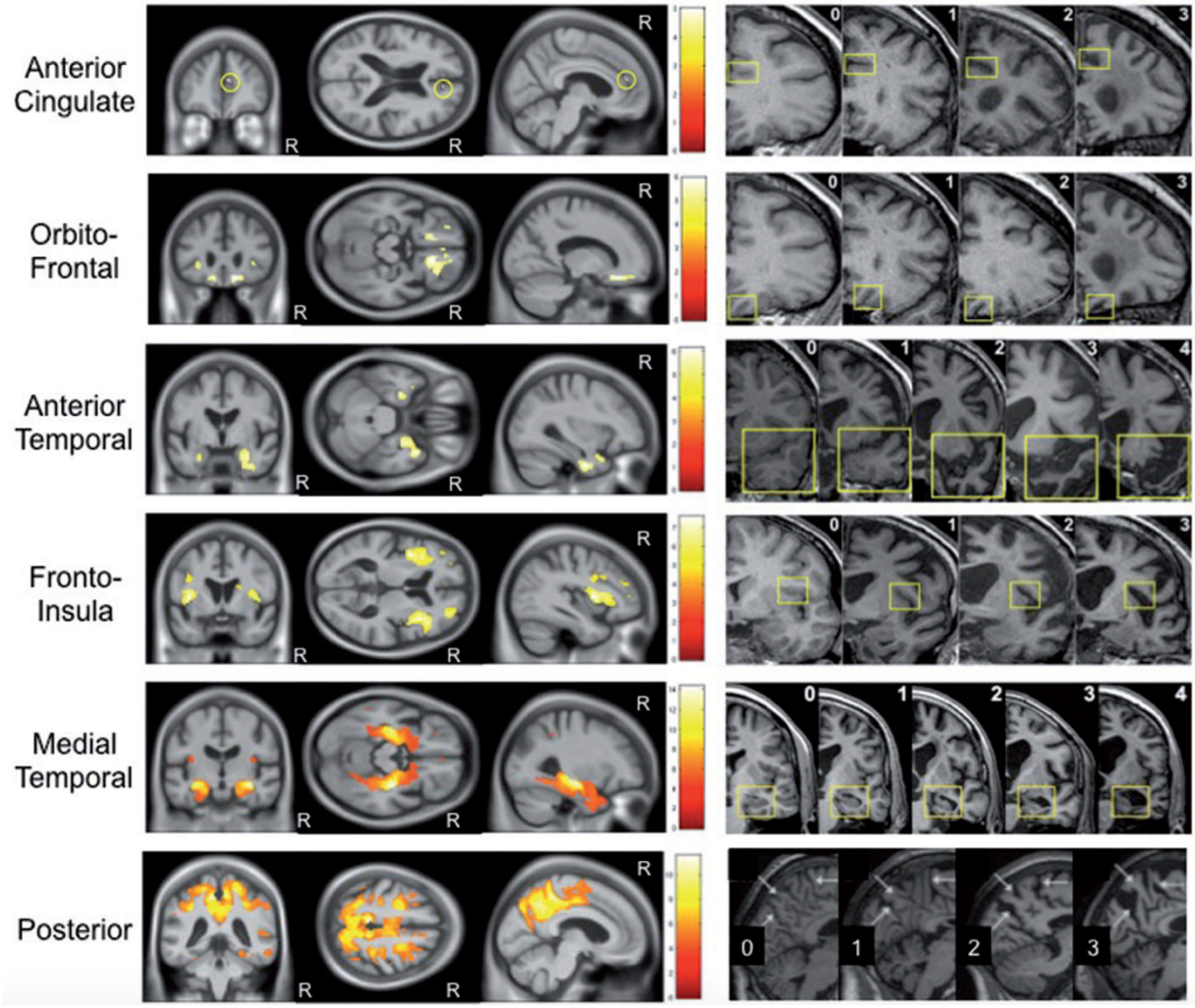


Figure 5. Six visual rating scales for semiquantitative assessment of brain atrophy with congruent correlation with grey matter volume, as presented by Harper et al (Harper et al., 2016).

More recently, the entorhinal cortex atrophy (ERICA) score was described (Enkirch et al., 2018), with the aim of detecting AD in an early phase, as the entorhinal cortex is one of the first brain structures affected by this disorder. This rating should be performed on a coronal reformat of a 3D T1-weighted sequence, perpendicular to the hippocampus, at the level of the mammillary bodies; a score of

at least 2 showed accurate discrimination between subjective cognitive decline and clinically manifest AD.

Alternatively, automated volumetric assessment of the brain is another option available, and is preferentially used, due to its potential higher accuracy, by many research groups and in some clinical trials (Haller et al., 2019). There are also some centers using several software tools for automatic MRI volumetry, however, there are some potential caveats associated with it, namely relating to interindividual physiological variability and external validation. Moreover, despite the increasing number of software tools that enable easier and quicker volumetric post-processing, it still requires an amount of time investment, which is enough to diminish its wider use in the daily clinical routine. These are the reasons why we decided to use the visual rating scales in this project, which are relatively easy to perform in the daily clinical routine and are, of course, widely available (i.e. only depends on the know-how by the rater).

ii. Microangiopathic burden assessment: the role of the Fazekas score

Cerebrovascular disease burden in the form of white matter hyperintensities on T2-weighted sequences has been shown to be a predictor of AD progression and can be routinely assessed by the Fazekas score (Ozge et al., 2023) on brain MRI. This is a three-point based scale (Fazekas et al., 1987), originally described almost four decades ago but still widely used in clinical practice, that independently rates deep and periventricular white matter lesions related to leukoaraiosis, with the former topography being frequently associated with microangiopathy (**Figure 6**). Moreover, it has been shown that amyloid-beta deposition and white matter lesions independently predict cognitive impairment, a notion that further supports the potential usefulness of assessing white matter damage (Gordon et al., 2015). Despite brain vascular pathology being a well-established comorbidity in AD, it is still underexplored how this burden differentially impacts PART compared to AD.

iii. Magnetic resonance imaging in Alzheimer's disease

The classic and most prominent imaging finding in patients with typical AD (i.e. with slowly progressive cognitive impairment, that typically begins with short-term memory loss) is hippocampal atrophy (Haller & Barkhof, 2018), commonly evaluated on MRI by the medial temporal lobe atrophy score described above; the most accepted cut-off is the one proposed by Pereira et al (Pereira et al., 2014) in 2014: in a patient with less than 75 years, a medial temporal score of at least 1.5 (mean score of both hemispheres) is considered pathological, while in a patient with more than 75 years, a medial temporal score of at least 2.0 is considered abnormal. In AD cases with presenile onset, however,

parietal/precuneus atrophy may be found in isolation (i.e. Koedam score of at least 2). Moreover, there are many recognized atypical phenotypes of AD that present with different brain atrophy patterns (Graff-Radford et al., 2021) – **figure 7**: (a) logopenic variant with left temporoparietal atrophy; (b) posterior cortical atrophy with parieto-occipital atrophy; (c) dysexecutive variant with frontoparietal atrophy; (d) cortical basal syndrome with left greater than right hemisphere atrophy, namely around the motor cortex; (e) behavioral variant with frontotemporal atrophy (predominantly temporal). It is paramount to keep in mind that these findings are highly unspecific, as, for instance, the behavioral variant of frontotemporal dementia can also present with hippocampal atrophy, as can also the latter stages of dementia with Lewy bodies (Haller et al., 2019).

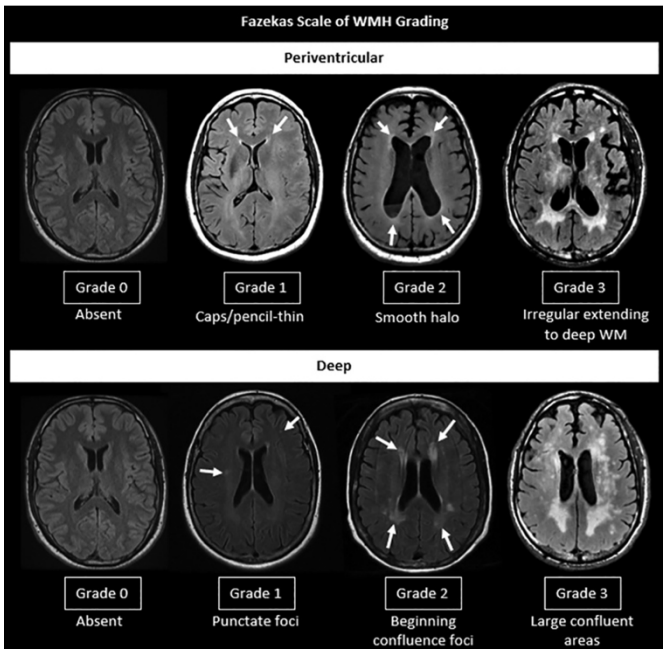


Figure 6. Fazekas rating scale for the periventricular and deep white matter, as presented by Mahammedi et al (Mahammedi et al., 2022).

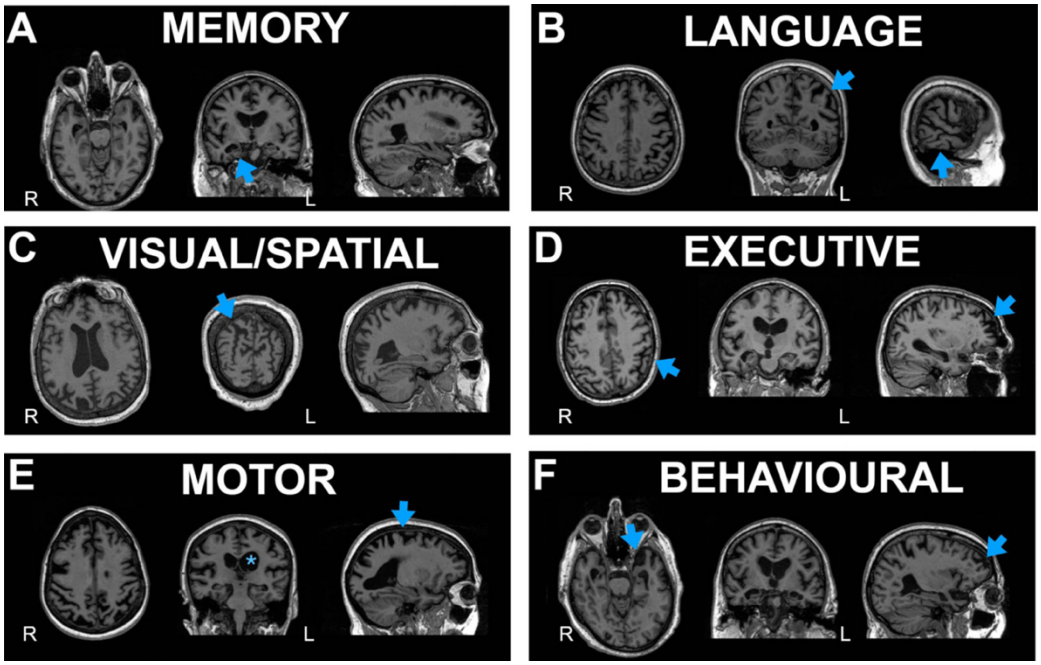


Figure 7. Magnetic resonance imaging across AD phenotypes, as presented by Graff-Radford et al (Graff-Radford et al., 2021).

It is important to keep in mind that these brain morphological changes typically start occurring immediately before the beginning of the memory-predominant mild cognitive impairment that latter might progress to AD (~ 50% of the cases), as depicted in **figure 8**.

As previously stated, T2 white matter hyperintensities, globally known as leukoaraiosis, are frequently found in patients with AD, with the deep white matter topography being frequently associated with small vessel disease (i.e. microangiopathy) (Fazekas et al., 1987; Mahammedi et al., 2022). Moreover, lobar cerebral microbleeds can also be found in some patients with AD (Haller & Barkhof, 2018), and, therefore, there is a current debate regarding partial overlap in amyloid deposition in AD and cerebral amyloid angiopathy (Haller & Barkhof, 2018), a cerebrovascular disorder caused by the brain accumulation of Aβ in the tunica media and adventitia of leptomeningeal and cortical vessels, that can lead to lobar cerebral microbleeds.

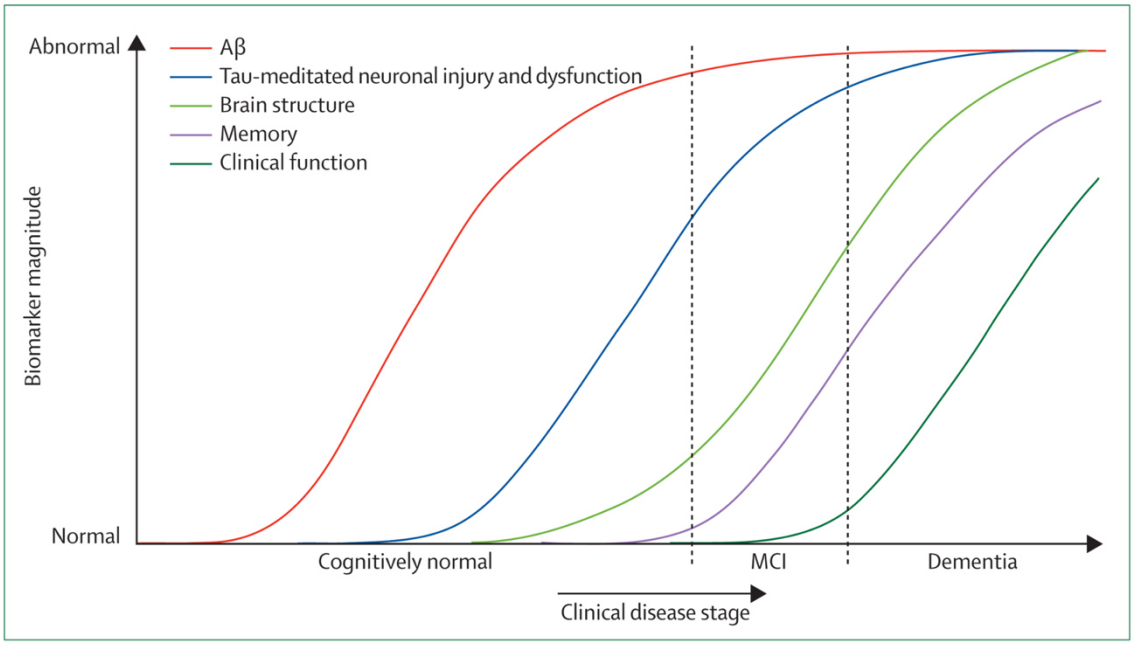


Figure 8. Dynamic biomarkers of the Alzheimer's pathological cascade, as presented by Jack et al (Jack et al., 2010).

Several studies have shown that the entorhinal cortex and the transentorhinal region are among the first brain structures to show pathologic changes in AD, even before similar changes take place in the hippocampus (Braak & Braak, 1991; Delacourte et al., 1999; Du et al., 2004; Khan et al., 2014), with the continuous decrease of the entorhinal cortex volume from preclinical stages of dementia to later stages of AD (Jessen et al., 2006). The ERICA score (**Figure 9**) was created precisely to detect these changes in the entorhinal cortex, potentially raising the early suspicion of AD development, with a score of at least 2 (with the "tentorial cleft sign") discriminating between subjective cognitive decline and clinically manifest AD with 91% accuracy (Enkirch et al., 2018). Moreover, this score showed significant correlations with other biomarkers of AD, such as cerebrospinal fluid and neuropsychological tests parameters (Enkirch et al., 2018).

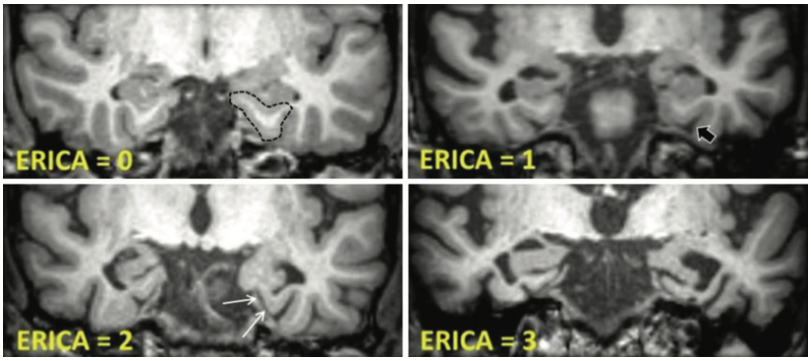


Figure 9. The ERICA score for the entorhinal cortex atrophy evaluation, as presented by Enkirch et al (Enkirch et al., 2018).

iv. Magnetic resonance imaging in primary age-related tauopathy

The first study to assess magnetic resonance imaging characteristics in individuals with PART was the one performed by Josephs et al in 2017 (Josephs, Murray, et al., 2017), that used a voxel-based morphometry approach to characterize the atrophy patterns of participants with "definite" PART, while also assessing its relationship with cognitive performance; it was found an association between Braak staging (i.e. NFTs deposition) and atrophy of the left head of the hippocampus, with the latter correlating with the preservation of the episodic memory. A couple of years later, by evaluating 26 cases with neuropathologically confirmed "definite" PART, and with the use of six semiquantitative previously validated visual rating scales that assess regional brain atrophy, we found a significant correlation between Braak staging and atrophy of the medial temporal lobe (**figure 10**) (Quintas-Neves et al., 2019), as well as an increase in medial temporal lobe atrophy with age (close to statistical threshold).

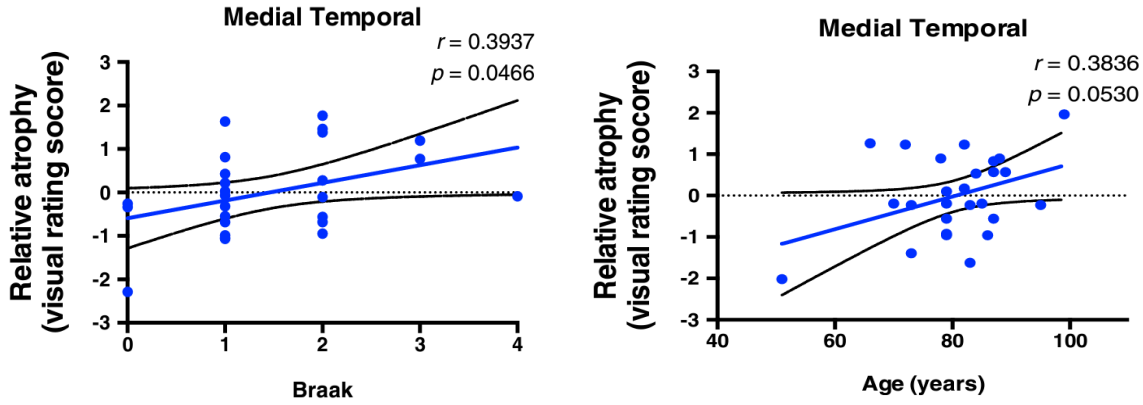


Figure 10. (Left) Medial temporal lobe atrophy significantly correlating with increasing Braak stage in "definite" PART participants, after correction for age. (Right) Medial temporal lobe atrophy increasing with age, after correction for Braak, close to the statistical threshold. Adapted from Quintas-Neves et al (Quintas-Neves et al., 2019).

Moreover, we also found that anterior and medial temporal lobe atrophy significantly correlated with worse performance on neuropsychological tests that evaluate the semantic memory/language domain, such as the vegetables (for both areas) and animals (for anterior temporal) naming (**Figure 11**) (Quintas-Neves et al., 2019).

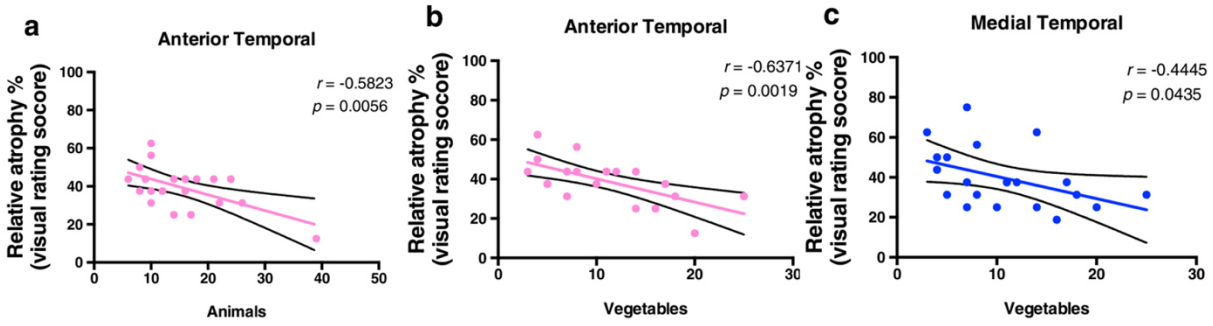


Figure 11. (a, b) Anterior temporal lobe atrophy significantly correlating with decreased semantic memory/language tests performance in "definite" PART participants, after correction for age, as also did medial temporal lobe atrophy (c). Adapted from Quintas-Neves et al (Quintas-Neves et al., 2019).

Adding to this, TAR DNA-binding protein 43 (TDP-43), a main component of the ubiquitinated inclusions found on several neurodegenerative conditions, it is known to be strikingly associated with amygdala and hippocampal atrophy in PART participants (Josephs et al., 2019), and, in AD patients, associated with worse memory loss (Josephs et al., 2014), atrophy of the hippocampus (Josephs et al., 2014), and faster rates of hippocampal atrophy (Josephs, Dickson, et al., 2017); these findings support the notion of TDP-43 being associated with temporal lobe atrophy across the entire range of amyloid-beta and NFTs deposition. Moreover, high levels of TDP-43 in participants with PART were associated with smaller brain volumes, faster rates of brain atrophy and acceleration of atrophy rates more than a decade prior to death, with deceleration occurring closer to death, particularly in the hippocampus (Josephs et al., 2020); additionally, it was found that the association between brain atrophy and TDP-43 in PART participants occurred 3 years later than in AD (Josephs et al., 2020). Despite these results, few studies have assessed the relationship between brain MRI and neuropathological findings in individuals with PART and AD, specially using semiquantitative visual rating scales to assess the degree of regional brain atrophy.

d. Aims

- To compare *in vivo* magnetic resonance imaging findings with neuropathological findings in individuals with "definite" PART (i.e. Braak stage higher than 0 and CERAD = 0) and AD, using visual rating regional atrophy scales (Harper et al., 2016), while also assessing the relationship between brain atrophy and the degree of clinical impairment in all groups, based on CDR metrics (Morris, 1993) and neuropsychological testing (Weintraub et al., 2018);
- To compare the microangiopathic burden evaluated by *in vivo* brain magnetic resonance imaging, using the Fazekas score (Fazekas et al., 1987), with neuropathological findings in patients with "definite" PART and AD, while assessing the relationship between brain microangiopathy and regional brain atrophy in all groups, using the previously mentioned visual rating scales;
- To assess potential differences in the entorhinal cortex by *in vivo* brain magnetic resonance imaging, using the semiquantitative visual rating scale ERICA (Enkirch et al., 2018), between individuals with "definite" PART and AD, while also assessing the relationship between the ERICA score and the degree of clinical impairment in all groups, based on CDR metrics (Morris, 1993).

e. References

Almeida, M. C., Eger, S. J., He, C., Audouard, M., Nikitina, A., Glasauer, S. M. K., Han, D., Mejia-Cupajita, B., Acosta-Uribe, J., Villalba-Moreno, N. D., Littau, J. L., Elcheikhali, M., Rivera, E. K., Carrettiero, D. C., Villegas-Lanau, C. A., Sepulveda-Falla, D., Lopera, F., & Kosik, K. S. (2024). Single-nucleus RNA sequencing demonstrates an autosomal dominant Alzheimer's disease profile and possible mechanisms of disease protection. *Neuron*, *112*(11), 1778-1794 e1777. https://doi.org/10.1016/j.neuron.2024.02.009

Bell, W. R., An, Y., Kageyama, Y., English, C., Rudow, G. L., Pletnikova, O., Thambisetty, M., O'Brien, R., Moghekar, A. R., Albert, M. S., Rabins, P. V., Resnick, S. M., & Troncoso, J. C. (2019). Neuropathologic, genetic, and longitudinal cognitive profiles in primary age-related tauopathy (PART) and Alzheimer's disease. *Alzheimers Dement*, *15*(1), 8-16. https://doi.org/10.1016/j.jalz.2018.07.215

Besser, L. M., Crary, J. F., Mock, C., & Kukull, W. A. (2017). Comparison of symptomatic and asymptomatic persons with primary age-related tauopathy. *Neurology*, *89*(16), 1707-1715. https://doi.org/10.1212/WNL.0000000000004521

Besser, L. M., Mock, C., Teylan, M. A., Hassenstab, J., Kukull, W. A., & Crary, J. F. (2019). Differences in Cognitive Impairment in Primary Age-Related Tauopathy Versus Alzheimer Disease. *J Neuropathol Exp Neurol*, *78*(3), 219-228. https://doi.org/10.1093/jnen/nly132

Braak, H., & Braak, E. (1991). Neuropathological stageing of Alzheimer-related changes. *Acta Neuropathol*, *82*(4), 239-259. https://doi.org/10.1007/BF00308809

Chapleau, M., Iaccarino, L., Soleimani-Meigooni, D., & Rabinovici, G. D. (2022). The Role of Amyloid PET in Imaging Neurodegenerative Disorders: A Review. *J Nucl Med*, *63*(Suppl 1), 13S-19S. https://doi.org/10.2967/jnumed.121.263195

Crary, J. F., Trojanowski, J. Q., Schneider, J. A., Abisambra, J. F., Abner, E. L., Alafuzoff, I., Arnold, S. E., Attems, J., Beach, T. G., Bigio, E. H., Cairns, N. J., Dickson, D. W., Gearing, M., Grinberg, L. T., Hof, P. R., Hyman, B. T., Jellinger, K., Jicha, G. A., Kovacs, G. G.,...Nelson, P. T. (2014). Primary age-related tauopathy (PART): a common pathology associated with human aging. *Acta Neuropathol*, *128*(6), 755-766. https://doi.org/10.1007/s00401-014-1349-0

Delacourte, A., David, J. P., Sergeant, N., Buee, L., Wattez, A., Vermersch, P., Ghozali, F., Fallet-Bianco, C., Pasquier, F., Lebert, F., Petit, H., & Di Menza, C. (1999). The biochemical pathway of neurofibrillary degeneration in aging and Alzheimer's disease. *Neurology*, *52*(6), 1158-1165. https://doi.org/10.1212/wnl.52.6.1158

Du, A. T., Schuff, N., Kramer, J. H., Ganzer, S., Zhu, X. P., Jagust, W. J., Miller, B. L., Reed, B. R., Mungas, D., Yaffe, K., Chui, H. C., & Weiner, M. W. (2004). Higher atrophy rate of entorhinal cortex than hippocampus in AD. *Neurology*, *62*(3), 422-427. https://doi.org/10.1212/01.wnl.0000106462.72282.90

Enkirch, S. J., Traschutz, A., Muller, A., Widmann, C. N., Gielen, G. H., Heneka, M. T., Jurcoane, A., Schild, H. H., & Hattingen, E. (2018). The ERICA Score: An MR Imaging-based Visual Scoring System for the Assessment of Entorhinal Cortex Atrophy in Alzheimer Disease. *Radiology*, *288*(1), 226-333. https://doi.org/10.1148/radiol.2018171888

Fazekas, F., Chawluk, J. B., Alavi, A., Hurtig, H. I., & Zimmerman, R. A. (1987). MR signal abnormalities at 1.5 T in Alzheimer's dementia and normal aging. *AJR Am J Roentgenol*, *149*(2), 351-356. https://doi.org/10.2214/ajr.149.2.351

Ginsberg, S. D., Che, S., Counts, S. E., & Mufson, E. J. (2006). Shift in the ratio of three-repeat tau and four-repeat tau mRNAs in individual cholinergic basal forebrain neurons in mild cognitive impairment and Alzheimer's disease. *J Neurochem*, *96*(5), 1401-1408. https://doi.org/10.1111/j.1471-4159.2005.03641.x

Godi, C., & Falini, A. (2019). Radiological Findings of Drug-Induced Neurotoxic Disorders. In F. Barkhof, R. Jager, M. Thurnher, & A. Rovira Cañellas (Eds.), *Clinical Neuroradiology: The ESNR Textbook* (pp. 1-27). Springer International Publishing. https://doi.org/10.1007/978-3-319-61423-6_67-1

Goedert, M. (2015). NEURODEGENERATION. Alzheimer's and Parkinson's diseases: The prion concept in relation to assembled Abeta, tau, and alpha-synuclein. *Science*, *349*(6248), 1255555. https://doi.org/10.1126/science.1255555

Gordon, B. A., Najmi, S., Hsu, P., Roe, C. M., Morris, J. C., & Benzinger, T. L. (2015). The effects of white matter hyperintensities and amyloid deposition on Alzheimer dementia. *Neuroimage Clin*, *8*, 246-252. https://doi.org/10.1016/j.nicl.2015.04.017

Graff-Radford, J., Yong, K. X. X., Apostolova, L. G., Bouwman, F. H., Carrillo, M., Dickerson, B. C., Rabinovici, G. D., Schott, J. M., Jones, D. T., & Murray, M. E. (2021). New insights into atypical Alzheimer's disease in the era of biomarkers. *Lancet Neurol*, *20*(3), 222-234. https://doi.org/10.1016/S1474-4422(20)30440-3

Guo, T., Zhang, D., Zeng, Y., Huang, T. Y., Xu, H., & Zhao, Y. (2020). Molecular and cellular mechanisms underlying the pathogenesis of Alzheimer's disease. *Mol Neurodegener*, *15*(1), 40. https://doi.org/10.1186/s13024-020-00391-7

Haass, C., & Selkoe, D. J. (2007). Soluble protein oligomers in neurodegeneration: lessons from the Alzheimer's amyloid beta-peptide. *Nat Rev Mol Cell Biol*, *8*(2), 101-112. https://doi.org/10.1038/nrm2101

Haller, S., & Barkhof, F. (2018). Neuroimaging in Dementia: A Clinical Approach.

Haller, S., Garibotto, V., & Barkhof, F. (2019). Neurodegenerative disorders: classification and imaging strategy. *Clin Neuroradiol*, 1251-1275.

Haller, S., Garibotto, V., & Schwarz, S. (2018). Neuroimaging in Movement Disorders. *Clinical Neuroradiology. Cham, Switzerland: Springer*, 1-36.

Harper, L., Fumagalli, G. G., Barkhof, F., Scheltens, P., O'Brien, J. T., Bouwman, F., Burton, E. J., Rohrer, J. D., Fox, N. C., Ridgway, G. R., & Schott, J. M. (2016). MRI visual rating scales in the diagnosis of dementia: evaluation in 184 post-mortem confirmed cases. *Brain*, *139*(Pt 4), 1211-1225. https://doi.org/10.1093/brain/aww005

Hyman, B. T., Phelps, C. H., Beach, T. G., Bigio, E. H., Cairns, N. J., Carrillo, M. C., Dickson, D. W., Duyckaerts, C., Frosch, M. P., Masliah, E., Mirra, S. S., Nelson, P. T., Schneider, J. A., Thal, D. R., Thies, B., Trojanowski, J. Q., Vinters, H. V., & Montine, T. J. (2012). National Institute on Aging-Alzheimer's Association guidelines for the neuropathologic assessment of Alzheimer's disease. *Alzheimers Dement*, *8*(1), 1-13. https://doi.org/10.1016/j.jalz.2011.10.007

Jack, C. R., Jr., Andrews, J. S., Beach, T. G., Buracchio, T., Dunn, B., Graf, A., Hansson, O., Ho, C., Jagust, W., McDade, E., Molinuevo, J. L., Okonkwo, O. C., Pani, L., Rafii, M. S., Scheltens, P., Siemers, E., Snyder, H. M., Sperling, R., Teunissen, C. E., & Carrillo, M. C. (2024). Revised criteria for diagnosis and staging of Alzheimer's disease: Alzheimer's Association Workgroup. *Alzheimers Dement*, *20*(8), 5143-5169. https://doi.org/10.1002/alz.13859

Jack, C. R., Jr., Bennett, D. A., Blennow, K., Carrillo, M. C., Dunn, B., Haeberlein, S. B., Holtzman, D. M., Jagust, W., Jessen, F., Karlawish, J., Liu, E., Molinuevo, J. L., Montine, T., Phelps, C., Rankin, K. P., Rowe, C. C., Scheltens, P., Siemers, E., Snyder, H. M.,...Contributors. (2018). NIA-AA Research Framework: Toward a biological definition of Alzheimer's disease. *Alzheimers Dement*, *14*(4), 535-562. https://doi.org/10.1016/j.jalz.2018.02.018

Jack, C. R., Jr., Knopman, D. S., Jagust, W. J., Shaw, L. M., Aisen, P. S., Weiner, M. W., Petersen, R. C., & Trojanowski, J. Q. (2010). Hypothetical model of dynamic biomarkers of the Alzheimer's pathological cascade. *Lancet Neurol*, *9*(1), 119-128. https://doi.org/10.1016/S1474-4422(09)70299-6

Jessen, F., Feyen, L., Freymann, K., Tepest, R., Maier, W., Heun, R., Schild, H. H., & Scheef, L. (2006). Volume reduction of the entorhinal cortex in subjective memory impairment. *Neurobiol Aging*, *27*(12), 1751-1756. https://doi.org/10.1016/j.neurobiolaging.2005.10.010

Josephs, K. A., Dickson, D. W., Tosakulwong, N., Weigand, S. D., Murray, M. E., Petrucelli, L., Liesinger, A. M., Senjem, M. L., Spychalla, A. J., Knopman, D. S., Parisi, J. E., Petersen, R. C., Jack, C. R., Jr., & Whitwell, J. L. (2017). Rates of hippocampal atrophy and presence of post-mortem TDP-43 in patients with Alzheimer's disease: a longitudinal retrospective study. *Lancet Neurol*, *16*(11), 917-924. https://doi.org/10.1016/S1474-4422(17)30284-3

Josephs, K. A., Martin, P. R., Weigand, S. D., Tosakulwong, N., Buciuc, M., Murray, M. E., Petrucelli, L., Senjem, M. L., Spychalla, A. J., Knopman, D. S., Boeve, B. F., Petersen, R. C., Parisi, J. E., Dickson, D. W., Jack, C. R., & Whitwell, J. L. (2020). Protein contributions to brain atrophy acceleration in Alzheimer's disease and primary age-related tauopathy. *Brain*, *143*(11), 3463-3476. https://doi.org/10.1093/brain/awaa299

Josephs, K. A., Murray, M. E., Tosakulwong, N., Weigand, S. D., Knopman, D. S., Petersen, R. C., Jack, C. R., Jr., Whitwell, J. L., & Dickson, D. W. (2019). Brain atrophy in primary age-related tauopathy is linked to transactive response DNA-binding protein of 43 kDa. *Alzheimers Dement*, *15*(6), 799-806. https://doi.org/10.1016/j.jalz.2019.03.003

Josephs, K. A., Murray, M. E., Tosakulwong, N., Whitwell, J. L., Knopman, D. S., Machulda, M. M., Weigand, S. D., Boeve, B. F., Kantarci, K., Petrucelli, L., Lowe, V. J., Jack, C. R., Jr., Petersen, R. C., Parisi, J. E., & Dickson, D. W. (2017). Tau aggregation influences cognition and hippocampal atrophy in the absence of beta-amyloid: a clinico-imaging-pathological study of primary age-related tauopathy (PART). *Acta Neuropathol*, *133*(5), 705-715. https://doi.org/10.1007/s00401-017-1681-2

Josephs, K. A., Whitwell, J. L., Weigand, S. D., Murray, M. E., Tosakulwong, N., Liesinger, A. M., Petrucelli, L., Senjem, M. L., Knopman, D. S., Boeve, B. F., Ivnik, R. J., Smith, G. E., Jack, C. R., Jr., Parisi, J. E., Petersen, R. C., & Dickson, D. W. (2014). TDP-43 is a key player in the clinical features associated with Alzheimer's disease. *Acta Neuropathol*, *127*(6), 811-824. https://doi.org/10.1007/s00401-014-1269-z

Karran, E., Mercken, M., & De Strooper, B. (2011). The amyloid cascade hypothesis for Alzheimer's disease: an appraisal for the development of therapeutics. *Nat Rev Drug Discov*, *10*(9), 698-712. https://doi.org/10.1038/nrd3505

Kepp, K. P., Robakis, N. K., Hoilund-Carlsen, P. F., Sensi, S. L., & Vissel, B. (2023). The amyloid cascade hypothesis: an updated critical review. *Brain*, *146*(10), 3969-3990. https://doi.org/10.1093/brain/awad159

Khan, U. A., Liu, L., Provenzano, F. A., Berman, D. E., Profaci, C. P., Sloan, R., Mayeux, R., Duff, K. E., & Small, S. A. (2014). Molecular drivers and cortical spread of lateral entorhinal cortex dysfunction in preclinical Alzheimer's disease. *Nat Neurosci*, *17*(2), 304-311. https://doi.org/10.1038/nn.3606

Knopman, D. S., Amieva, H., Petersen, R. C., Chetelat, G., Holtzman, D. M., Hyman, B. T., Nixon, R. A., & Jones, D. T. (2021). Alzheimer disease. *Nat Rev Dis Primers*, *7*(1), 33. https://doi.org/10.1038/s41572-021-00269-y

Koedam, E. L., Lehmann, M., van der Flier, W. M., Scheltens, P., Pijnenburg, Y. A., Fox, N., Barkhof, F., & Wattjes, M. P. (2011). Visual assessment of posterior atrophy development of a MRI rating scale. *Eur Radiol*, *21*(12), 2618-2625. https://doi.org/10.1007/s00330-011-2205-4

Liu, A. K., Chang, R. C., Pearce, R. K., & Gentleman, S. M. (2015). Nucleus basalis of Meynert revisited: anatomy, history and differential involvement in Alzheimer's and Parkinson's disease. *Acta Neuropathol*, *129*(4), 527-540. https://doi.org/10.1007/s00401-015-1392-5

Mahammedi, A., Wang, L. L., Williamson, B. J., Khatri, P., Kissela, B., Sawyer, R. P., Shatz, R., Khandwala, V., & Vagal, A. (2022). Small Vessel Disease, a Marker of Brain Health: What the Radiologist Needs to Know. *AJNR Am J Neuroradiol*, *43*(5), 650-660. https://doi.org/10.3174/ajnr.A7302

Mirra, S. S., Heyman, A., McKeel, D., Sumi, S. M., Crain, B. J., Brownlee, L. M., Vogel, F. S., Hughes, J. P., van Belle, G., & Berg, L. (1991). The Consortium to Establish a Registry for Alzheimer's Disease (CERAD). Part II. Standardization of the neuropathologic assessment of Alzheimer's disease. *Neurology*, *41*(4), 479-486. https://doi.org/10.1212/wnl.41.4.479

Morris, J. C. (1993). The Clinical Dementia Rating (CDR): current version and scoring rules. *Neurology*, *43*(11), 2412-2414. https://doi.org/10.1212/wnl.43.11.2412-a

Nagy, Z., Yilmazer-Hanke, D. M., Braak, H., Braak, E., Schultz, C., & Hanke, J. (1998). Assessment of the pathological stages of Alzheimer's disease in thin paraffin sections: a comparative study. *Dement Geriatr Cogn Disord*, *9*(3), 140-144. https://doi.org/10.1159/000017038

Ozge, A., Ghouri, R., Oksuz, N., & Tasdelen, B. (2023). Predictive factors for Alzheimer's disease progression: a comprehensive retrospective analysis of 3,553 cases with 211 months follow-up. *Front Neurol*, *14*, 1239995. https://doi.org/10.3389/fneur.2023.1239995

Pereira, J. B., Cavallin, L., Spulber, G., Aguilar, C., Mecocci, P., Vellas, B., Tsolaki, M., Kloszewska, I., Soininen, H., Spenger, C., Aarsland, D., Lovestone, S., Simmons, A., Wahlund, L. O., Westman, E., AddNeuroMed, c., & for the Alzheimer's Disease Neuroimaging, I. (2014). Influence of age, disease onset and ApoE4 on visual medial temporal lobe atrophy cut-offs. *J Intern Med*, *275*(3), 317-330. https://doi.org/10.1111/joim.12148

Quintas-Neves, M., Teylan, M. A., Besser, L., Soares-Fernandes, J., Mock, C. N., Kukull, W. A., Crary, J. F., & Oliveira, T. G. (2019). Magnetic resonance imaging brain atrophy assessment in primary age-related tauopathy (PART). *Acta Neuropathol Commun*, *7*(1), 204. https://doi.org/10.1186/s40478-019-0842-z

Schilling, S., Pradhan, A., Heesch, A., Helbig, A., Blennow, K., Koch, C., Bertgen, L., Koo, E. H., Brinkmalm, G., Zetterberg, H., Kins, S., & Eggert, S. (2023). Differential effects of familial Alzheimer's disease-causing mutations on amyloid precursor protein (APP) trafficking, proteolytic conversion, and synaptogenic activity. *Acta Neuropathol Commun*, *11*(1), 87. https://doi.org/10.1186/s40478-023-01577-y

Tanzi, R. E., & Bertram, L. (2005). Twenty years of the Alzheimer's disease amyloid hypothesis: a genetic perspective. *Cell*, *120*(4), 545-555. https://doi.org/10.1016/j.cell.2005.02.008

Teylan, M., Besser, L. M., Crary, J. F., Mock, C., Gauthreaux, K., Thomas, N. M., Chen, Y. C., & Kukull, W. A. (2019). Clinical diagnoses among individuals with primary age-related tauopathy versus Alzheimer's neuropathology. *Lab Invest*, *99*(7), 1049-1055. https://doi.org/10.1038/s41374-019-0186-0

Teylan, M., Mock, C., Gauthreaux, K., Chen, Y. C., Chan, K. C. G., Hassenstab, J., Besser, L. M., Kukull, W. A., & Crary, J. F. (2020). Cognitive trajectory in mild cognitive impairment due to primary age-related tauopathy. *Brain*, *143*(2), 611-621. https://doi.org/10.1093/brain/awz403

Weintraub, S., Besser, L., Dodge, H. H., Teylan, M., Ferris, S., Goldstein, F. C., Giordani, B., Kramer, J., Loewenstein, D., Marson, D., Mungas, D., Salmon, D., Welsh-Bohmer, K., Zhou, X. H., Shirk, S. D., Atri, A., Kukull, W. A., Phelps, C., & Morris, J. C. (2018). Version 3 of the Alzheimer Disease Centers' Neuropsychological Test Battery in the Uniform Data Set (UDS). *Alzheimer Dis Assoc Disord*, *32*(1), 10-17. https://doi.org/10.1097/WAD.0000000000000223

Wu, W., Ji, Y., Wang, Z., Wu, X., Li, J., Gu, F., Chen, Z., & Wang, Z. (2023). The FDA-approved anti-amyloid-beta monoclonal antibodies for the treatment of Alzheimer's disease: a systematic

review and meta-analysis of randomized controlled trials. *Eur J Med Res*, *28*(1), 544. https://doi.org/10.1186/s40001-023-01512-w

Zhang, Y., Chen, J., Li, Y., Jiao, B., & Luo, S. (2024). Disease-modifying therapies for Alzheimer's disease: clinical trial progress and opportunity. *Ageing Res Rev*, 102595. https://doi.org/10.1016/j.arr.2024.102595

Chapter 2.1

Miguel Quintas-Neves, Merilee A. Teylan, Rafaela Morais-Ribeiro, Francisco Almeida, Charles N. Mock, Walter A. Kukull, John F. Crary, Tiago Gil Oliveira

Divergent magnetic resonance imaging atrophy patterns in Alzheimer's disease and primary age-related tauopathy

Neurobiology of Aging (2022) 117:1-11

Doi: 10.1016/j.neurobiolaging.2022.04.013

Neurobiology of Aging 117 (2022) 1–11

Contents lists available at ScienceDirect

Neurobiology of Aging

journal homepage: www.elsevier.com/locate/neuaging.org

Divergent magnetic resonance imaging atrophy patterns in Alzheimer's disease and primary age-related tauopathy

Miguel Quintas-Neves[a,b,c], Merilee A. Teylan[d], Rafaela Morais-Ribeiro[b,c], Francisco Almeida[b,c], Charles N. Mock[d], Walter A. Kukull[d], John F. Crary[e], Tiago Gil Oliveira[a,b,c,*]

[a] Department of Neuroradiology, Hospital de Braga, Braga, Portugal
[b] Life and Health Sciences Research Institute (ICVS), School of Medicine, University of Minho, Braga, Portugal
[c] ICVS/3B's—PT Government Associate Laboratory, Braga/Guimarães, Portugal
[d] Department of Epidemiology, National Alzheimer's Coordinating Center, University of Washington, Seattle, WA, USA
[e] Neuropathology Brain Bank & Research Core, Department of Pathology, Nash Family Department of Neuroscience, Department of Artificial Intelligence & Human Health, Friedman Brain Institute, Ronald M. Loeb Center for Alzheimer's Disease, Icahn School of Medicine at Mount Sinai, New York, NY, USA

ARTICLE INFO

Article history:
Received 18 October 2021
Revised 18 April 2022
Accepted 19 April 2022
Available online 1 May 2022

Keywords:
Primary age-related tauopathy
Alzheimer's disease
MRI
Brain imaging

ABSTRACT

Our study compared brain MRI with neuropathological findings in patients with primary age-related tauopathy (PART) and Alzheimer's disease (AD), while assessing the relationship between brain atrophy and clinical impairment. We analyzed 233 participants: 32 with no plaques ("definite" PART—BRAAK stage higher than 0 and CERAD 0), and 201 cases within the AD spectrum, with 25 with sparse (CERAD 1), 76 with moderate (CERAD 2), and 100 with severe (CERAD 3) degrees of neuritic plaques. Upon correcting for age, sex, and age difference at MRI and death, there were significantly higher levels of atrophy in CERAD 3 compared to CERAD 1–2 and a trend compared to PART ($p = 0.06$). In the anterior temporal region, there was a trend for higher levels of atrophy in PART compared to Alzheimer's disease spectrum cases with CERAD 1 ($p = 0.08$). We then assessed the correlation between regional brain atrophy and CDR sum of boxes score for PART and AD, and found that overall cognition deficits are directly correlated with regional atrophy in the AD continuum, but not in definite PART. We further observed correlations between regional brain atrophy with multiple neuropsychological metrics in AD, with PART showing specific correlations between language deficits and anterior temporal atrophy. Overall, these findings support PART as an independent pathologic process from AD.

© 2022 Elsevier Inc. All rights reserved.

1. Introduction

Primary age-related tauopathy (PART) is a pathological process characterized by the presence of tau-positive neurofibrillary tangles (NFTs) and no amyloid-beta (Aβ) deposition ("definite PART") (Crary et al., 2014). Currently, the diagnosis of PART is histologically assessed by the presence of tau positive NFT with Braak staging (which can generally go from I to IV), and a Thal Aβ phase $\leq$2 or a Consortium to Establish a Registry for Alzheimer's disease (CERAD) Aβ stage of 0 (Crary et al., 2014).

Alzheimer's disease is clinically characterized by slowly progressive neurocognitive impairment predominantly characterized by short-term memory loss (typical senile Alzheimer's disease) and with disease progression, multiple neurocognitive domains can be involved, such as language impairment or mood disbalance (Kelley and Petersen, 2007). At the level of neuropathology, Alzheimer's disease diagnosis consists of grading the "ABC score," which is achieved by grading amyloid plaques (A) by Thal phases, NFT by Braak staging (B) and the neuritic plaque score by CERAD assessment (C) (Hyman et al., 2012).

Abbreviations: Aβ, amyloid-beta; AC, anterior cingulate; ADCs, Alzheimer's disease centers; AT, anterior temporal; CDR, CDR Dementia Staging Instrument; CDR-SB, clinical dementia rating sum of boxes; CERAD, Consortium to Establish a Registry for Alzheimer's disease; FI, frontoinsular; LATE, limbic-predominant age-related TDP-43 encephalopathy; MTA, medial temporal lobe atrophy; NACC, National Alzheimer's Coordinating Center; NIA-AA, National Institute on Aging and Alzheimer's Association; NFTs, neurofibrillary tangles; NP, neuritic plaque; OF, orbitofrontal; PART, primary age-related tauopathy; Post, posterior region; TDP-43, TAR DNA-binding protein 43; UDS, uniform data set.

* Corresponding author at: Life and Health Sciences Research Institute (ICVS), School of Medicine, University of Minho, Campus Gualtar, 4710-057 Braga, Portugal. Tel.: +351253604923.
E-mail address: tiago@med.uminho.pt (T.G. Oliveira).

0197-4580/$ – see front matter © 2022 Elsevier Inc. All rights reserved.
https://doi.org/10.1016/j.neurobiolaging.2022.04.013

The clinical characteristics of patients eventually identified as having *post mortem* PART can be divided as "symptomatic" (when dementia or cognitive deterioration were present up to the time of death) or "asymptomatic" (with no cognitive deficits) (Besser et al., 2017). However, the clinical presentation and the specific types of neuropsychological deficits in PART participants are still under scrutiny. Regarding this, "definite" PART participants showed sparing of semantic memory/language compared to Alzheimer's disease, and, when stratified by global Clinical Dementia Rating (CDR), presented sparing of memory (CDR of 0.5 or 1) or attention (CDR of 2 or 3), when compared to Alzheimer's disease patients (Besser et al., 2019). Moreover, it was shown that patients with PART had slower cognitive decline than Alzheimer's disease patients across multiple neuropsychological domains (Bell et al., 2019; Teylan et al., 2020). Alzheimer's disease patients showed a significantly steeper decline after becoming clinically symptomatic than those with PART (Teylan et al., 2020) and temporal lobe atrophy in PART specifically correlated with semantic memory/language deficits (Quintas-Neves et al., 2019). Also, it was shown that PART patients had significantly slower rates of decline on measures of memory, language and visuospatial performance, when compared to Alzheimer's disease patients (Bell et al., 2019). Furthermore, PART with dementia was originally described as being a disorder that typically affects older patients than the ones with Alzheimer's disease (Crary et al., 2014), which is supported by follow-up studies that included a higher number of cases (Besser et al., 2019; Teylan et al., 2020).

Given that Alzheimer's disease is diagnosed more than 50% of the time in PART cases with mild cognitive impairment or dementia (Teylan et al., 2019), there is a need for in vivo diagnostic tools to differentiate PART from other dementias during life, particularly Alzheimer's disease, by assessing the cognitive domains involved, cerebrospinal fluid (CSF) biomarkers, and brain magnetic resonance imaging (MRI) findings, in accordance with the research framework recommended by the National Institute on Aging and Alzheimer's Association (NIA-AA), specifically the AT(N) criteria (Jack et al., 2018). In line with this, brain MRI of "definite" PART patients showed an association between Braak staging and atrophy of the left head of the hippocampus, which was correlated with the preservation of episodic memory (Josephs et al., 2017b). Moreover, MRI of "definite" PART participants showed a correlation between Braak staging and aging with atrophy of the medial temporal lobe (Quintas-Neves et al., 2019). Despite these results, few studies have assessed the relationship between brain MRI and neuropathological findings of patients with PART and Alzheimer's disease.

Here, we compared the in vivo brain MRI findings with neuropathological findings in patients with definite PART (i.e., BRAAK stage higher than 0 and CERAD = 0) and Alzheimer's disease (i.e., CERAD = 1–3), using visual rating regional atrophy scales (Harper et al., 2016). Additionally, we assessed the relationship between brain atrophy and the degree of clinical impairment in all groups, based on CDR metrics (Morris, 1993) and neuropsychological testing (Weintraub et al., 2018).

2. Methods

2.1. Participants

Data was obtained from the National Alzheimer's Coordinating Center (NACC), a repository for data collected at the Alzheimer's Disease Centers (ADCs) located across the United States of America. Such ADCs collect standardized clinical data via the Uniform Data Set (UDS) and neuropathological evaluations obtained at autopsy to the Neuropathology Data Set. The UDS and Neuropathology Data Set data have been described in detail (Beekly et al., 2007; Besser et al., 2018; Morris et al., 2006; Weintraub et al., 2009, 2018).

2.2. Selection criteria

Our sample was obtained from the September 2019 data freeze (n = 38,836 patients), which included 4192 patients with clinical UDS data within 2 years from death and neuritic plaque (NP) burden assessed at autopsy. At this point, all UDS visits of participants with MRI scans performed no more than 4 years before the date of death and who had neuropathology data available were collected (n = 334 patients); only the last UDS visit and respective brain MRI scan before death were considered for the analysis. We excluded participants: (a) with neuropathological evidence of frontotemporal lobar degeneration, Lewy body disease, amyotrophic lateral sclerosis, prion disease, or argyrophilic grains; (b) with clinical evidence of dementia with Lewy bodies, Parkinson disease, Down syndrome, Huntington disease, prion disease, corticobasal degeneration, or progressive supranuclear palsy; (c) with other brain lesions that biased atrophy assessment (e.g., brain tumor; brain herniation; vascular malformation; lymphocytic meningoencephalitis; traumatic brain injury; demyelinating disease). Patients with a BRAAK stage of 0 (without evidence of neurofibrillary tangles), and a simultaneous CERAD score of 0 (absence of neuritic plaques on autopsy) were excluded. With the application of these exclusion criteria, 233 participants remained (Table 1). PART patients were defined as having a higher BRAAK stage than 0, considered as having neuropathological evidence of varying degrees of neurofibrillary tangles, and a CERAD score of 0 (absence of neuritic plaques).

2.3. Neuropathology data

As referred above, the neuropathological data was collected by the ADCs by using a standardized Neuropathology Form on those patients who died and consented to autopsy and neuropathologic examination. With such data, participants were categorized according to the Braak stage for neurofibrillary degeneration and CERAD stage. TAR DNA-binding protein 43 (TDP-43) data was considered in a small subset of cases that had been assessed by the ADCs. Details on brain tissue preparation and staining within the NACC Neuropathology dataset have been previously described (Besser et al., 2018).

2.4. Brain MRI data

The MRI examinations were performed on 1.5T or 3T scanners, both from Philips, Siemens, or GE manufacturers. Although there were several imaging protocols performed by different centers, for our imaging analysis we used T1-weighted acquisitions in order to grade the degree of regional brain atrophy.

2.5. Image analysis

We previously applied validated visual rating scales to assess brain atrophy of the following regions: anterior cingulate, orbitofrontal, anterior temporal, frontoinsular, medial temporal, and posterior regions (Quintas-Neves et al., 2019). Here we define atrophy as cross-sectional, corresponding to the score attributed on the basis of these rating scales. As previously described by the simplified version: orbitofrontal (OF) and anterior cingulate (AC) regions were rated on the first anterior slice where the corpus callosum becomes visible; the frontoinsular (FI) was rated over three slices, starting on the first anterior slice where the anterior cingulate becomes visible and moving posteriorly; the anterior temporal (AT)

Table 1
Characterization of patients according to the density of neocortical neuritic plaques (CERAD score)

	PART	AD spectrum			
	CERAD 0 (None) (n = 32)	CERAD 1 (Sparse) (n = 25)	CERAD 2 (Moderate) (n = 76)	CERAD 3 (Severe) (n = 100)	p
Male sex, n (%)[a]	24 (75)	11 (44.0)	48 (63.2)	64 (64.0)	X^2 (3) = 11.34; p = 0.01
Age at death, mean (SD)[b]	79.0 (±11.06)	87.7 (±6.29)	82.2 (±8.84)	77.4 (±11.15)	$F(3, 229) = 8.464$, $p < 10^{-3}$
Age at last MRI, mean (SD)[c]	77.2 (±11.3)	85.9 (±5.75)	80.1 (±8.75)	75.0 (±11.1)	$F(3, 229) = 9.95$, $p < 10^{-3}$
Age MRI-death, mean (SD)[d]	2.0 (±1.05)	1.8 (±1.40)	2.1 (±1.18)	2.4 (±1.14)	$F(3, 229) = 2.557$, $p = 0.06$
CDR-SB[e]	6.6 (±5.54)	3.8 (±4.83)	5.9 (±4.57)	8.5 (±4.24)	$F(3, 229) = 9.77$, $p < 10^{-3}$
Global CDR[e]	1.2 (±0.89)	0.7 (±0.8)	1.1 (±0.75)	1.4 (±0.73)	$F(3, 229) = 8.529$, $p < 10^{-3}$
Braak stage, n (%)[f]					
None	0 (0)	0 (0.0)	1 (1.3)	0 (0.0)	
I	14 (43.8)	3 (12.0)	4 (5.3)	1 (1.0)	
II	12 (37.5)	8 (32.0)	10 (13.2)	0 (0.0)	
III	3 (9.37)	8 (32.0)	13 (17.1)	2 (2.0)	
IV	3 (9.37)	4 (16.0)	18 (23.7)	8 (8.0)	
V	0 (0.0)	2 (8.0)	17 (22.4)	24 (24.0)	
VI	0 (0.0)	0 (0.0)	13 (17.1)	65 (65.0)	
Braak stage, mean (SD)	1.8 (±0.95)	2.8 (±1.13)	3.9 (±1.5)	5.5 (±0.86)	$F(3, 229) = 100.5$, $p < 10^{-3}$

The table shows the summarized demographic characteristics of a total cohort of 245 patients, separated according to PART (CERAD 0 and BRAAK stage higher than 0) or AD spectrum with presence (CERAD 1—mild; CERAD 2—moderate; CERAD 3—severe) of neocortical neuritic plaques after neuropathological evaluation.
*$p < 0.05$ considered as significant for one-way ANOVA or χ^2 test, as appropriate.
[a]Male sex refers to the absolute mean and relative percentage of male patients in a given group, represented as n (%).
[b]Age at death is the subject age at the time of death.
[c]Age at last MRI is the subject age at the time the last MRI was performed.
[d]Age MRI-death is the difference between the subject age at the last performed MRI and time of death. These three variables are reported in years as [a] continuous variable with mean and standard deviation (SD).
[e]CDR-SB refers to the sum of boxes score from the CDR Dementia Staging Instrument and global CDR refers to the global Clinical Dementia Rating [s]core; they are both attributed to the subject in the last clinical visit and are also reported as continuous variables with mean and standard deviation.
[f]For each Braak stage (from none to VI) values are represented as number of cases and percentage of total. Data presented as n (%) and mean (±SD).

was rated at the level of the temporal pole, just anterior to where the "temporal stem" connects the frontal and temporal lobes; the medial temporal was rated according to the medial temporal lobe atrophy (MTA) score—performed on the hippocampus at the level of the anterior pons; the posterior region (Post) was rated according to the four-point posterior atrophy scale described by Koedam (Koedam et al., 2011)—overall score based on the presence of atrophy in sagittal (widening of the posterior cingulate and parieto-occipital sulcus, and atrophy of the precuneus on left and right by considering paramedian sagittal images), axial (widening of the posterior cingulate sulcus and sulcal dilatation in parietal lobes on axial images) and coronal (widening of the posterior cingulate sulcus and parietal lobes on coronal images) orientations, assessed for left and right separately (Harper et al., 2016). Two independent classifiers with 7 years and 4 years, respectively, of experience in clinical neuroradiology were responsible for rating the images. Visual raters were blind to clinical diagnosis. For each brain region scale, the average of both hemispheres was calculated and an average of both classifiers was used. In order to aid the rating process, reference images for each rating scale were provided to the classifiers based on Harper et al. (Harper et al., 2016).

2.6. Neuropsychological assessment

Local ADCs assessed participants using the CDR and the UDS version 2 neuropsychological test battery (Weintraub et al., 2009). Here, we used the global CDR, CDR-SB, and neuropsychological tests conducted at the last UDS visit prior to death. The so-called Washington University CDR was reviewed by Morris and collaborators in 1993. (Morris et al., 1993) with the purpose of staging the severity of Alzheimer's disease, and takes into consideration the following six cognitive categories: memory, orientation, judgment and problem solving, community affairs, home and hobbies, and personal care; it is based on a five point scale in which none = 0, questionable = 0.5, mild = 1, moderate = 2, and severe = 3. The global CDR is calculated using a proprietary algorithm according to clinical scoring rules, with CDR 0 = no dementia, CDR 0.5 = questionable dementia, CDR 1 = mild dementia, CDR 2 = moderate dementia and CDR 3 = severe dementia. The CDR-SB is calculated by summing the ratings of each of the six cognitive domains and it reflects a more quantitative global measure; it ranges from 0 (normal) to 18 (severe dementia) (O'Bryant et al., 2008). Several other tests of memory, executive function, language and processing speed were considered in our analysis. Executive function was assessed by the Trail Making Test (TMT) A and B, which globally tests attention, visual scanning and search skills, and psychomotor speed and coordination (Reitan, 1955); TMT A can independently assess processing speed, while TMT B assesses set switching; on both parts of this test (i.e., A and B), the total number of seconds to complete the test, the number of commission errors, and number of correct lines were recorded; the Wechsler Adult Intelligence Scale digit symbol test (WAIS) was also considered to provide an estimate of processing speed (Wechsler, 1939). Semantic memory/language was assessed by category (vegetables and animals) verbal fluency (Lezak and Lezak, 2004), consisting of a test on registering the total number of vegetables and animals named in 60 s; the Boston naming test (Kaplan et al., 1983), which also assesses the effect of language function, more precisely the confrontational word retrieval, was included in this evaluation, and consisted of showing pictures (up to 60) to the patient, and wait up to 20 seconds for the patients to name them. Attention and working memory was evaluated by Digit span forward (DSF) and

backward test (DSB) (Jensen and Figueroa, 1975), consisting on registering the ability of recalling a sequence of numbers shown, and the total length of numbers successfully achieved (DSF L and DSB L, respectively). Logical memory was evaluated using Logical Memory Immediate and Delayed Recall tests (Logical Mem; Mem Unit), in which an orally presented verbal story is asked to be recalled immediately and 20 minutes after (Abikoff et al., 1987). Mini-Mental State Examination (MMSE) (Folstein et al., 1975) was performed as a brief cognitive screening instrument that provides a measure of global cognition.

2.7. Statistical analysis

We divided our data into four groups of participants according to the CERAD score (i.e., density of neocortical neuritic plaques): CERAD 0 (None); CERAD 1 (Sparse); CERAD 2 (Moderate); CERAD 3 (Severe); "definite" PART being considered CERAD 0. To assess potential differences between these groups in terms of baseline characteristics, one-way analysis of variance (ANOVA) was performed, followed by a Tukey post hoc analysis whenever these characteristics were significantly different between groups ($p < 0.05$). With the purpose of assessing the rating acuity between both classifiers, Spearman's correlation coefficient was calculated for the pair of classifiers per each region, and no significant differences were found between each observer. The standardized residuals for age and Braak were calculated after linear regression for sex, age difference at MRI and death and BRAAK staging or age at MRI, respectively. Correlation data analysis for regional brain atrophy scores and CDR-SB score for groups with absent (i.e., definite PART) versus present (i.e., Alzheimer's disease) neuritic plaques was performed using the linear regression model and Pearson correlation coefficients and values expressed as (R) and statistically significant values considered for $p < 0.05$. Moreover, multiple linear regression was used to compare slopes between groups for each brain area with CDR-SB as a continuous independent variable. Z-scores for each neuropsychological test were calculated by subtracting the score from the mean test score among cognitively unimpaired participants and dividing it by the standard deviation. Tests were then grouped by cognitive domains (i.e., episodic memory, attention, language/semantic memory, executive function) (Teylan et al., 2020), which were established by (Hayden et al., 2011) using factor analysis. Tests within a cognitive domain were averaged to calculate a domain z-score. A global composite score was created by averaging the domain z-scores (Global). These were then correlated with the residuals of the visual rating scores for each brain region after linear regression with age, in PART and Alzheimer's disease using the Pearson coefficient. SPSS Statistics version 26, and GraphPad Software version 9.0.0 were used for Figs. 1 and 2, and RStudio Version 1.4.1103 was used for Figs. 3 and 4.

2.8. Standard protocol approvals, registrations, and patient consents

All participants provided written informed consent at each local ADC, and the study protocols were approved by the respective institutional review boards. The participants that contributed to the Neuropathology Data Set gave consent for autopsy. All participants provided written informed consent at each ADC.

2.9. Data availability

The datasets used and/or analyzed during the current study are available upon request on the NACC database.

3. Results

About 233 participants were included in this study: 32 with no ("definite" PART—CERAD 0 and BRAAK stage higher than 0), 25 with sparse ("possible" PART or mild Alzheimer's disease—CERAD 1), 76 with moderate (CERAD 2), and 100 with severe (CERAD 3) neuritic plaques. There was a global male predominance among groups (more than 50%), with significant changes in sex proportions across groups due to the Alzheimer's disease spectrum CERAD 1 group, where we found a slight female preponderance (Table 1). The mean age at death was significantly lower for groups CERAD 0 and 3 (79.0 ± 11.06 and 77.4 ± 11.15 years old, respectively), and higher for group CERAD 1 (87.7 ± 6.29 years old) (Table 1). Braak staging was also statistically different between groups, with a predominance of lower grades (Braak - I and II) in PART and higher grades (Braak - V and VI) in the Alzheimer's disease spectrum CERAD 3 cases (Table 1). The global CDR and CDR-SB were significantly higher for the Alzheimer's disease spectrum CERAD 3 group (1.4 ± 0.73 and 8.5 ± 4.24, respectively) (Table 1 and Supplementary Table 1).

After calculating the standardized residuals for age, sex and difference between age of death and age at MRI, there was a statistically significant higher brain atrophy on the AT in CERAD 3 versus CERAD 1 ($p < 0.01$; diff = 0.74; 95%CI [0.18; 1.31], Fig. 1C). There was a nonsignificant trend for higher atrophy in PART versus Alzheimer's disease spectrum cases with CERAD 1 ($p = 0.08$; diff = −0.63; 95%CI [−1.30; 0.04], Fig. 1C). In MTA, brain atrophy was higher in CERAD 3 versus CERAD 2 ($p < 0.01$; diff = 0.47; 95%CI [0.089; 0.84], Fig. 1E) and CERAD 3 versus CERAD 1 ($p < 0.01$; diff = 0.87; 95%CI [0.31; 1.42], Fig. 1E). There was also a nonsignificant trend in Alzheimer's disease spectrum with CERAD 3 versus PART ($p = 0.06$; diff = 0.49; 95%CI [−0.013; 0.99], Fig. 1E). For the other regions, there were no significant differences in relative atrophy between groups (Fig. 1A, B, D, F). Upon correction for Braak stage, the AT region showed a nonsignificant trend for higher brain atrophy in PART versus Alzheimer's disease spectrum cases with CERAD 1 ($p = 0.09$, diff = −0.62; 95%CI [−1.30; 0.059], Fig. 2C). For the other regions, there were no significant differences in relative atrophy between groups (Fig. 2). Since TDP-43 has been proposed to be a relevant determinant of atrophy in PART (Josephs et al., 2020), in the small subset of cases that had TDP-43 data available, we observed that indeed "TDP-43 positive / PART" showed higher relative medial temporal lobe atrophy compared to the "TDP-43 negative / PART" group ($p < 0.01$; diff = 53.03; 95%CI [10.85; 95.21]; Supplementary Fig. 1). On the other hand, we do not find statistically significant differences for the Alzheimer's disease group.

After computing the correlation between regional brain atrophy scores and CDR-SB scores for PART (CERAD 0) and Alzheimer's disease (CERAD 1–3) (Fig. 3A–F), significant correlations were found between CDR-SB and relative atrophy in all the brain regions evaluated in patients with Alzheimer's disease ($R = 0.2$, $p = 0.0045$; $R = 0.17$, $p = 0.016$; $R = 0.3$, $p = 1.4e{-}05$; $R = 0.29$, $p = 3.9e{-}05$; $R = 0.3$, $p = 1.3e{-}06$; $R = 0.34$, $p = 7.3e{-}0.7$; for AC, OF, AT, FI, medial temporal and posterior regions, respectively). On the other hand, patients with PART showed no significant correlations between relative regional brain atrophy and CDR-SB ($R = 0.23$, $p = 0.2$; $R = 0.24$, $p = 0.19$; $R = -0.07$, $p = 0.7$; $R = 0.015$, $p = 0.94$; $R = 0.034$, $p = 0.85$; $R = -0.12$, $p = 0.52$; for AC, OF, AT, FI, medial temporal, and posterior regions, respectively). Moreover, significant differences were found between the regression lines of both groups in the AT and posterior regions (Fig. 3; Supplementary Table 2). After correcting for age, brain atrophy scores were correlated with z-scores for the neuropsychological tests. We found that AD shows a widespread pattern of negative correlations

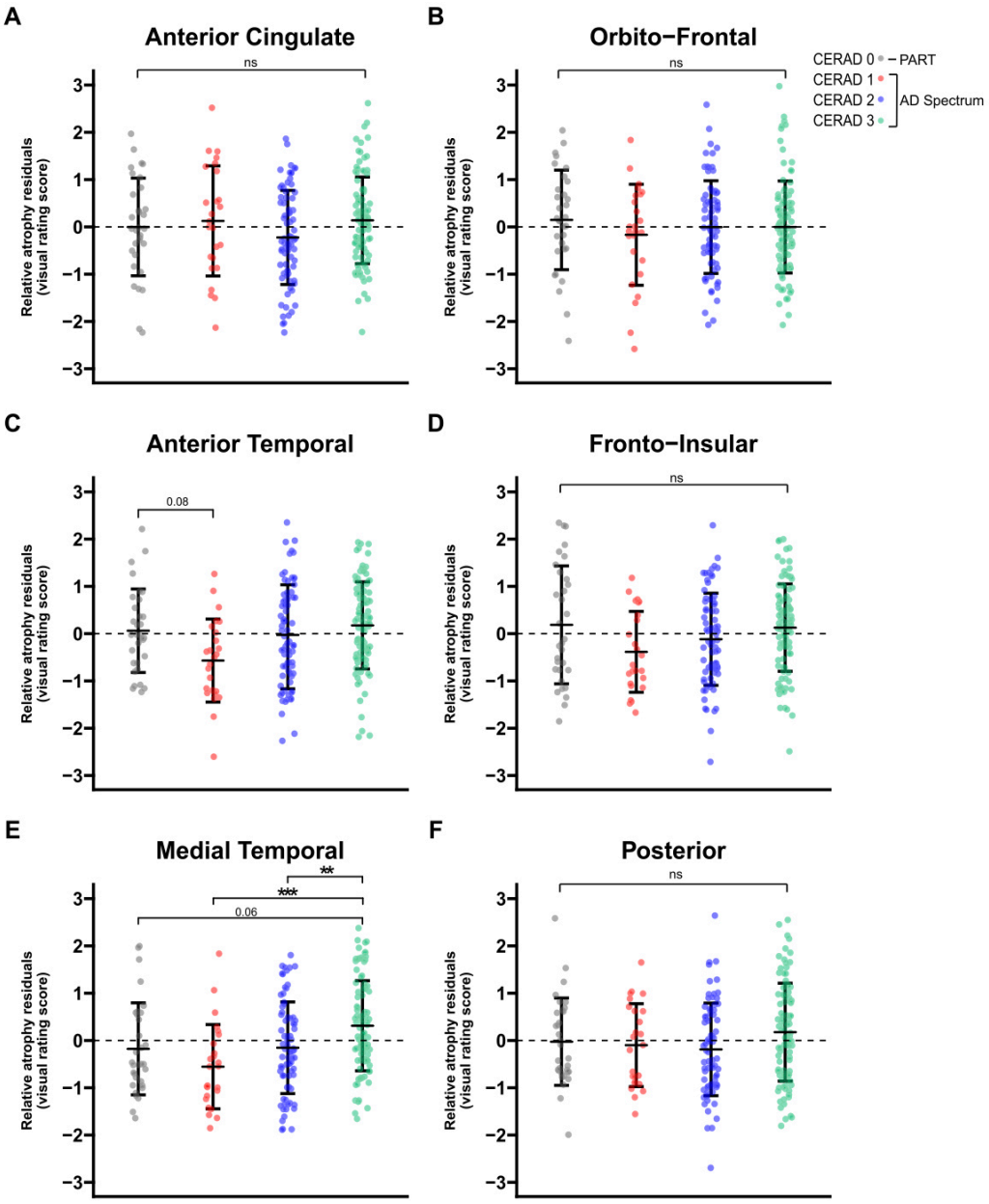


Fig. 1. Age-c relative regional brain atrophy shows differential patterns in PART and Alzheimer's disease spectrum CERAD groups. Standardized residuals corrected for age for each specific region of brain atrophy among 4 groups of participants, distributed according to PART (CERAD 0 and BRAAK stage higher than 0) or Alzheimer's disease spectrum with presence (CERAD 1—mild; CERAD 2—moderate; CERAD 3—severe) of neocortical neuritic plaques after neuropathological evaluation. The regions evaluated are (A) anterior cingulate, (B) orbitofrontal, (C) anterior temporal, (D) frontoinsular, (E) medial temporal, and (F) posterior. * $p < 0.05$, ** $p < 0.01$, and *** $p < 0.001$. "ns" represents nonsignificant differences between groups.

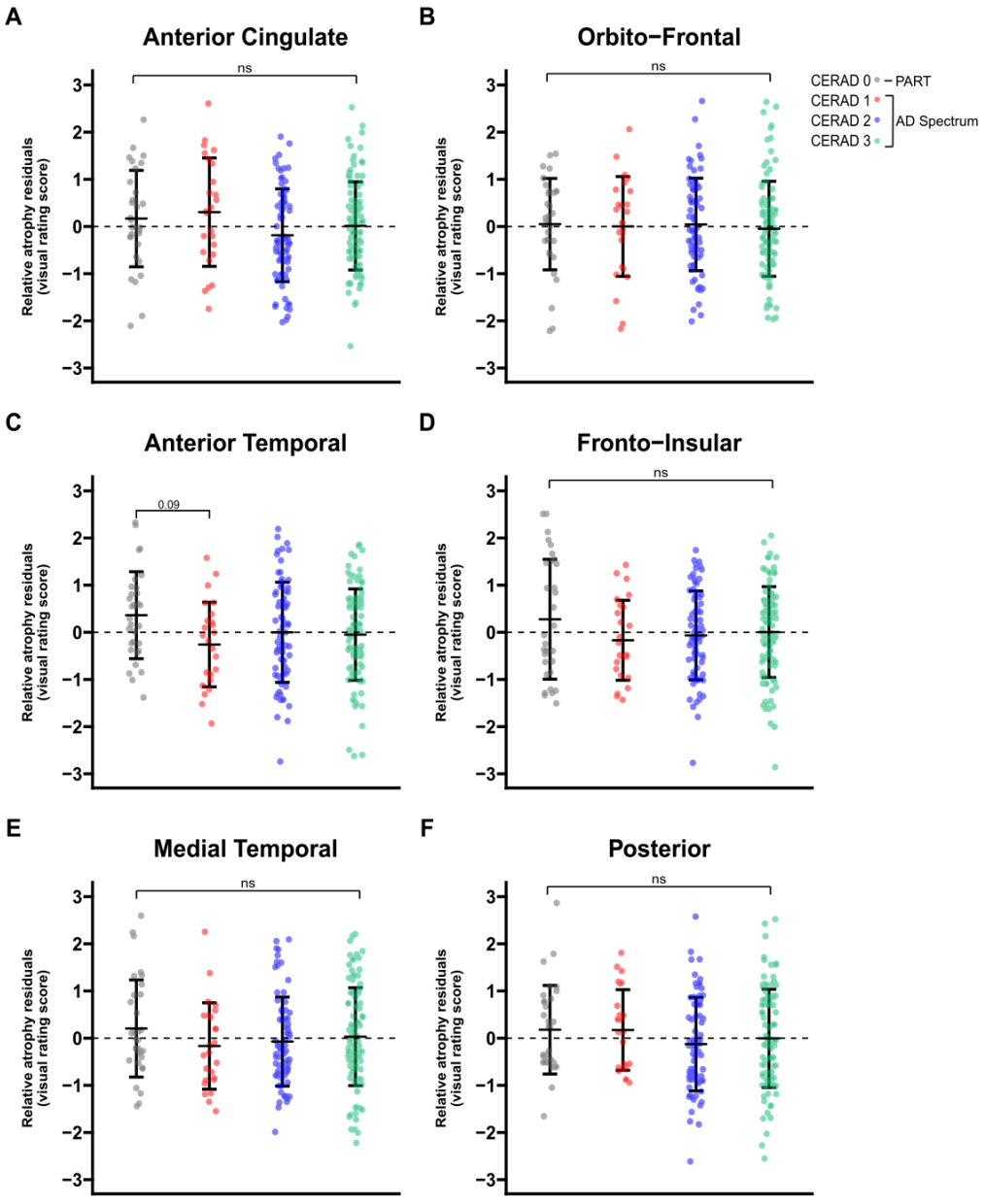


Fig. 2. Braak-corrected relative regional brain atrophy shows no significant changes in PART and Alzheimer's disease spectrum CERAD groups. Standardized residuals corrected for Braak for each specific region of brain atrophy among 4 groups of participants, distributed according to PART (CERAD 0 and BRAAK stage higher than 0) or Alzheimer's disease spectrum with presence (CERAD 1—mild; CERAD 2—moderate; CERAD 3—severe) of neocortical neuritic plaques after neuropathological evaluation. The regions evaluated are (A) anterior cingulate, (B) orbitofrontal, (C) anterior temporal, (D) frontoinsular, (E) medial temporal, and (F) posterior. * $p < 0.05$. "ns" represents nonsignificant differences between groups.

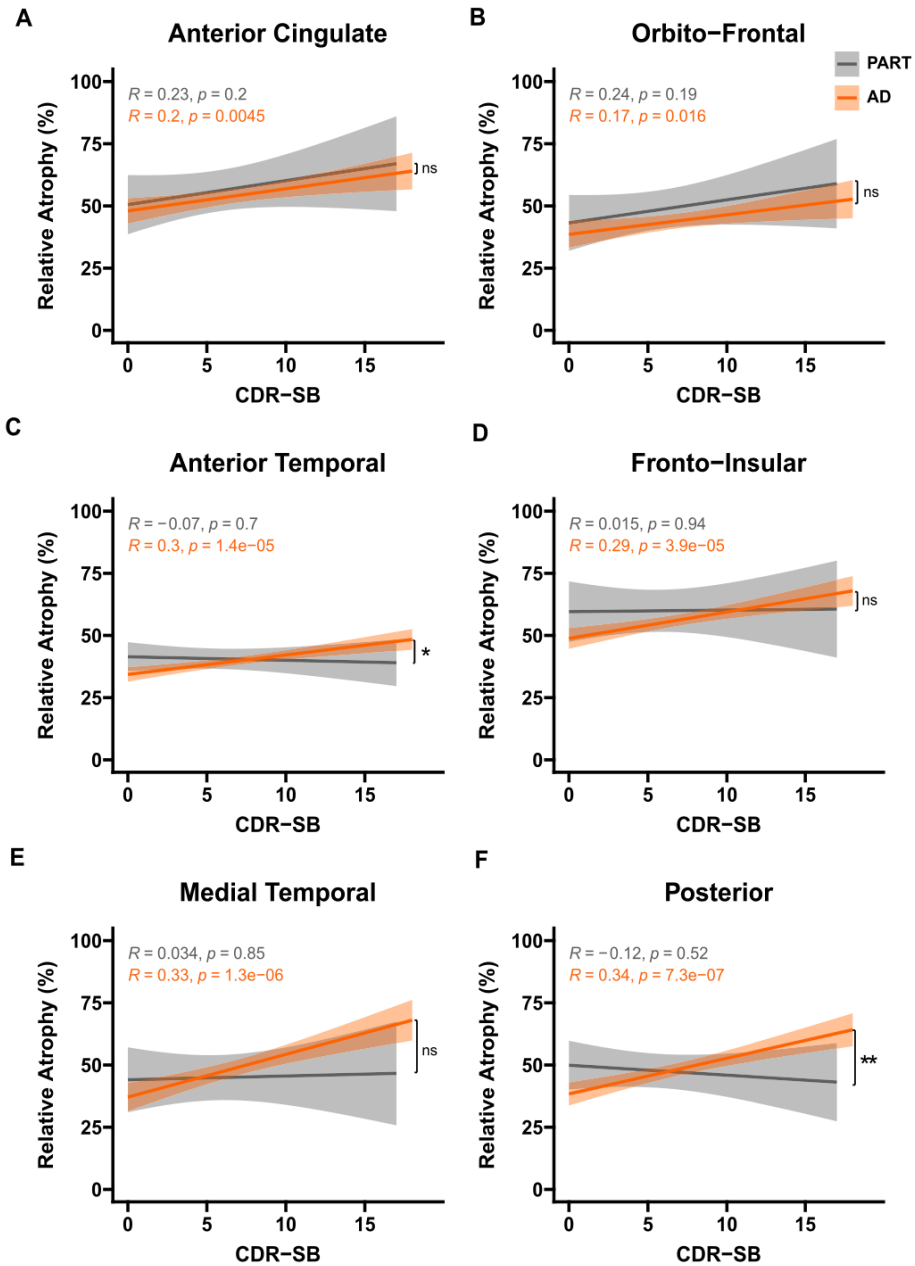


Fig. 3. Correlation analysis between relative regional brain atrophy and CDR shows differential patterns in Alzheimer's disease and PART. Pearson correlation analysis and linear regressions of relative brain atrophy per region versus CDR Dementia Staging Instrument (CDR) Sum of Boxes among 2 groups of participants, distributed according to the absence (PART) or presence (Alzheimer's disease) of neocortical neuritic plaques after neuropathological evaluation. The regions evaluated are (A) anterior cingulate (AC), (B) orbitofrontal (OF), (C) anterior temporal (AT), (D) frontoinsular (FI), (E) medial temporal, and (F) posterior. Correlation coefficients (*R*). *p* values of the correlation analysis considered significant if $p < 0.05$. $^{*}p < 0.05$, $^{**}p < 0.01$, and $^{***}p < 0.001$ represent statistically significant differences between the regression lines of both groups in multiple linear regression. "ns" represents nonsignificant differences between the regression lines of both groups.

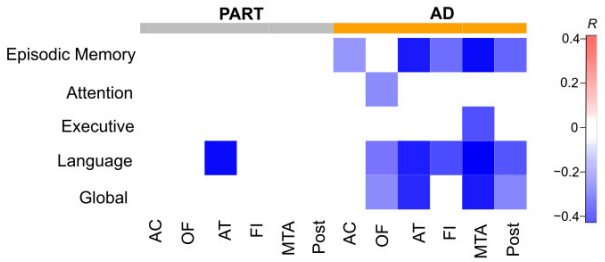


Fig. 4. Correlation analysis between relative regional brain atrophy and neuropsychological assessment shows differential patterns in Alzheimer's disease and PART. Pearson correlation analysis of relative brain atrophy residuals after linear regression with age per region versus *z*-scores of neuropsychological test composites among 2 groups of participants, distributed according to the absence (PART) or presence (Alzheimer's disease) of neocortical neuritic plaques after neuropathological evaluation. Only showing pairs with $p < 0.05$ in the correlational analysis. Color indicates *R*Pearson coefficient. Anterior cingulate (AC), orbitofrontal (OF), anterior temporal (AT), frontoinsular (FI), medial temporal (MT), and posterior (Post).

between regional atrophy and z-scores of most neuropsychological tests (Fig. 4; Supplementary Fig. 2). On the other hand, PART showed a specific negative correlation between AT atrophy and z-scores on the Boston naming test ($R = -0.554$, $p = 0.003$; Supplementary Fig. 2), which is reflected on the language composite score ($R = -0.397$; $p = 0.045$; Fig. 4). When comparing the z-scores between PART and AD, the latter group is more deeply affected in practically all tests, but not in the language composite (Table S3).

4. Discussion

The main goal of this study was to compare in vivo brain MRI findings of PART and Alzheimer's disease participants using previously validated visual rating scales that are commonly deployed in clinical settings (Harper et al., 2016). Additionally, we assessed the relationship between brain atrophy and the degree of clinical impairment, based on CDR-SB. Our results suggest that while Alzheimer's disease participants show a stepwise increase in relative age-corrected atrophy in the medial temporal lobe region with increasing CERAD scores (1 to 3), PART cases present intermediate relative atrophy levels (Fig. 1). A similar nonsignificant trend was also observed for AT regions (Fig. 1). Since there has been debate whether PART is a pre-Alzheimer's disease condition (Duyckaerts et al., 2015; Weigand et al., 2020), these findings indicate that PART could be an independent pathologic process from Alzheimer's disease (Bell et al., 2019; Besser et al., 2019; Crary et al., 2014; Josephs et al., 2020; Teylan et al., 2019, 2020).

Overall, "definite" PART patients (i.e., CERAD 0 and BRAAK stage higher than 0) showed higher mean relative age-corrected atrophy than CERAD 1 group (i.e., sparse NP—"possible" PART / mild Alzheimer's disease) in all brain regions evaluated, and lower mean relative age-corrected atrophy than the CERAD 3 group (i.e., advanced Alzheimer's disease) in the medial temporal region. This supports a more benign nature of this pathology when compared to severe Alzheimer's disease, but more severe when compared to mild Alzheimer's disease. It is interesting to observe that CERAD 1 cases are older at death, have a slight female preponderance and have lower levels of age-corrected relative atrophy when compared to the other pathological groups. This is in accordance with recent observations that show that disease onset at a younger age tends to be associated with more advanced pathology (Jack et al., 2020; Vogel et al., 2021; Whitwell et al., 2019). This suggests that CERAD 1, also considered "possible PART" by some authors, could be the basis to identify a state of Alzheimer's disease pathology resistance, while CERAD 0, corresponding to "definite PART," could represent an entirely different pathological process.

Given that NPs are only present in mild Alzheimer's disease, other pathophysiological mechanisms might explain this difference, such as deposition of TDP-43. This protein was first described in 2006 as a main component of the ubiquitinated inclusions found at autopsy of patients with frontotemporal lobar degeneration (FTLD) (Neumann et al., 2006). Over time, it has been described to be present in several other pathologies (so-called TDP-43 proteinopathies), and can be divided in two groups: primary and mixed (i.e., secondary). PART and Alzheimer's disease are considered within the mixed group. In Alzheimer's disease, TDP-43 has been found to be associated with worse memory loss (Josephs et al., 2014), atrophy of the hippocampus (Josephs et al., 2014), and faster rates of hippocampal atrophy (Josephs et al., 2017a). Concomitantly, in patients with PART, TDP-43 is strikingly associated with amygdala and hippocampal atrophy (Josephs et al., 2019), which supports TDP-43 as being associated with temporal lobe atrophy across the entire range of Aβ and NFT deposition. Interestingly, in PART patients, there seems to be a topographic predilection for TDP-43 accumulation, as more inclusions were found in the atrophic left anteromedial temporal lobe region, compared to the right (Josephs et al., 2019). This is different from what is found in Alzheimer's disease patients, where a bilateral pattern of atrophy is associated with TDP-43 (Josephs et al., 2014), and similar to what is found in FTLD type C, a disorder clinically associated with semantic dementia, as seems to be the case with PART (Josephs et al., 2017b; Quintas-Neves et al., 2019). Moreover, high TDP-43 levels in PART was associated with smaller brain volumes, faster rates of brain atrophy and acceleration of atrophy rates, more than a decade prior to death, with deceleration occurring closer to death, particularly in the hippocampus compared to neocortical regions (Josephs et al., 2020). Additionally, TDP-43 and brain atrophy association in PART occurred 3 years later than in Alzheimer's disease (Josephs et al., 2020). Even though we were only able to analyze the impact of TDP-43 in a small subset of cases, our data further supports that TDP-43 contributes to atrophy in PART, but to a lesser extent in Alzheimer's disease. Overall, these observations suggest that tau (i.e., Braak stage) and TDP-43 contribute differently to the rate of brain atrophy over time in patients with PART or Alzheimer's disease.

Globally, after controlling for Braak, we found no major differences in the mean relative atrophy of the several regions evaluated between the four groups, suggesting that atrophy patterns are mainly Braak-dependent (i.e., dependent on the NFT deposition grade) and nondependent of the Aβ deposition. Since correcting for the effect of Braak staging globally nullifies the differences between PART and Alzheimer's disease spectrum CERAD 1–3 groups,

these observations remarkably confirm the widely known correlation between tau NFTs with regional brain atrophy and cognitive deficits, when compared to Aβ plaque distribution (Nelson et al., 2012). In the AT region, we found a nonsignificant trend for higher atrophy in "definite" PART versus the CERAD 1 group. This an interesting finding, which could be partially explained by the fact that Braak staging does not consider the most anterior part of the temporal lobe for grading (Braak and Braak, 1991). The fact that PART patients show a level of atrophy comparable to higher CERAD levels indicates that tau itself can exert neurodegenerative effects in PART without the concomitant presence of neuritic plaques. This is in agreement with animal studies showing increased brain atrophy in mice overexpressing human tau and in patients with tauopathy conditions (Wang and Mandelkow, 2016).

Interestingly, patients diagnosed with PART and dementia were previously shown to be older (eighth to ninth decades) than Alzheimer's disease patients, making unlikely the Aβ deposition starting at that point (Crary, 2016; Crary et al., 2014). In our study, patients with PART presented a mean age at death significantly lower than the sparse (CERAD 1) group and not significantly different from the moderate (CERAD 2) and severe (CERAD 3) groups. Moreover, despite not being older than the CERAD 1 and 2 groups, there was a tendency for PART patients to die at the same age (77.1 $\pm$ 12.4) as patients with severe Alzheimer's disease (77.4 $\pm$ 11.2). It has been shown that PART patients have slower cognitive decline than Alzheimer's disease patients across multiple neuropsychological domains (Teylan et al., 2020). Additionally, both "definite" and "possible" PART patients exhibit longitudinal cognitive decline that increases in severity with higher levels of NFT pathology (Jefferson-George et al., 2017).

The previously mentioned differences in the patterns of atrophy between PART and Alzheimer's disease patients are potentially important, as it has been described that, although clinicians recognize a distinction in the clinical presentation between Alzheimer's disease and PART, diagnosing Alzheimer's disease less frequently in patients with PART, clinical Alzheimer's disease can be diagnosed more than 50% of the time in PART patients with mild cognitive impairment or dementia (Teylan et al., 2019). This clinical remark makes brain MRI an important tool to differentiate PART from Alzheimer's disease, or to follow longitudinally PART patients identified by other biomarkers such as CSF or PET. However, given the scarcity of PART patients with Braak stages of III and IV, this is something to be tackled by future studies. We believe that in order to validate MRI as a clinical routine tool to use in PART patients, an easy to apply and practical visual rating scale could be a relevant tool to be used. Importantly, our results are globally in accordance with what others observed using volumetric approaches (Josephs et al., 2017b).

PET studies assessing in vivo Aβ and tau deposition are overall in agreement with our results showing that concomitant Aβ and tau pathology synergizes to lead to higher levels of brain atrophy and worse clinical outcome (Jack et al., 2019; Weigand et al., 2020). However, these studies do not segregate Aβ deposition, as performed for the CERAD staging. In the present study, we identified different pathological characteristics based on different CERAD stages, and in light of recent observations in PET-MRI studies that there are 4 subtypes of tau spreading patterns that also differ in their clinical characteristics (Vogel et al., 2021), it would be interesting to assess how these CERAD stages correlate with those identified tau pathology subtypes, that challenge the concept of "typical Alzheimer's disease."

Studies that assessed cognitive status using the CDR scoring system found that within the same stratum of CDR scores, individuals with PART had relative sparing of semantic memory/language in comparison to Alzheimer's disease (Besser et al., 2019). Moreover, participants with Alzheimer's disease had a significantly steeper decline after becoming clinically symptomatic than those with PART (Teylan et al., 2020). Our results showed that overall cognition deficits (given by CDR-SB) are directly correlated with regional atrophy in patients with Alzheimer's disease, but not in patients with PART (Fig. 3A–F). Additionally, we observe significant differences between the regression lines of both groups (i.e., PART vs. Alzheimer's disease) for the AT and posterior regions. These results indicate that PART and Alzheimer's disease show different atrophy patterns, which correlate poorly with global cognitive deficits in patients with PART. This is in accordance with the previously mentioned steeper decline that Alzheimer's disease patients experience, when compared to PART (Teylan et al., 2020). This dissociation might be due to other comorbid pathologies that were shown to contribute to cognitive impairment in patients with PART, such as cerebrovascular disease (Fulcher et al., 2014). Therefore, in the future, it would be relevant to identify and characterize how brain MRI markers of vascular pathology affect the brains of patients with PART.

Additionally, our results focusing on a broader neuropsychological assessment show a focal deficit of language in PART correlating with AT atrophy, whereas in AD we find widespread correlations between regional atrophy and cognitive deficits. This is in accordance with our previous study showing that the anterior temporal region in PART correlates with semantic memory/fluency tests (Quintas-Neves et al., 2019) and other reports showing longitudinal semantic cognitive decline (Jefferson-George et al., 2017) and higher deficits in PART compared to neuropathology negative controls (Weigand et al., 2020). Importantly, the more widespread and differential pattern of cognitive impairment in Alzheimer's disease is in line with the literature (Savola et al., 2021; Teylan et al., 2020; Weigand et al., 2020).

This study had important limitations. First, it was based on a convenience, autopsy-based sample, which limits its extrapolation. The NACC database has limitations in its generalizability, given that participants tend to be more often Caucasian and more affluent than the general population. However, there was no additional selection bias of the participants considered in our sample, as we chose all eligible participants with neuropathologically defined PART or Alzheimer's disease who had an MRI available at most 4 years before death. Second, the use of visual rating scales, even when performed by trained neuroradiologists, is associated with interobserver variability. However, with training and neuroradiologic experience, using a reference visual scale during the rating process reduces this bias effect. Third, the variability in scanner manufacturers and field strengths were potential sources of biases/variability. Fourth, the patients included in our sample had incomplete clinical information on other co-morbidities that could be associated with brain atrophy, such as hypertension or dyslipidemia, or on other neuropathologic features, such as TDP-43 pathology. Fifth, Braak staging is considered an incomplete measure of tau burden and it would be beneficial to have additional quantitative measures of such parameter. However, this requires additional special staining, a process that is time-consuming and not currently performed at most centers. Furthermore, it is not available in the NACC neuropathology database (Neltner et al., 2012; Walker et al., 2017). Finally, the retrospective nature of the study is also a potential source of bias. For instance, since the only difference in selecting the participants was having performed an MRI scan, we hypothesize this contingency in patient selection, could partially explain the discrepancies in the age at death comparing with other studies using the NACC database (Teylan et al., 2019). Despite the aforementioned limitations, this study has several major strengths: the use of multicentric data on a large group of individuals across the USA, the constantly performed standard-

ized process of collecting global CDR (among other clinical variables) in every UDS visit, the use of standardized neuropathological criteria to assess pathology at autopsy (Montine et al., 2016), the preferential use of volumetric acquisitions, and a relevant number of participants with PART and Alzheimer's disease.

In conclusion, the findings of this study support the hypothesis that PART is a separate pathological process from the Alzheimer's disease "continuum." Future studies should address and expand: the independent or cumulative impact of Aβ, tau and other aggregates, such as TDP-43, on brain regional atrophy, using cases of Alzheimer's disease, PART and, eventually, the recently proposed pathological entity limbic-predominant age-related TDP-43 encephalopathy (LATE) (Nelson et al., 2019). Finally, the characterization of PET and CSF findings in symptomatic and asymptomatic PART patients could provide diagnostic biomarkers to follow their longitudinal evolution.

Disclosure statement

The authors report no conflicts of interest.

Authors' contributions

T.G.O. and J.F.C. conceived the idea. T.G.O., J.F.C., C.M., F.A., R.M., M.A.T., and M.Q. designed and planned the analysis. T.G.O. and M.Q. performed neuroimaging analysis. W.A.K., C.M., and MAT contributed with subject data.

T.G.O., M.Q., R.M., and F.A. conducted data analysis. T.G.O., M.Q., and F.A. wrote the manuscript. All authors reviewed and corrected the manuscript. All authors read and approved the final manuscript.

Acknowledgements

The NACC database is funded by NIA/NIH Grant U01 AG016976 and U24 AG072122. NACC data are contributed by the NIA-funded ADCs: P30 AG019610 (PI Eric Reiman, MD), P30 AG013846 (PI Neil Kowall, MD), P30 AG062428-01 (PI James Leverenz, MD) P50 AG008702 (PI Scott Small, MD), P50 AG025688 (PI Allan Levey, MD, PhD), P50 AG047266 (PI Todd Golde, MD, PhD), P30 AG010133 (PI Andrew Saykin, PsyD), P50 AG005146 (PI Marilyn Albert, PhD), P30 AG062421-01 (PI Bradley Hyman, MD, PhD), P30 AG062422-01 (PI Ronald Petersen, MD, PhD), P50 AG005138 (PI Mary Sano, PhD), P30 AG008051 (PI Thomas Wisniewski, MD), P30 AG013854 (PI Robert Vassar, PhD), P30 AG008017 (PI Jeffrey Kaye, MD), P30 AG010161 (PI David Bennett, MD), P50 AG047366 (PI Victor Henderson, MD, MS), P30 AG010129 (PI Charles DeCarli, MD), P50 AG016573 (PI Frank LaFerla, PhD), P30 AG062429-01(PI James Brewer, MD, PhD), P50 AG023501 (PI Bruce Miller, MD), P30 AG035982 (PI Russell Swerdlow, MD), P30 AG028383 (PI Linda Van Eldik, PhD), P30 AG053760 (PI Henry Paulson, MD, PhD), P30 AG010124 (PI John Trojanowski, MD, PhD), P50 AG005133 (PI Oscar Lopez, MD), P50 AG005142 (PI Helena Chui, MD), P30 AG012300 (PI Roger Rosenberg, MD), P30 AG049638 (PI Suzanne Craft, PhD), P50 AG005136 (PI Thomas Grabowski, MD), P30 AG062715-01 (PI Sanjay Asthana, MD, FRCP), P50 AG005681 (PI John Morris, MD), P50 AG047270 (PI Stephen Strittmatter, MD, PhD); R01 AG054008, R01 NS095252, R01 AG060961, R01 NS086736, and the Tau Consortium (PI John F. Crary MD, PhD). This work was funded by the Portuguese Foundation for Science and Technology (FCT) - project UIDB/50026/2020 and UIDP/50026/2020.

Supplementary materials

Supplementary material associated with this article can be found, in the online version, at doi:10.1016/j.neurobiolaging.2022.04.013.

References

Abikoff, H., Alvir, J., Hong, G., Sukoff, R., Orazio, J., Solomon, S., Saravay, S., 1987. Logical memory subtest of the Wechsler Memory Scale: age and education norms and alternate-form reliability of two scoring systems. J. Clin. Exp. Neuropsychol. 9 (4), 435–448.

Beekly, D.L., Ramos, E.M., Lee, W.W., Deitrich, W.D., Jacka, M.E., Wu, J., Hubbard, J.L., Koepsell, T.D., Morris, J.C., Kukull, W.A., Centers, N.I.A.A.s.D., 2007. The National Alzheimer's Coordinating Center (NACC) database: the Uniform Data Set. Alzheimer Dis. Assoc. Disord. 21 (3), 249–258.

Bell, W.R., An, Y., Kageyama, Y., English, C., Rudow, G.L., Pletnikova, O., Thambisetty, M., O'Brien, R., Moghekar, A.R., Albert, M.S., Rabins, P.V., Resnick, S.M., Troncoso, J.C., 2019. Neuropathologic, genetic, and longitudinal cognitive profiles in primary age-related tauopathy (PART) and Alzheimer's disease. Alzheimers Dement. 15 (1), 8–16.

Besser, L.M., Crary, J.F., Mock, C., Kukull, W.A., 2017. Comparison of symptomatic and asymptomatic persons with primary age-related tauopathy. Neurology 89 (16), 1707–1715.

Besser, L.M., Kukull, W.A., Teylan, M.A., Bigio, E.H., Cairns, N.J., Kofler, J.K., Montine, T.J., Schneider, J.A., Nelson, P.T., 2018. The revised National Alzheimer's Coordinating Center's Neuropathology Form—available data and new analyses. J. Neuropathol. Exp. Neurol. 77 (8), 717–726.

Besser, L.M., Mock, C., Teylan, M.A., Hassenstab, J., Kukull, W.A., Crary, J.F., 2019. Differences in cognitive impairment in primary age-related tauopathy versus Alzheimer disease. J. Neuropathol. Exp. Neurol. 78 (3), 219–228.

Braak, H., Braak, E., 1991. Neuropathological stageing of Alzheimer-related changes. Acta Neuropathol. 82 (4), 239–259.

Crary, J.F., 2016. Primary age-related tauopathy and the amyloid cascade hypothesis: the exception that proves the rule? J. Neurol. Neuromed. 1 (6), 53–57.

Crary, J.F., Trojanowski, J.Q., Schneider, J.A., Abisambra, J.F., Abner, E.L., Alafuzoff, I., Arnold, S.E., Attems, J., Beach, T.G., Bigio, E.H., Cairns, N.J., Dickson, D.W., Gearing, M., Grinberg, L.T., Hof, P.R., Hyman, B.T., Jellinger, K., Jicha, G.A., Kovacs, G.G., Knopman, D.S., Kofler, J., Kukull, W.A., Mackenzie, I.R., Masliah, E., McKee, A., Montine, T.J., Murray, M.E., Neltner, J.H., Santa-Maria, I., Seeley, W.W., Serrano-Pozo, A., Shelanski, M.L., Stein, T., Takao, M., Thal, D.R., Toledo, J.B., Troncoso, J.C., Vonsattel, J.P., White 3rd, C.L., Wisniewski, T., Woltjer, R.L., Yamada, M., Nelson, P.T., 2014. Primary age-related tauopathy (PART): a common pathology associated with human aging. Acta Neuropathol. 128 (6), 755–766.

Duyckaerts, C., Braak, H., Brion, J.P., Buee, L., Del Tredici, K., Goedert, M., Halliday, G., Neumann, M., Spillantini, M.G., Tolnay, M., Uchihara, T., 2015. PART is part of Alzheimer disease. Acta Neuropathol. 129 (5), 749–756.

Folstein, M.F., Folstein, S.E., McHugh, P.R., 1975. "Mini-mental state". A practical method for grading the cognitive state of patients for the clinician. J. Psychiatr. Res. 12 (3), 189–198.

Fulcher, K.K., Alosco, M.L., Miller, L., Spitznagel, M.B., Cohen, R., Raz, N., Sweet, L., Colbert, L.H., Josephson, R., Hughes, J., Rosneck, J., Gunstad, J., 2014. Greater physical activity is associated with better cognitive function in heart failure. Health Psychol. 33 (11), 1337–1343.

Harper, L., Fumagalli, G.G., Barkhof, F., Scheltens, P., O'Brien, J.T., Bouwman, F., Burton, E.J., Rohrer, J.D., Fox, N.C., Ridgway, G.R., Schott, J.M., 2016. MRI visual rating scales in the diagnosis of dementia: evaluation in 184 post-mortem confirmed cases. Brain 139, 1211–1225 Pt 4.

Hayden, K.M., Jones, R.N., Zimmer, C., Plassman, B.L., Browndyke, J.N., Pieper, C., Warren, L.H., Welsh-Bohmer, K.A., 2011. Factor structure of the National Alzheimer's Coordinating Centers uniform dataset neuropsychological battery: an evaluation of invariance between and within groups over time. Alzheimer Dis. Assoc. Disord. 25 (2), 128–137.

Hyman, B.T., Phelps, C.H., Beach, T.G., Bigio, E.H., Cairns, N.J., Carrillo, M.C., Dickson, D.W., Duyckaerts, C., Frosch, M.P., Masliah, E., Mirra, S.S., Nelson, P.T., Schneider, J.A., Thal, D.R., Thies, B., Trojanowski, J.Q., Vinters, H.V., Montine, T.J., 2012. National Institute on Aging-Alzheimer's Association guidelines for the neuropathologic assessment of Alzheimer's disease. Alzheimers Dement. 8 (1), 1–13.

Jack Jr., C.R., Bennett, D.A., Blennow, K., Carrillo, M.C., Dunn, B., Haeberlein, S.B., Holtzman, D.M., Jagust, W., Jessen, F., Karlawish, J., Liu, E., Molinuevo, J.L., Montine, T., Phelps, C., Rankin, K.P., Rowe, C.C., Scheltens, P., Siemers, E., Snyder, H.M., Sperling, R.Contributors, 2018. NIA-AA research framework: toward a biological definition of Alzheimer's disease. Alzheimers Dement. 14 (4), 535–562.

Jack Jr., C.R., Wiste, H.J., Therneau, T.M., Weigand, S.D., Knopman, D.S., Mielke, M.M., Lowe, V.J., Vemuri, P., Machulda, M.M., Schwarz, C.G., Gunter, J.L., Senjem, M.L., Graff-Radford, J., Jones, D.T., Roberts, R.O., Rocca, W.A., Petersen, R.C., 2019. Associations of amyloid, tau, and neurodegeneration biomarker profiles with rates of memory decline among individuals without dementia. JAMA 321 (23), 2316–2325.

Jack, C.R., Wiste, H.J., Weigand, S.D., Therneau, T.M., Lowe, V.J., Knopman, D.S., Botha, H., Graff-Radford, J., Jones, D.T., Ferman, T.J., Boeve, B.F., Kantarci, K., Vemuri, P., Mielke, M.M., Whitwell, J., Josephs, K., Schwarz, C.G., Senjem, M.L., Gunter, J.L., Petersen, R.C., 2020. Predicting future rates of tau accumulation on PET. Brain 143 (10), 3136–3150.

Jefferson-George, K.S., Wolk, D.A., Lee, E.B., McMillan, C.T., 2017. Cognitive decline associated with pathological burden in primary age-related tauopathy. Alzheimers Dement. 13 (9), 1048–1053.

Jensen, A.R., Figueroa, R.A., 1975. Forward and backward digit span interaction with race and IQ: predictions from Jensen's theory. J. Educ. Psychol. 67 (6), 882–893.

Josephs, K.A., Dickson, D.W., Tosakulwong, N., Weigand, S.D., Murray, M.E., Petrucelli, L., Liesinger, A.M., Senjem, M.L., Spychalla, A.J., Knopman, D.S., Parisi, J.E., Petersen, R.C., Jack Jr., C.R., Whitwell, J.L., 2017a. Rates of hippocampal atrophy and presence of post-mortem TDP-43 in patients with Alzheimer's disease: a longitudinal retrospective study. Lancet Neurol. 16 (11), 917–924.

Josephs, K.A., Martin, P.R., Weigand, S.D., Tosakulwong, N., Buciuc, M., Murray, M.E., Petrucelli, L., Senjem, M.L., Spychalla, A.J., Knopman, D.S., Boeve, B.F., Petersen, R.C., Parisi, J.E., Dickson, D.W., Jack, C.R., Whitwell, J.L., 2020. Protein contributions to brain atrophy acceleration in Alzheimer's disease and primary age-related tauopathy. Brain 143 (11), 3463–3476.

Josephs, K.A., Murray, M.E., Tosakulwong, N., Weigand, S.D., Knopman, D.S., Petersen, R.C., Jack Jr., C.R., Whitwell, J.L., Dickson, D.W., 2019. Brain atrophy in primary age-related tauopathy is linked to transactive response DNA-binding protein of 43 kDa. Alzheimers Dement. 15 (6), 799–806.

Josephs, K.A., Murray, M.E., Tosakulwong, N., Whitwell, J.L., Knopman, D.S., Machulda, M.M., Weigand, S.D., Boeve, B.F., Kantarci, K., Petrucelli, L., Lowe, V.J., Jack Jr., C.R., Petersen, R.C., Parisi, J.E., Dickson, D.W., 2017b. Tau aggregation influences cognition and hippocampal atrophy in the absence of beta-amyloid: a clinico-imaging-pathological study of primary age-related tauopathy (PART). Acta Neuropathol. 133 (5), 705–715.

Josephs, K.A., Whitwell, J.L., Weigand, S.D., Murray, M.E., Tosakulwong, N., Liesinger, A.M., Petrucelli, L., Senjem, M.L., Knopman, D.S., Boeve, B.F., Ivnik, R.J., Smith, G.E., Jack Jr., C.R., Parisi, J.E., Petersen, R.C., Dickson, D.W., 2014. TDP-43 is a key player in the clinical features associated with Alzheimer's disease. Acta Neuropathol. 127 (6), 811–824.

Kaplan, E., Goodglass, H., Weintraub, S., Brand, S., 1983. Boston Naming Test. Lea & Febiger, Philadelphia, PA..

Kelley, B.J., Petersen, R.C., 2007. Alzheimer's disease and mild cognitive impairment. Neurol. Clin. 25 (3), 577–609 v.

Koedam, E.L., Lehmann, M., van der Flier, W.M., Scheltens, P., Pijnenburg, Y.A., Fox, N., Barkhof, F., Wattjes, M.P., 2011. Visual assessment of posterior atrophy development of a MRI rating scale. Eur. Radiol. 21 (12), 2618–2625.

Lezak, M.D., Lezak, M.D., 2004. Neuropsychological Assessment, fourth ed. Oxford University Press, Oxford; New York.

Montine, T.J., Monsell, S.E., Beach, T.G., Bigio, E.H., Bu, Y., Cairns, N.J., Frosch, M., Henriksen, J., Kofler, J., Kukull, W.A., Lee, E.B., Nelson, P.T., Schantz, A.M., Schneider, J.A., Sonnen, J.A., Trojanowski, J.Q., Vinters, H.V., Zhou, X.H., Hyman, B.T., 2016. Multisite assessment of NIA-AA guidelines for the neuropathologic evaluation of Alzheimer's disease. Alzheimers Dement. 12 (2), 164–169.

Morris, J.C., 1993. The Clinical Dementia Rating (CDR): current version and scoring rules. Neurology 43 (11), 2412–2414.

Morris, J.C., Edland, S., Clark, C., Galasko, D., Koss, E., Mohs, R., van Belle, G., Fillenbaum, G., Heyman, A., 1993. The consortium to establish a registry for Alzheimer's disease (CERAD). Part IV. Rates of cognitive change in the longitudinal assessment of probable Alzheimer's disease. Neurology 43 (12), 2457–2465.

Morris, J.C., Weintraub, S., Chui, H.C., Cummings, J., Decarli, C., Ferris, S., Foster, N.L., Galasko, D., Graff-Radford, N., Peskind, E.R., Beekly, D., Ramos, E.M., Kukull, W.A., 2006. The Uniform Data Set (UDS): clinical and cognitive variables and descriptive data from Alzheimer Disease Centers. Alzheimer Dis. Assoc. Disord. 20 (4), 210–216.

Nelson, P.T., Alafuzoff, I., Bigio, E.H., Bouras, C., Braak, H., Cairns, N.J., Castellani, R.J., Crain, B.J., Davies, P., Del Tredici, K., Duyckaerts, C., Frosch, M.P., Haroutunian, V., Hof, P.R., Hulette, C.M., Hyman, B.T., Iwatsubo, T., Jellinger, K.A., Jicha, G.A., Kovari, E., Kukull, W.A., Leverenz, J.B., Love, S., Mackenzie, I.R., Mann, D.M., Masliah, E., McKee, A.C., Montine, T.J., Morris, J.C., Schneider, J.A., Sonnen, J.A., Thal, D.R., Trojanowski, J.Q., Troncoso, J.C., Wisniewski, T., Woltjer, R.L., Beach, T.G., 2012. Correlation of Alzheimer disease neuropathologic changes with cognitive status: a review of the literature. J. Neuropathol. Exp. Neurol. 71 (5), 362–381.

Nelson, P.T., Dickson, D.W., Trojanowski, J.Q., Jack, C.R., Boyle, P.A., Arfanakis, K., Rademakers, R., Alafuzoff, I., Attems, J., Brayne, C., Coyle-Gilchrist, I.T.S., Chui, H.C., Fardo, D.W., Flanagan, M.E., Halliday, G., Hokkanen, S.R.K., Hunter, S., Jicha, G.A., Katsumata, Y., Kawas, C.H., Keene, C.D., Kovacs, G.G., Kukull, W.A., Levey, A.I., Makkinejad, N., Montine, T.J., Murayama, S., Murray, M.E., Nag, S., Rissman, R.A., Seeley, W.W., Sperling, R.A., White Iii, C.L., Yu, L., Schneider, J.A., 2019. Limbic-predominant age-related TDP-43 encephalopathy (LATE): consensus working group report. Brain 142 (6), 1503–1527.

Neltner, J.H., Abner, E.L., Schmitt, F.A., Denison, S.K., Anderson, S., Patel, E., Nelson, P.T., 2012. Digital pathology and image analysis for robust high-throughput quantitative assessment of Alzheimer disease neuropathologic changes. J. Neuropathol. Exp. Neurol. 71 (12), 1075–1085.

Neumann, M., Sampathu, D.M., Kwong, L.K., Truax, A.C., Micsenyi, M.C., Chou, T.T., Bruce, J., Schuck, T., Grossman, M., Clark, C.M., McCluskey, L.F., Miller, B.L., Masliah, E., Mackenzie, I.R., Feldman, H., Feiden, W., Kretzschmar, H.A., Trojanowski, J.Q., Lee, V.M., 2006. Ubiquitinated TDP-43 in frontotemporal lobar degeneration and amyotrophic lateral sclerosis. Science 314 (5796), 130–133.

O'Bryant, S.E., Waring, S.C., Cullum, C.M., Hall, J., Lacritz, L., Massman, P.J., Lupo, P.J., Reisch, J.S., Doody, R., Texas Alzheimer's Research, C., 2008. Staging dementia using Clinical Dementia Rating Scale Sum of Boxes scores: a Texas Alzheimer's research consortium study. Arch Neurol. 65 (8), 1091–1095.

Quintas-Neves, M., Teylan, M.A., Besser, L., Soares-Fernandes, J., Mock, C.N., Kukull, W.A., Crary, J.F., Oliveira, T.G., 2019. Magnetic resonance imaging brain atrophy assessment in primary age-related tauopathy (PART). Acta Neuropathol. Commun. 7 (1), 204.

Reitan, R.M., 1955. The relation of the trail making test to organic brain damage. J. Consult. Psychol. 19 (5), 393–394.

Savola, S., Kaivola, K., Raunio, A., Kero, M., Makela, M., Parn, K., Palta, P., Tanskanen, M., Tuimala, J., Polvikoski, T., Tienari, P.J., Paetau, A., Myllykangas, L., 2021. Primary age-related tauopathy in a Finnish population-based study of the oldest old (Vantaa 85+). Neuropathol. Appl. Neurobiol. 48 (3), e12788.

Teylan, M., Besser, L.M., Crary, J.F., Mock, C., Gauthreaux, K., Thomas, N.M., Chen, Y.C., Kukull, W.A., 2019. Clinical diagnoses among individuals with primary age-related tauopathy versus Alzheimer's neuropathology. Lab. Invest. 99 (7), 1049–1055.

Teylan, M., Mock, C., Gauthreaux, K., Chen, Y.C., Chan, K.C.G., Hassenstab, J., Besser, L.M., Kukull, W.A., Crary, J.F., 2020. Cognitive trajectory in mild cognitive impairment due to primary age-related tauopathy. Brain 143 (2), 611–621.

Vogel, J.W., Young, A.L., Oxtoby, N.P., Smith, R., Ossenkoppele, R., Strandberg, O.T., La Joie, R., Aksman, L.M., Grothe, M.J., Iturria-Medina, Y., Alzheimer's Disease Neuroimaging, I., Pontecorvo, M.J., Devous, M.D., Rabinovici, G.D., Alexander, D.C., Lyoo, C.H., Evans, A.C., Hansson, O., 2021. Four distinct trajectories of tau deposition identified in Alzheimer's disease. Nat. Med. 27 (5), 871–881.

Walker, L., McAleese, K.E., Johnson, M., Khundakar, A.A., Erskine, D., Thomas, A.J., McKeith, I.G., Attems, J., 2017. Quantitative neuropathology: an update on automated methodologies and implications for large scale cohorts. J. Neural Transm. (Vienna) 124 (6), 671–683.

Wang, Y., Mandelkow, E., 2016. Tau in physiology and pathology. Nat. Rev. Neurosci. 17 (1), 5–21.

Wechsler, D., 1939. The Measurement of Adult Intelligence. The Williams & Wilkins Company, Baltimore.

Weigand, A.J., Bangen, K.J., Thomas, K.R., Delano-Wood, L., Gilbert, P.E., Brickman, A.M., Bondi, M.W., Alzheimer's Disease Neuroimaging, I., 2020. Is tau in the absence of amyloid on the Alzheimer's continuum?: A study of discordant PET positivity. Brain Commun. 2 (1) fcz046.

Weintraub, S., Besser, L., Dodge, H.H., Teylan, M., Ferris, S., Goldstein, F.C., Giordani, B., Kramer, J., Loewenstein, D., Marson, D., Mungas, D., Salmon, D., Welsh-Bohmer, K., Zhou, X.H., Shirk, S.D., Atri, A., Kukull, W.A., Phelps, C., Morris, J.C., 2018. Version 3 of the Alzheimer Disease Centers' neuropsychological test battery in the Uniform Data Set (UDS). Alzheimer Dis. Assoc. Disord. 32 (1), 10–17.

Weintraub, S., Salmon, D., Mercaldo, N., Ferris, S., Graff-Radford, N.R., Chui, H., Cummings, J., DeCarli, C., Foster, N.L., Galasko, D., Peskind, E., Dietrich, W., Beekly, D.L., Kukull, W.A., Morris, J.C., 2009. The Alzheimer's Disease Centers' Uniform Data Set (UDS): the neuropsychologic test battery. Alzheimer Dis. Assoc. Disord. 23 (2), 91–101.

Whitwell, J.L., Martin, P., Graff-Radford, J., Machulda, M.M., Senjem, M.L., Schwarz, C.G., Weigand, S.D., Spychalla, A.J., Drubach, D.A., Jack Jr., C.R., Lowe, V.J., Josephs, K.A., 2019. The role of age on tau PET uptake and gray matter atrophy in atypical Alzheimer's disease. Alzheimers Dement. 15 (5), 675–685.

SUPPLEMENTARY TABLES

Supplementary Table 1. Post hoc analysis of variables significantly different between groups of patients according to the density of neocortical neuritic plaques - CERAD score.

	Age at death, *p*	Braak stage, *p*	Age at last MRI, *p*	CDR-SB, *p*	Global CDR, *p*
CERAD 0 – CERAD 1	0.007	0.017	0.006	0.442	0.404
CERAD 0 – CERAD 2	0.458	0.000	0.520	0.994	0.983
CERAD 0 – CERAD 3	0.841	0.000	0.694	0.013	0.027
CERAD 1 – CERAD 2	0.078	0.000	0.059	0.204	0.144
CERAD 1 – CERAD 3	0.000	0.000	0.000	0.000	0.000
CERAD 2 – CERAD 3	0.010	0.000	0.005	0.001	0.007

The table shows the summarized pair-wise comparisons between groups for the variables age at death, Braak stage, age at last MRI, CDR-SB and global CDR using a *P*-value obtained by a Tukey post hoc analysis. There are significant differences at the age of death between groups CERAD 0 and 1, CERAD 1 and 3, and CERAD 2 and 3. When the Braak stage is considered, all groups are significantly different among them. There are significant differences at the age of last MRI between groups CERAD 0 and 1, CERAD 1 and 3, and CERAD 2 and 3. Significant differences are also observed in CDR-SB and global CDR between groups CERAD 1 and 3, and CERAD 2 and 3. $p < 0.05$ considered as statistically significant. For more details see Table 1.

Supplementary Table 2. Multiple Linear Regression Coefficient estimates and p values for regional brain atrophy dependent upon Group and CDR Sum Of Boxes.

	Intercept	Group	CDR-SB	Group*CDR-SB
AC	50.521***	-2.514	0.967	0.918
OF	43.191***	-4.614	0.928	-0.142
AT	41.423***	-7.080*	-0.141	0.922*
FI	59.547***	-10.743*	0.062	0.999
MT	44.065***	-6.969*	0.1515	1.567
Post	49.914***	-11.528*	-0.399	1.831**

The analyses presented here are relating to Figure 3. The Groups considered were "PART", which included cases with CERAD = 0; and "Alzheimer's disease spectrum" which included cases with CERAD = 1-3. Multiple Linear Regression Coefficient estimates are relative to brain regional atrophy and CDR-SB, with group dummy coded as Alzheimer's disease = 1, PART = 0. The brain regions considered were anterior cingulate (AC), orbito-frontal (OF), anterior temporal (AT), fronto-insular (FI), medial temporal (MT) and posterior (Post). *p* value: *** < 0.001, ** < 0.01 and * < 0.05, considered as significant.

Supplementary Table 3. Comparison of Neuropsychological Test z-scores between PART and Alzheimer's disease.

	PART (n=32)	**Alzheimer's disease (n=201)**	**Statistics and p-value**
MMSE, mean	(n = 26) -2.872	(n = 166) -5.533	**t(45.453) = -3.475; p-value = 0.001; 95%CI [-4.20 -1.12]**
Logical Memory immediate recall, mean	(n = 26) -0.989	(n = 154) -1.841	**t(31.294) = -2.627; p-value = 0.013; 95%CI [-1.51 -0.191]**
Logical Memory delayed recall, mean	(n = 26) -1.088	(n = 154) -1.820	**t(30.961) = -2.438; p-value = 0.021; 95%CI [-1.343 -0.119]**
Digit Span Forward – trials correct, mean	(n = 26) -0.374	(n = 155) -0.753	t(36.213) = -1.5732; p-value = 0.1244; 95%CI [-0.868 0.110]
Digit Span Forward - length, mean	(n = 26) -0.387	(n = 155) -0.898	t(37.135) = -1.8038; p-value = 0.079; 95%CI [-1.085 0.0629]
Digit Span Backward – trials correct, mean	(n = 26) -0.802	(n = 155) -0.912	t(35.444) = -0.514; p-value = 0.6098; 95%CI [-0.543 0.323]
Digit Span Backward - length, mean	(n = 26) -0.903	(n = 155) -0.956	t(35.318) = -0.221; p-value = 0.826; 95%CI [-0.539 0.432]
Category Fluency -Animals, mean	(n = 26) -1.267	(n = 155) -1.686	t(32.847) = -1.8813; p-value = 0.068; 95%CI [-0.871 0.034]
Category Fluency - Vegetables, mean	(n = 26) -1.808	(n = 158) -1.953	t(29.663) -0.580; p-value = 0.566; 95%CI [-0.656 0.365]
Boston Naming Task, mean	(n = 26) -1.108	(n = 155) -1.908	**t(38.211) = -2.098; p-value = 0.0425; 95%CI [-1.572 -0.0283]**
Trail A, mean	(n = 25) -2.827	(n = 140) -2.781	t(30.815) = 0.071; p-value = 0.943; 95%CI [-1.28 1.376]
Trail B, mean	(n = 19) -1.183	(n = 112) -2.374	**t(24.534) = -3.079; p-value = 0.005; 95%CI [-1.989 -0.39]**
WAIS, mean	(n = 22) -1.262	(n = 131) -1.849	**t(26.595) = -2.15; p-value = 0.040; 95%CI [-1.15 -0.027]**
Epimem, mean	(n = 26) -1.039	(n = 154) -1.830	**t(31.048) = -2.595; p-value = 0.014; 95%CI [-1.413 -0.169]**
Attent, mean	(n = 26) -0.616	(n = 155) -0.880	t(37.13) = -1.229; p-value = 0.226; 95%CI [-0.697 0.170]
Exec, mean	(n = 17) -1.024	(n = 106) -1.969	**t(21.107) = -2.603; p-value = 0.016; 95%CI [-1.699 -0.190]**
Lang, mean	(n = 26) -1.394	(n = 155) -1.829	t(34.407) = -1.812; p-value = 0.079; 95%CI [-0.921 0.052]
Global, mean	(n = 17) -0.832	(n = 106) -1.433	**t(19.55) = -2.425; p-value = 0.025; 95%CI [-1.12 -0.083]**

The table shows the comparison of z-scores of each neuropsychological test or composite between PART and Alzheimer's disease. Welch's two-sample t-test. $p < 0.05$ considered as significant.

Supplementary Table 4. TDP-43 in PART and Alzheimer's disease.

	PART (n=14)	**Alzheimer's disease (n=39)**
TDP-43 + (%)	3 (21)	7 (18)
TDP-43 - (%)	11 (79)	32 (82)

The table shows the distribution of TDP-43 inclusions in the subsample of the data in which this data is available.

SUPPLEMENTARY FIGURES

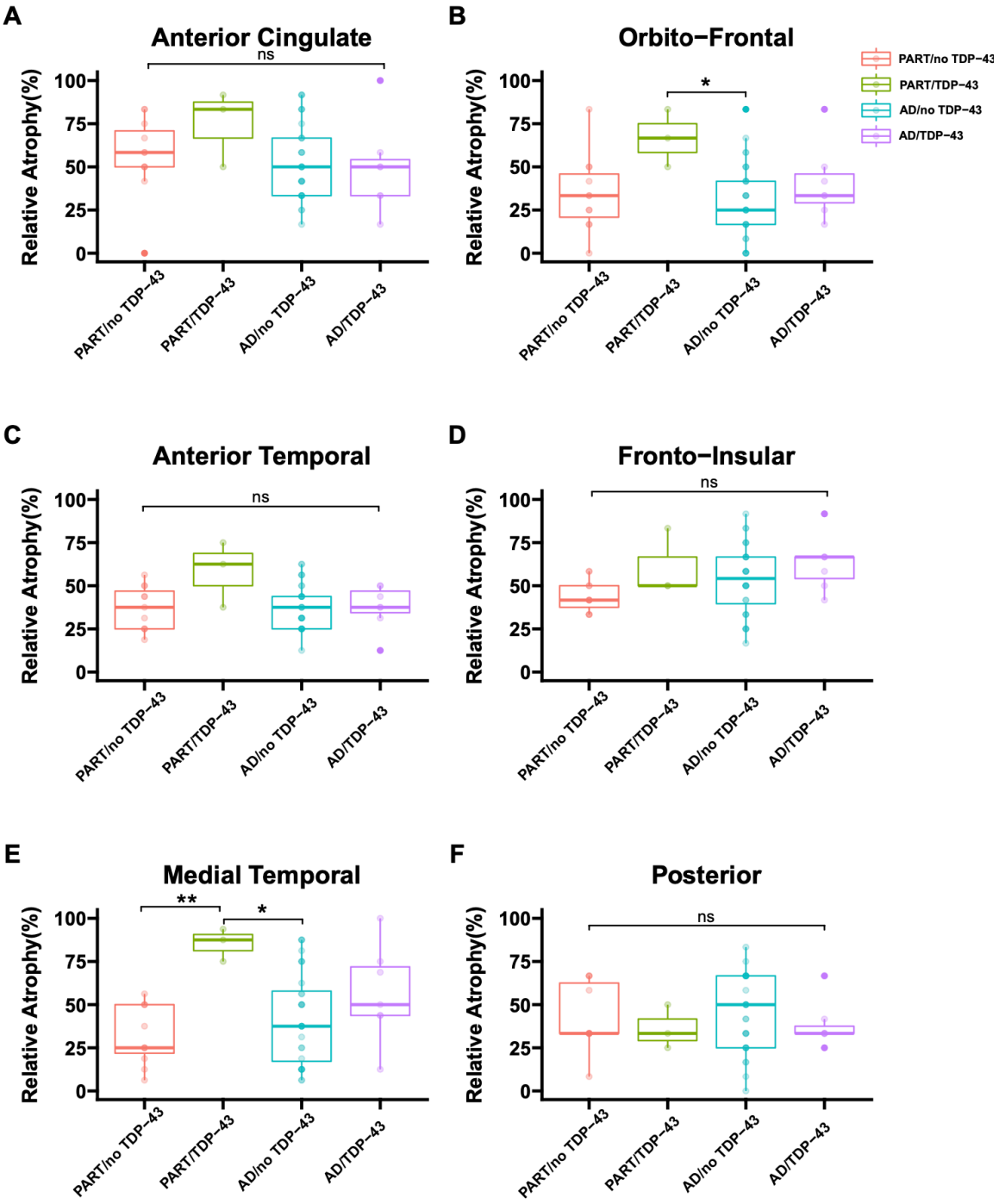


Figure S1. Braak and age-corrected relative regional brain atrophy shows significant changes between CERAD groups with and without TDP-43, predominantly in the medial temporal region. Standardized residuals corrected for Braak and age for each specific region of brain atrophy among 4 groups of participants, distributed according to the absence (CERAD 0) or presence (CERAD 1 – mild; CERAD 2 – moderate; CERAD 3 – severe) of neocortical neuritic plaques, as well as absence or presence of TDP-43, after neuropathological evaluation. The regions evaluated are **(A)** Anterior Cingulate, **(B)** Orbito-

Frontal, **(C)** Anterior Temporal, **(D)** Fronto-Insular, **(E)** Medial Temporal, and **(F)** Posterior. * $p < 0.05$. 'ns' represents non-significant differences between groups.

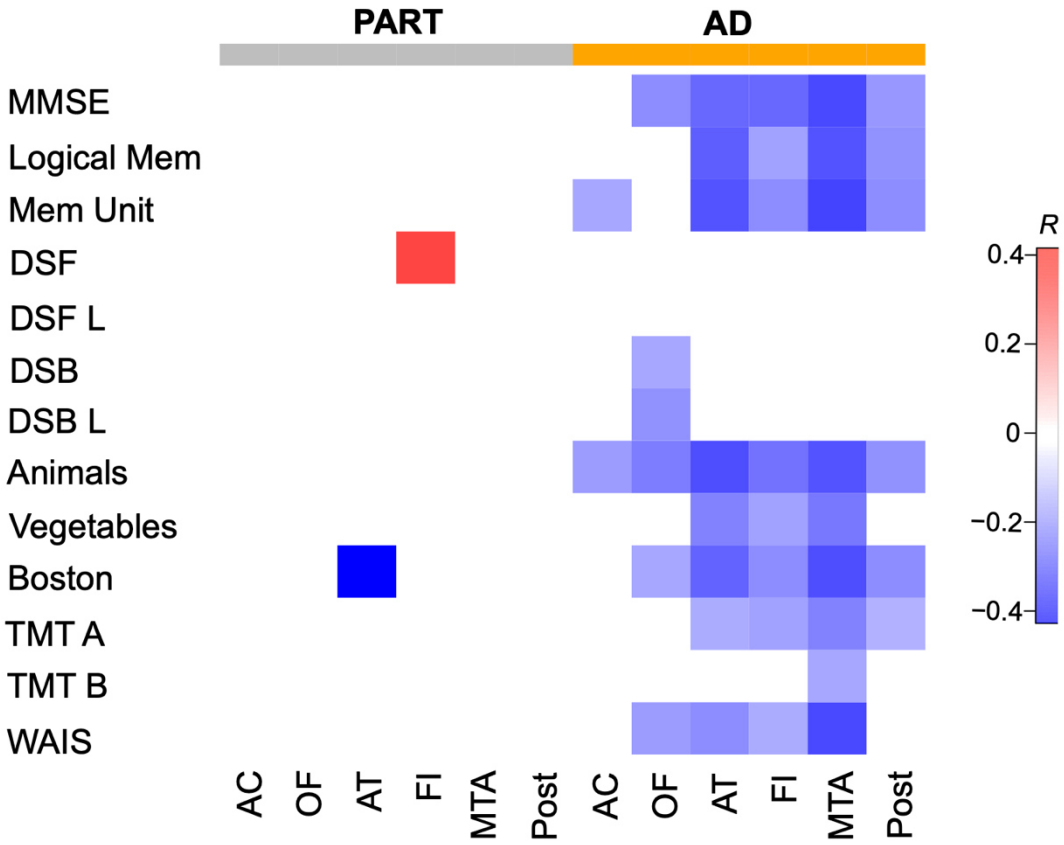


Figure S2. Pearson correlation analysis of relative brain atrophy per region after age correction versus neuropsychological test z-scores. Pearson correlation analysis of relative brain atrophy residuals after linear regression with age per region versus z-scores of neuropsychological tests among 2 groups of participants, distributed according to the absence (PART) or presence (Alzheimer's disease) of neocortical neuritic plaques after neuropathological evaluation. Only showing pairs with *p*- values < 0.05 in the correlational analysis. Colour indicates *R* Pearson coefficient. Anterior Cingulate (AC), Orbito-Frontal (OF), Anterior Temporal (AT), Fronto-Insular (FI), Medial Temporal (MT) and Posterior (Post).

Chapter 2.2

Miguel Quintas-Neves, Francisco C. Almeida, Kathryn Gauthreaux, Merilee A. Teylan, Charles N. Mock, Walter A. Kukull, John F. Crary, Tiago Gil Oliveira

Fazekas scale Magnetic Resonance Imaging assessment in Alzheimer's disease and primary age-related tauopathy

Neuroradiology (2024) 66(12):2185-93

Doi: 10.1007/s00234-024-03464-2

Neuroradiology (2024) 66:2185–2193
https://doi.org/10.1007/s00234-024-03464-2

DIAGNOSTIC NEURORADIOLOGY

Fazekas scale magnetic resonance imaging assessment in Alzheimer's disease and primary age-related tauopathy

Miguel Quintas-Neves[1,2,3] · Francisco C. Almeida[1,2,4] · Kathryn Gauthreaux[5] · Merilee A. Teylan[5] · Charles N. Mock[5] · Walter A. Kukull[5] · John F. Crary[6] · Tiago Gil Oliveira[1,2,3]

Received: 7 May 2024 / Accepted: 2 September 2024 / Published online: 26 September 2024
© The Author(s) 2024

Abstract

Background Brain vascular pathology is an important comorbidity in Alzheimer's disease (AD), with white matter damage independently predicting cognitive impairment. However, it is still unknown how vascular pathology differentially impacts primary age-related tauopathy (PART) compared to AD. Therefore, our objectives were to compare the brain microangiopathic burden in patients with PART and AD, evaluated by MRI, while assessing its relation with neuropathological findings, patterns of brain atrophy and degree of clinical impairment.

Methods Clinical information, brain MRI (T1 and T2-FLAIR) and neuropathological data were obtained from the National Alzheimer's Coordinating Centre ongoing study, with a total sample of 167 patients identified, that were divided according to the presence of neuritic plaques in Consortium to Establish a Registry for Alzheimer's disease (CERAD) 0 to 3. Microangiopathic burden and brain atrophy were evaluated by two certified neuroradiologists, using, respectively, the Fazekas score and previously validated visual rating scales to assess brain regional atrophy.

Results Significant correlations were found between the Fazekas score and atrophy in the fronto-insular and medial temporal regions on both groups, with PART showing overall stronger positive correlations than in AD, especially in the fronto-insular region. For this specific cohort, no significant correlations were found between the Fazekas score and the degree of clinical impairment.

Conclusion Our results show that PART presents different pathological consequences at the brain microvascular level compared with AD and further supports PART as an independent pathological entity from AD.

Keywords PART = Primary age-related tauopathy · AD = Alzheimer's disease · CERAD = Consortium to Establish a Registry for Alzheimer's disease

Introduction

Primary age-related tauopathy (PART) is a neuropathological condition, characterized by the postmortem finding of tau-positive neurofibrillary tangles in the brain, without neuritic plaque deposition ("definite" PART). Neurofibrillary tangle neuropathological classification is based on Braak staging, while amyloid-beta neuritic plaque pathology is classified by the Consortium to Establish a Registry for Alzheimer's disease (AD) (CERAD) staging, which

✉ Tiago Gil Oliveira
tiago@med.uminho.pt

1 School of Medicine, Life and Health Sciences Research Institute (ICVS), University of Minho, Braga, Portugal

2 ICVS/3B's—PT Government Associate Laboratory, Braga/Guimarães, Portugal

3 Department of Neuroradiology, Unidade Local de Saúde de Braga, Braga, Portugal

4 Department of Neuroradiology, Centro Hospitalar Universitário Do Porto, Porto, Portugal

5 Department of Epidemiology, National Alzheimer's Coordinating Center, University of Washington, Seattle, WA, U.S.A.

6 Neuropathology Brain Bank & Research Core, Department of Pathology, Nash Family Department of Neuroscience, Department of Artificial Intelligence, & Human Health, Friedman Brain Institute, Ronald M. Loeb Center for Alzheimer's Disease, Icahn School of Medicine at Mount Sinai, New York, NY, U.S.A.

in "definite" PART is 0, corresponding to the absence of neuritic plaques [1]. On the other hand, AD is diagnosed by the identification of both neurofibrillary tangles and amyloid-beta brain deposition, whether in vivo [using the so-called AT(N) biomarkers proposed by the National Institute on Aging and Alzheimer's Association (NIA-AA) 2018 Research Framework [2]] or postmortem [using the "ABC score", by grading amyloid plaques with Thal phases (A), neurofibrillary tangles with Braak staging (B) and neuritic plaques with CERAD assessment (C)] [3].

Several risk factors have been described for AD, such as genetic, age, traumatic brain injury or vascular disease [4]. Interestingly, cerebrovascular disease burden in the form of white matter T2 hyperintensities in brain MRI has been found to be a predictor of AD progression and can be clinically assessed by the Fazekas grading score [5]. This is a three-point based scale [6] that independently rates deep and periventricular white matter lesions related to leukoaraiosis, with the former being frequently associated with small vessel disease. Moreover, it is known that the amount of amyloid-beta deposition and white matter lesions independently predict cognitive impairment, which supports the diagnostic usefulness of assessing white matter damage [7]. Recently, a neuropathological study found a significant correlation between cognitive impairment and cerebrovascular disease in PART patients [8]. Despite the known importance of brain vascular pathology as a comorbidity in AD, it is still underexplored how brain vascular lesion burden differentially affects PART compared to AD, in terms of cognition and brain atrophy, namely by using clinically applicable visual rating scales [9–11]. Therefore, our study aimed to assess how PART and AD are differentially impacted by brain microangiopathy burden, evaluated by in vivo MRI.

This article follows the STROBE reporting guidelines.

Materials and methods

Study design, participants and selection criteria

This is a retrospective study based on data obtained from the National Alzheimer's Coordinating Center, a repository for data collected at the Alzheimer's Disease Centers located across the United States of America. Each Alzheimer's Disease Centers collected standardized clinical data via the Uniform Data Set and neuropathological evaluations obtained at autopsy to the Neuropathology Data Set. Both datasets have been described in detail elsewhere [12–16]. Our sample was obtained from the September 2019 data freeze (n = 38,836 patients), that included 4192 patients clinical Uniform Data Set data within 2 years from death and neuritic plaque burden assessed at autopsy. All Uniform Data Set visits from patients with MRI scans performed no more than 4 years before the date of death and who had neuropathology data available were collected (n = 334 patients); only the last Uniform Data Set visit and respective brain MRI scan were considered for the analysis. Participants with the following comorbidities were excluded: (a) neuropathological evidence of frontotemporal lobar degeneration, amyotrophic lateral sclerosis, prion disease, or argyrophilic grains; (b) with clinical evidence of dementia with Lewy bodies, Parkinson disease, Down syndrome, Huntington disease, prion disease, corticobasal degeneration, or progressive supranuclear palsy; (c) with other brain lesions that biased atrophy assessment (e.g., brain tumor, brain herniation, vascular malformation, lymphocytic meningoencephalitis, traumatic brain injury, demyelinating disease, large territorial ischemic lesion). After applying these exclusion criteria, participants with no T2-FLAIR sequence available on brain MRI were also excluded, after which a final sample of 167 participants was obtained. PART cases were defined as having no neuritic plaques (CERAD 0), that is, "definite" PART.

Neuropathology data

This information was collected by the Alzheimer's Disease Centers by the use of a standardized Neuropathology Form on those patients who died and consented to autopsy and neuropathologic examination. Afterwards, participants were categorized according to the Braak stage for neurofibrillary degeneration (i.e. neurofibrillary tangles distribution) and CERAD stage (i.e. neuritic plaques density). Details on brain tissue preparation and staining within the National Alzheimer's Coordinating Center Neuropathology dataset have been previously described [13].

Brain MRI data

MRI examinations were performed on 1.5 T or 3 T scanners, both from Philips, Siemens or GE manufacturers. Despite different protocols between centers, for our imaging analysis we only used 3D T1-weighted acquisitions (in order to grade the degree of regional brain atrophy) and 2D T2-FLAIR sequences (in order to grade leukoaraiosis).

Imaging analysis

In order to assess brain atrophy, we used a previously validated visual rating scale [9] that takes into account the following 6 regions: anterior cingulate, orbito-frontal, anterior temporal, fronto-insular, medial temporal, and posterior. We defined atrophy as a cross-sectional concept, corresponding to the score attributed on the basis of the aforementioned rating scales. As already described by the simplified version: orbito-frontal and anterior cingulate regions were both rated on the first anterior coronal slice where the corpus callosum

becomes visible; the fronto-insular was rated over three slices, starting on the first anterior coronal slice where the anterior cingulate becomes visible and moving posteriorly; the anterior temporal was rated at the level of the temporal pole, immediately anterior to where the "temporal stem" connects the frontal and temporal lobes; the medial temporal was rated according to the medial temporal lobe atrophy score [17], performed on the hippocampus at the same coronal section of the anterior pons; the posterior region was rated according to a four-point posterior atrophy scale described by Koedam [18], being the overall score based on the presence of atrophy in sagittal (widening of the posterior cingulate and parieto-occipital sulcus, and atrophy of the precuneus on both sides by considering paramedian sagittal sections), as well as axial and coronal (widening of the posterior cingulate sulcus and sulcal dilatation in parietal lobes) sections, assessed for left and right separately [9]. For each brain region scale, an average of both hemispheres was calculated. In order to aid and increase acuity of the rating process, reference imagens for each rating scale were provided to the classifiers based on Harper et al. [9].

In order to assess leukoaraiosis, the Fazekas scale was used [6], considering separately the periventricular and the deep white matter, according to a rating system ranging from 0 (none) to 3 (severe), as originally described. In order to aid and increase the acuity of the rating process, reference images for the deep and periventricular Fazekas scales were provided to the classifiers [19].

Two independent classifiers (unaware of the clinical diagnosis) with 11 and 7 years, respectively, of experience in clinical neuroradiology were responsible for rating the images. In all cases, an average of both classifiers was used. Figure 1 depicts an example of a patient in which this rating method was performed.

Neuropsychological assessment

Local Alzheimer's Disease Centers assessed participants using the CDR and the Uniform Data Set version 2 neuropsychological test battery [15]. We used the CDR Sum of Boxes (CDR-SB) performed at the last Uniform Data Set visit prior to death. The Washington University CDR was reviewed by Morris and collaborators in 1993 [20] with the purpose of staging the severity of AD, and takes into consideration six cognitive categories: orientation, memory, judgment and problem solving, community affairs, home and hobbies, and personal care; it is based on a five-point scale in which none = 0, questionable = 0.5, mild = 1, moderate = 2, and severe = 3. The CDR-SB is calculated by summing the ratings of the previously mentioned six cognitive domains and, therefore, reflects a quantitative global measure, that ranges from 0 (normal) to 18 (severe dementia) [21].

Statistical analysis and *bias* control

Part of our analysis was based on the division into four groups according to the CERAD score (ie, density of neocortical neuritic plaques): CERAD 0 (none – "definite" PART); CERAD 1 (sparse – mild AD); CERAD 2 (moderate – moderate AD); CERAD 3 (severe – severe AD). One-way

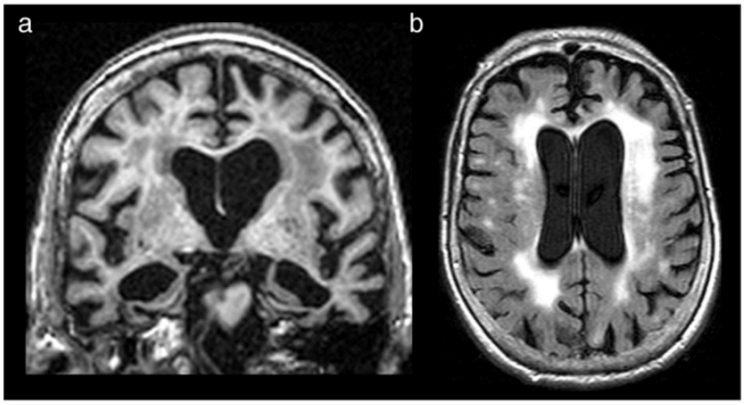


Fig. 1 Representative case of a 91 year-old male patient with AD. (**a**) Coronal reformat of a 3D T1-weighted sequence shows severe widening of the choroid fissures and severe enlargement of the temporal horns, with marked atrophy of both hippocampi (medial temporal lobe atrophy – MTA – score of 4). (**b**) Axial T2-FLAIR sequence reveals hyperintensities involving the periventricular and the deep white matter, with irregular periventricular signal extending to the deep white matter in the former and severe confluence in the latter (periventricular and deep Fazekas score of 3)

ANOVA was performed in order to assess potential differences between groups in terms of baseline characteristics, followed by Tukey post hoc analysis or χ^2 test whenever these characteristics were significantly different ($p < 0.05$). Intraclass correlation coefficients were calculated for checking the acuity of the rating process between both classifiers per each region evaluated for atrophy and for the Fazekas grading (periventricular and deep), with significant correlations obtained between classifiers for each variable (Online Resource 1), and overall good reliability (> 0.75). One-way ANOVA was also performed in order to check for statistically significant differences between Fazekas grading in the 4 groups of CERAD, followed by Tukey post hoc analysis whenever significant results were obtained ($p < 0.05$), without correcting for other factors and after correcting for Braak and age; the same method was applied to check differences between groups with absence (i.e. "definite" PART) and presence (i.e. AD neuropathological change) of neuritic plaques.

Linear regression models and Pearson correlation coefficients were used in order to assess the relation between the Fazekas score (periventricular and deep) and the CDR-SB, uncorrected and after correction for age and Braak, in "definite" PART versus AD; values were expressed as (R) and considered statistically significant when $p < 0.05$. Linear regression models and Pearson correlation coefficients were also used to assess the relation between the Fazekas score (periventricular and deep) and the percentage of relative atrophy in the several evaluated brain regions, after correction for age. ANCOVA was then performed in order to compare the slopes of the regression lines obtained. All statistical analyses and graphical representation were performed on SPSS Statistics version 29 and GraphPad software version 10.0.0.

Results

167 participants were included: 29 with no ("definite" PART – CERAD 0), 17 with sparse (CERAD 1), 54 with moderate (CERAD 2), and 67 with severe (CERAD 3) neuritic plaques density. CERAD 0, 2 and 3 showed a male predominance (more than 50%), while CERAD 1 had a female predominance (approximately 65%); there was, however, no significant differences in gender between groups (Table 1). Mean age at death and mean age at last MRI were significantly different between groups, with lower values on CERAD 0 (78.1 ± 12.4 and 76.0 ± 12.9 years old, respectively) and 3 (80.4 ± 8.5 and 77.8 ± 8.7 years old, respectively) and higher values on CERAD 1 (88.8 ± 6.1 and 86.8 ± 5.4 years old, respectively) (Table 1). The global CDR and CDR-SB were significantly lower for CERAD 1 (0.8 ± 0.9 and 4.5 ± 5.2, respectively) and 2 (1.0 ± 0.7 and 5.2 ± 4.2, respectively), and higher for CERAD 3 (1.4 ± 0.7 and 8.4 ± 4.5, respectively); moreover, CERAD 0 presented values of CDR between those of CERAD 2 and 3, with no statistically significant differences between them. Braak staging was also significantly different between groups, with a predominance of lower grades (Braak I and II) in PART and higher grades (Braak V and VI) in the more advanced AD spectrum CERAD 3 cases (Table 1).

No statistically significant differences were found in the periventricular or deep Fazekas scores considering groups from CERAD 0 to 3, without correction for potential confounding factors ($p = 0.116$ and 0.132, respectively) and after correction for age and Braak ($p = 0.059$ and 0.311, respectively) (Online Resource 2). Although statistically significant differences were found in periventricular and deep Fazekas scores between "definite" PART (CERAD 0) and the AD spectrum (CERAD 1–3) ($p < 0.05$ – Fig. 2), no significant differences remained after correcting for age and Braak ($p = 0.182$ and 0.634, respectively).

No significant correlations were found between the Fazekas scores (periventricular or deep) and the CDR-SB on both "definite" PART and AD participants, without correction for other factors and after correcting for age and Braak (Online Resource 2).

In AD patients, significant positive correlations ($p < 0.05$) were found between the Fazekas score (periventricular and deep) and atrophy in the medial temporal ($R = 0.30$ for both), anterior temporal ($R = 0.19$ and 0.20, respectively) and fronto-insular regions ($R = 0.27$ and 0.18, respectively), and between the periventricular Fazekas and the orbito-frontal ($R = 0.19$) and the anterior cingulate ($R = 0.21$) regions, while in PART patients, significant positive correlations ($p < 0.05$) were found between the Fazekas score (periventricular and deep) and atrophy in the medial temporal ($R = 0.39$ and 0.47, respectively) and fronto-insular regions ($R = 0.53$ and 0.62, respectively) (Fig. 3). Moreover, a significant difference was found ($p < 0.05$) between the regression lines assessing atrophy in the fronto-insular region and the deep Fazekas score in AD versus PART patients (Online Resource 1).

Discussion

Previous evidence suggested that AD and PART could have differential cerebrovascular disease associated co-pathologies [8]. Using the Fazekas score as an MRI-based surrogate for leukoaraiosis, with the deep white matter hyperintensities predominantly reflecting small vessel disease, we observed no major statistically significant differences between groups of CERAD 0 to 3 or between "definite" PART and AD patients. However, significant correlations were found between the Fazekas score and regional atrophy patterns on

Table 1 Characterization of patients according to the density of neocortical neuritic plaques (CERAD score)

	PART	AD			
	CERAD 0 (None) (n = 29)	CERAD 1 (Sparse) (n = 17)	CERAD 2 (Moderate) (n = 54)	CERAD 3 (Severe) (n = 67)	*p*
Male sex, n (%)[a]	19 (65.5)	6 (35.3)	30 (55.6)	45 (67.2)	0.087
Age at death, mean (SD)[b]	78.1 (± 12.4)	88.8 (± 6.1)	83.1 (± 8.4)	80.4 (± 8.5)	< 0.001
Age at last MRI, mean (SD)[c]	76.0 (± 12.9)	86.8 (± 5.4)	81.0 (± 8.5)	77.8 (± 8.7)	< 0.001
Age MRI-Death, mean (SD)[d]	2.1 (± 1.1)	2.0 (± 1.4)	2.1 (± 1.2)	2.5 (± 1.1)	0.118
CDR-SB[e]	6.1 (± 6.3)	4.5 (± 5.2)	5.2 (± 4.2)	8.4 (± 4.5)	< 0.001
Global CDR[e]	1.2 (± 1.1)	0.8 (± 0.9)	1.0 (± 0.7)	1.4 (± 0.7)	0.003
Braak stage, n (%)[f]					0.000
None	6 (20.7)	0 (0.0)	1 (1.9)	0 (0.0)	
I	10 (34.5)	1 (5.9)	1 (1.9)	0 (0.0)	
II	8 (27.6)	6 (35.3)	9 (16.7)	0 (0.0)	
III	3 (10.3)	7 (41.2)	12 (22.2)	2 (3.0)	
IV	2 (6.9)	1 (5.9)	11 (20.4)	7 (10.4)	
V	0 (0.0)	2 (11.8)	12 (22.2)	21 (31.3)	
VI	0 (0.0)	0 (0.0)	8 (14.8)	37 (55.2)	
Braak stage, mean (SD)	1.5 (± 1.2)	2.8 (± 1.1)	3.8 (± 1.5)	5.4 (± 0.8)	< 0.001

[a]Male sex refers to the absolute mean and relative percentage of male patients in a given group, represented as n (%)

[b]Age at death is the subject age at the time of death

[c]Age at last MRI is the subject age at the time the last MRI was performed

[d]Age MRI-Death is the difference between the subject age at the last performed MRI and time of death. These three variables are reported in years as a continuous variable with mean and standard deviation (SD)

[e]CDR-SB refers to the sum of boxes score from the CDR® Dementia Staging Instrument and global CDR refers to the global Clinical Dementia Rating score; they are both attributed to the subject in the last clinical visit and are also reported as continuous variables with mean and standard deviation

[f]For each Braak stage (from none to VI) values are represented as number of cases and percentage of total. Data presented as n (%) and mean (± SD)

p value for One-way ANOVA or chi-square test, as appropriate. $p < 0.05$ considered as significant

both groups, with PART showing overall stronger positive correlations than in AD, particularly in the fronto-insular region. Even though cerebrovascular co-pathology, in this case represented by small vessel disease, does not substantially differ between PART and AD at the MRI level, it might be differentially contributing to regional brain atrophy. These results provide additional evidence that PART and AD might be two different entities, with potentially different pathological consequences at the brain microvascular level.

It was shown that significant cerebrovascular disease (co-defined as a Fazekas score ≥ 2) was a potential neurodegeneration driver in patients with no significant altered amyloid-beta pathology in PET (i.e. in suspected non-Alzheimer pathology – "SNAP") [22]. Moreover, levels of amyloid deposition, as well as ratings of periventricular and deep Fazekas scores, have been found to discriminate between cognitively normal and demented individuals [7]. One of the described possibilities to potentially explain the link between cognitive impairment and periventricular white matter hyperintensities is the disruption of fibers in cognitive circuits across the brain, such as cholinergic projections from the basal forebrain to the cortex [23]. Moreover, elevated levels of activated microglia in periventricular white matter hyperintensities suggest an intrinsic neuroinflammatory response following the disruption of the blood–brain barrier [23]. This is not the case, however, for the subcortical/deep location [24], where white matter hyperintensities volume has been associated with lipid peroxidation in the blood, in the setting of hypertension, supporting the hypothesis of a vascular etiology in this location [25]. Adding to this, two recent studies [26, 27] found evidence that, in AD patients, white matter hyperintensities can develop in the setting of vascular disease and also secondary to AD pathology (i.e. AD-related white matter hyperintensities), with the latter potentially being explained by the following pathophysiological mechanisms: (a) axonal/Wallerian degeneration secondary to neurofibrillary tangles; (b) toxicity of amyloid-beta oligomers that can also lead to axonal degeneration; (c) neuroinflammation and microglial activation that could be involved in the pathogenesis and progression of AD. As such, AD-related processes, such as parenchymal/vessel amyloidosis and neurodegeneration, might be responsible

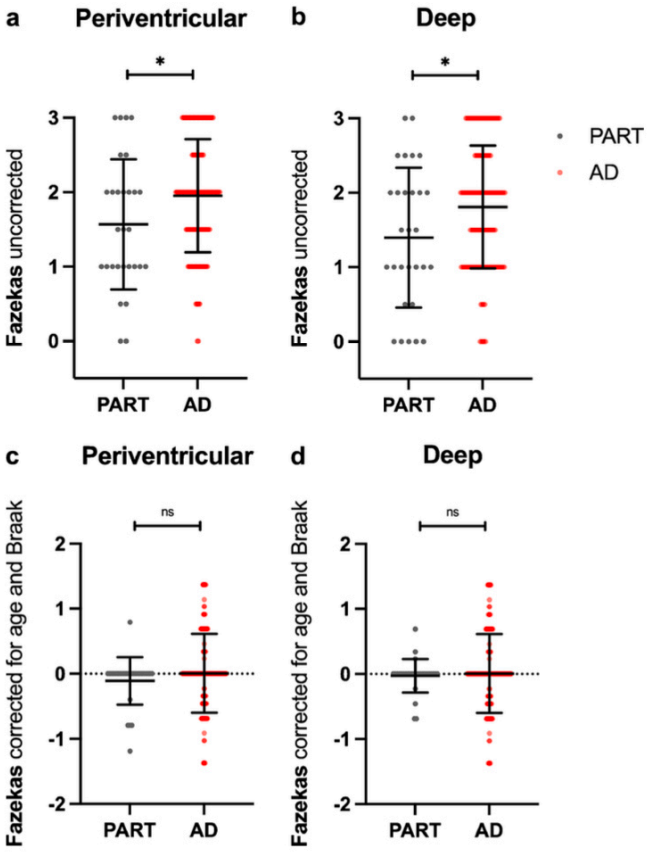


Fig. 2 No significant differences were found in the Fazekas grading between patients with PART and AD. Uncorrected (**a**, **b**) and standardized residuals for age and Braak (**c**, **d**) for deep and periventricular Fazekas scores among patients with absence (i.e. PART) or presence (i.e. AD) of neocortical neuritic plaques after neuropathological evaluation. * $p < 0.05$. 'ns' represents non-significant differences between groups



Fig. 3 Correlation analysis between relative regional brain atrophy and Fazekas scores, corrected for age, shows differential patterns in AD and PART. Pearson correlation analysis of relative brain atrophy residuals after linear regression with age per region versus Fazekas scores (periventricular and deep) among 2 groups of participants, distributed according to the absence (i.e. PART) or presence (i.e. AD) of neocortical neuritic plaques after neuropathological evaluation. The regions evaluated are anterior cingulate (AC), orbito-frontal (OF), fronto-insular (FI), medial temporal (MTA) and posterior (Post). Only showing pairs with $p < 0.05$ in the correlational analysis. Color indicates *R* Pearson coefficient

for a large proportion of the increased white matter lesion volume found in AD and, therefore, the presence of elevated white matter hyperintensities in these patients may not necessarily reflect the presence of mixed vascular and AD pathologies [27], something future studies should better assess, possibly by correlating imaging findings (i.e. the Fazekas scores) with neuropathological findings at autopsy on those regions. It is also noteworthy that some literature favors a posterior predominance of white matter hyperintensities in AD (i.e. parieto-occipital and posterior periventricular areas) [28, 29], with the splenium of the corpus callosum being described as a potentially core feature of AD associated with worse cognition [26]. Future studies should evaluate this anteroposterior gradient and compare it to the commonly used Fazekas score (deep and periventricular), while also correlating with the number and type of basal ganglia lesions, as defined by the European Task Force on Age-Related White Matter Changes [30].

Even though we found no significant correlations between the Fazekas scores and the CDR-SB, which is arguably explained by the sample size, we observed significant correlations between the Fazekas scores and the degree of atrophy in several brain regions, further supporting the concept that cerebrovascular co-pathology, represented by leukoaraiosis and, most specifically, small vessel disease, might play an important role in the pathophysiology of PART and AD. Interestingly, the magnitude of correlation between microangiopathy and atrophy in the fronto-insular region was more pronounced in PART than in AD, which suggests that, in PART, atrophy patterns might be less relying on neuropathological changes than in AD. This is in line with previous evidence that showed a strong association between cerebrovascular disease and cognitive impairment in PART patients [8]. As PART cases with mild cognitive impairment or dementia are diagnosed as AD more than 50% of the time [31], these findings might contribute to a potential future distinction between these two entities at the clinical presentation level. We believe that by using validated visual rating scales that can be easily applied in a routine clinical setting might contribute to the progressive translation from the neuropathological diagnosis of PART to its clinical characterization.

This study has important limitations. It was based on a convenience, autopsy-based, sample, which limits its extrapolation. The National Alzheimer's Coordinating Center database has inherent limitations of generalizability, given the participants tended to be more often caucasian and more affluent than the general population [32]. Moreover, in our sample, there was a tendency towards higher neuropathological burden in younger ages. Secondly, the use of visual rating scales, despite performed by trained neuroradiologists, is invariably associated with interobserver variability; however, in our case, significant correlations between both raters, with overall good interobserver agreement, was found. Also, the variability in MRI scanners and field strengths were potential sources of bias and the patients included in our sample had incomplete clinical information on other comorbidities that could be associated with brain atrophy and microangiopathy, such as hypertension or dyslipidemia, or on other neuropathologic features, such as TAR DNA-binding protein 43 pathology. Also, we did not assess other manifestations of small vessel disease, such as cerebral microbleeds, intracerebral hemorrhage, cortical superficial siderosis or lacunar infarcts, something future studies should tackle. Another limitation is that Braak staging is an incomplete measure of tau burden and, therefore, it would be beneficial to have other quantitative measures, such as tau PET. Finally, the retrospective nature of the study is a potential source of bias. Despite these limitations, the study has also major strengths, such as the use of multicentric data on a large group of individuals across the US, the persistently performed standardized process of collecting several clinical variables in every Uniform Data Set visit, the use of standardized neuropathological criteria to assess pathology at autopsy [33], and the unique nature of a database with antemortem clinically validated MRI sequences (T1 and T2-FLAIR) with gold-standard neuropathology postmortem diagnosis of PART and AD.

Conclusions

Our study further supports the concept that PART might be a different neuropathological entity from AD, by showing different correlations between brain microangiopathy and atrophy in several brain regions, particularly in PART.

Supplementary Information The online version contains supplementary material available at https://doi.org/10.1007/s00234-024-03464-2.

Funding Open access funding provided by FCT|FCCN (b-on). The National Alzheimer's Coordinating Center database is funded by NIA/NIH Grant U24 AG072122. NACC data are contributed by the NIA-funded ADRCs: P30 AG062429 (PI James Brewer, MD, PhD), P30 AG066468 (PI Oscar Lopez, MD), P30 AG062421 (PI Bradley Hyman, MD, PhD), P30 AG066509 (PI Thomas Grabowski, MD), P30 AG066514 (PI Mary Sano, PhD), P30 AG066530 (PI Helena Chui, MD), P30 AG066507 (PI Marilyn Albert, PhD), P30 AG066444 (PI John Morris, MD), P30 AG066518 (PI Jeffrey Kaye, MD), P30 AG066512 (PI Thomas Wisniewski, MD), P30 AG066462 (PI Scott Small, MD), P30 AG072979 (PI David Wolk, MD), P30 AG072972 (PI Charles DeCarli, MD), P30 AG072976 (PI Andrew Saykin, PsyD), P30 AG072975 (PI David Bennett, MD), P30 AG072978 (PI Neil Kowall, MD), P30 AG072977 (PI Robert Vassar, PhD), P30 AG066519 (PI Frank LaFerla, PhD), P30 AG062677 (PI Ronald Petersen, MD, PhD), P30 AG079280 (PI Eric Reiman, MD), P30 AG062422 (PI Gil Rabinovici, MD), P30 AG066511 (PI Allan Levey, MD, PhD), P30 AG072946 (PI Linda Van Eldik, PhD), P30 AG062715 (PI Sanjay Asthana, MD, FRCP), P30 AG072973 (PI Russell Swerdlow, MD), P30 AG066506 (PI Todd Golde, MD, PhD), P30 AG066508 (PI Stephen Strittmatter, MD, PhD), P30 AG066515 (PI Victor Henderson, MD, MS), P30 AG072947 (PI Suzanne Craft, PhD),

P30 AG072931 (PI Henry Paulson, MD, PhD), P30 AG066546 (PI Sudha Seshadri, MD), P20 AG068024 (PI Erik Roberson, MD, PhD), P20 AG068053 (PI Justin Miller, PhD), P20 AG068077 (PI Gary Rosenberg, MD), P20 AG068082 (PI Angela Jefferson, PhD), P30 AG072958 (PI Heather Whitson, MD), P30 AG072959 (PI James Leverenz, MD), R01 AG054008, R01 NS095252, R01 AG060961, R01 NS086736, and the Tau Consortium (PI John F. Crary MD, PhD). This work has been funded by Portuguese national funds, through the Foundation for Science and Technology (FCT)—UIDB/50026/2020 and UIDP/50026/2020. T.G.O. has been funded by Fundação Amélia de Mello (FAM/2022).

Data availability The data used in this study is available upon request on the National Alzheimer's Coordinating Center database.

Declarations

Ethics approval Study protocols were approved by the respective institutional review boards at each local Alzheimer's Disease Centers.

Informed consent Written informed consent was provided by all participants at each local Alzheimer's Disease Centers, and participants that contributed to the National Alzheimer's Coordinating Center Neuropathology Data Set gave consent to autopsy.

Competing interests M.Q.N. is an Editorial Board Member of this journal, namely in Head and Neck/ENT Radiology Section. T.G.O. is a scientific advisor and shareholder of Ceracuity Inc, has been a consultant for Sonae and Guidepoint, has received fees as a speaker from Eisai and conference fees covered from Roche.

Open Access This article is licensed under a Creative Commons Attribution 4.0 International License, which permits use, sharing, adaptation, distribution and reproduction in any medium or format, as long as you give appropriate credit to the original author(s) and the source, provide a link to the Creative Commons licence, and indicate if changes were made. The images or other third party material in this article are included in the article's Creative Commons licence, unless indicated otherwise in a credit line to the material. If material is not included in the article's Creative Commons licence and your intended use is not permitted by statutory regulation or exceeds the permitted use, you will need to obtain permission directly from the copyright holder. To view a copy of this licence, visit http://creativecommons.org/licenses/by/4.0/.

References

1. Crary JF, Trojanowski JQ, Schneider JA, Abisambra JF, Abner EL, Alafuzoff I et al (2014) Primary age-related tauopathy (PART): a common pathology associated with human aging. Acta Neuropathol 128(6):755–766. https://doi.org/10.1007/s00401-014-1349-0
2. Jack CR Jr, Bennett DA, Blennow K, Carrillo MC, Dunn B, Haeberlein SB et al (2018) NIA-AA Research Framework: Toward a biological definition of Alzheimer's disease. Alzheimers Dement 14(4):535–562. https://doi.org/10.1016/j.jalz.2018.02.018
3. Hyman BT, Phelps CH, Beach TG, Bigio EH, Cairns NJ, Carrillo MC et al (2012) National Institute on Aging-Alzheimer's Association guidelines for the neuropathologic assessment of Alzheimer's disease. Alzheimers Dement 8(1):1–13. https://doi.org/10.1016/j.jalz.2011.10.007
4. Aa R (2019) Risk factors for Alzheimer's disease. Folia Neuropathol 57(2):87–105. https://doi.org/10.5114/fn.2019.85929
5. Ozge A, Ghouri R, Oksuz N, Tasdelen B (2023) Predictive factors for Alzheimer's disease progression: a comprehensive retrospective analysis of 3,553 cases with 211 months follow-up. Front Neurol 14:1239995. https://doi.org/10.3389/fneur.2023.1239995
6. Fazekas F, Chawluk JB, Alavi A, Hurtig HI, Zimmerman RA (1987) MR signal abnormalities at 1.5 T in Alzheimer's dementia and normal aging. AJR Am J Roentgenol 149(2):351–6. https://doi.org/10.2214/ajr.149.2.351
7. Gordon BA, Najmi S, Hsu P, Roe CM, Morris JC, Benzinger TL (2015) The effects of white matter hyperintensities and amyloid deposition on Alzheimer dementia. Neuroimage Clin 8:246–252. https://doi.org/10.1016/j.nicl.2015.04.017
8. Iida MA, Farrell K, Walker JM, Richardson TE, Marx GA, Bryce CH et al (2021) Predictors of cognitive impairment in primary age-related tauopathy: an autopsy study. Acta Neuropathol Commun 9(1):134. https://doi.org/10.1186/s40478-021-01233-3
9. Harper L, Fumagalli GG, Barkhof F, Scheltens P, O'Brien JT, Bouwman F et al (2016) MRI visual rating scales in the diagnosis of dementia: evaluation in 184 post-mortem confirmed cases. Brain 139(Pt 4):1211–1225. https://doi.org/10.1093/brain/aww005
10. Quintas-Neves M, Teylan MA, Besser L, Soares-Fernandes J, Mock CN, Kukull WA et al (2019) Magnetic resonance imaging brain atrophy assessment in primary age-related tauopathy (PART). Acta Neuropathol Commun 7(1):204. https://doi.org/10.1186/s40478-019-0842-z
11. Quintas-Neves M, Teylan MA, Morais-Ribeiro R, Almeida F, Mock CN, Kukull WA et al (2022) Divergent magnetic resonance imaging atrophy patterns in Alzheimer's disease and primary age-related tauopathy. Neurobiol Aging 117:1–11. https://doi.org/10.1016/j.neurobiolaging.2022.04.013
12. Beekly DL, Ramos EM, Lee WW, Deitrich WD, Jacka ME, Wu J et al (2007) The National Alzheimer's Coordinating Center (NACC) database: the Uniform Data Set. Alzheimer Dis Assoc Disord 21(3):249–258. https://doi.org/10.1097/WAD.0b013e318142774e
13. Besser LM, Kukull WA, Teylan MA, Bigio EH, Cairns NJ, Kofler JK et al (2018) The Revised National Alzheimer's Coordinating Center's Neuropathology Form-Available Data and New Analyses. J Neuropathol Exp Neurol 77(8):717–726. https://doi.org/10.1093/jnen/nly049
14. Morris JC, Weintraub S, Chui HC, Cummings J, Decarli C, Ferris S et al (2006) The Uniform Data Set (UDS): clinical and cognitive variables and descriptive data from Alzheimer Disease Centers. Alzheimer Dis Assoc Disord 20(4):210–216. https://doi.org/10.1097/01.wad.0000213865.09806.92
15. Weintraub S, Salmon D, Mercaldo N, Ferris S, Graff-Radford NR, Chui H et al (2009) The Alzheimer's Disease Centers' Uniform Data Set (UDS): the neuropsychologic test battery. Alzheimer Dis Assoc Disord 23(2):91–101. https://doi.org/10.1097/WAD.0b013e318191c7dd
16. Weintraub S, Besser L, Dodge HH, Teylan M, Ferris S, Goldstein FC et al (2018) Version 3 of the Alzheimer Disease Centers' Neuropsychological Test Battery in the Uniform Data Set (UDS). Alzheimer Dis Assoc Disord 32(1):10–17. https://doi.org/10.1097/WAD.0000000000000223
17. Scheltens P, Leys D, Barkhof F, Huglo D, Weinstein HC, Vermersch P et al (1992) Atrophy of medial temporal lobes on MRI in "probable" Alzheimer's disease and normal ageing: diagnostic value and neuropsychological correlates. J Neurol Neurosurg Psychiatry 55(10):967–972. https://doi.org/10.1136/jnnp.55.10.967
18. Koedam EL, Lehmann M, van der Flier WM, Scheltens P, Pijnenburg YA, Fox N et al (2011) Visual assessment of posterior atrophy development of a MRI rating scale. Eur Radiol 21(12):2618–2625. https://doi.org/10.1007/s00330-011-2205-4
19. Mahammedi A, Wang LL, Williamson BJ, Khatri P, Kissela B, Sawyer RP et al (2022) Small Vessel Disease, a Marker of Brain

Health: What the Radiologist Needs to Know. AJNR Am J Neuroradiol 43(5):650–660. https://doi.org/10.3174/ajnr.A7302
20. Morris JC (1993) The Clinical Dementia Rating (CDR): current version and scoring rules. Neurology 43(11):2412–2414. https://doi.org/10.1212/wnl.43.11.2412-a
21. O'Bryant SE, Waring SC, Cullum CM, Hall J, Lacritz L, Massman PJ et al (2008) Staging dementia using Clinical Dementia Rating Scale Sum of Boxes scores: a Texas Alzheimer's research consortium study. Arch Neurol 65(8):1091–1095. https://doi.org/10.1001/archneur.65.8.1091
22. Saridin FN, Chew KA, Reilhac A, Gyanwali B, Villaraza SG, Tanaka T et al (2022) Cerebrovascular disease in suspected non-Alzheimer's pathophysiology and cognitive decline over time. Eur J Neurol 29(7):1922–1929. https://doi.org/10.1111/ene.15337
23. Alber J, Alladi S, Bae HJ, Barton DA, Beckett LA, Bell JM et al (2019) White matter hyperintensities in vascular contributions to cognitive impairment and dementia (VCID): Knowledge gaps and opportunities. Alzheimers Dement (N Y) 5:107–117. https://doi.org/10.1016/j.trci.2019.02.001
24. Simpson JE, Fernando MS, Clark L, Ince PG, Matthews F, Forster G et al (2007) White matter lesions in an unselected cohort of the elderly: astrocytic, microglial and oligodendrocyte precursor cell responses. Neuropathol Appl Neurobiol 33(4):410–419. https://doi.org/10.1111/j.1365-2990.2007.00828.x
25. Swardfager W, Yu D, Scola G, Cogo-Moreira H, Chan P, Zou Y et al (2017) Peripheral lipid oxidative stress markers are related to vascular risk factors and subcortical small vessel disease. Neurobiol Aging 59:91–97. https://doi.org/10.1016/j.neurobiolaging.2017.06.029
26. Garnier-Crussard A, Cotton F, Krolak-Salmon P, Chetelat G (2023) White matter hyperintensities in Alzheimer's disease: Beyond vascular contribution. Alzheimers Dement 19(8):3738–3748. https://doi.org/10.1002/alz.13057
27. Shirzadi Z, Schultz SA, Yau WW, Joseph-Mathurin N, Fitzpatrick CD, Levin R et al (2023) Etiology of White Matter Hyperintensities in Autosomal Dominant and Sporadic Alzheimer Disease. JAMA Neurol 80(12):1353–1363. https://doi.org/10.1001/jamaneurol.2023.3618
28. Weaver NA, Doeven T, Barkhof F, Biesbroek JM, Groeneveld ON, Kuijf HJ et al (2019) Cerebral amyloid burden is associated with white matter hyperintensity location in specific posterior white matter regions. Neurobiol Aging 84:225–234. https://doi.org/10.1016/j.neurobiolaging.2019.08.001
29. Brickman AM, Zahodne LB, Guzman VA, Narkhede A, Meier IB, Griffith EY et al (2015) Reconsidering harbingers of dementia: progression of parietal lobe white matter hyperintensities predicts Alzheimer's disease incidence. Neurobiol Aging 36(1):27–32. https://doi.org/10.1016/j.neurobiolaging.2014.07.019
30. Wahlund LO, Barkhof F, Fazekas F, Bronge L, Augustin M, Sjogren M et al (2001) A new rating scale for age-related white matter changes applicable to MRI and CT. Stroke 32(6):1318–1322. https://doi.org/10.1161/01.str.32.6.1318
31. Teylan M, Besser LM, Crary JF, Mock C, Gauthreaux K, Thomas NM et al (2019) Clinical diagnoses among individuals with primary age-related tauopathy versus Alzheimer's neuropathology. Lab Invest 99(7):1049–1055. https://doi.org/10.1038/s41374-019-0186-0
32. Besser LM, Mock C, Teylan MA, Hassenstab J, Kukull WA, Crary JF (2019) Differences in Cognitive Impairment in Primary Age-Related Tauopathy Versus Alzheimer Disease. J Neuropathol Exp Neurol 78(3):219–228. https://doi.org/10.1093/jnen/nly132
33. Montine TJ, Monsell SE, Beach TG, Bigio EH, Bu Y, Cairns NJ et al (2016) Multisite assessment of NIA-AA guidelines for the neuropathologic evaluation of Alzheimer's disease. Alzheimers Dement 12(2):164–169. https://doi.org/10.1016/j.jalz.2015.07.492

Publisher's Note Springer Nature remains neutral with regard to jurisdictional claims in published maps and institutional affiliations.

SUPPLEMENTARY TABLES

Table S1. Correlation analysis between CDR Sum Of Boxes and the Fazekas scores in patients with Alzheimer's disease and primary age-related tauopathy, before and after adjusting for age and Braak.

Uncorrected	AD				PART			
	Fazekas perivent		Fazekas deep		Fazekas perivent		Fazekas deep	
	R	*p*	*R*	*p*	*R*	*p*	*R*	*p*
CDR-SB	-0.08	0.384	-0.11	0.184	-0.15	0.443	-0.16	0.404

Corrected age & Braak	AD				PART			
	Fazekas perivent		Fazekas deep		Fazekas perivent		Fazekas deep	
	R	*p*	*R*	*p*	*R*	*p*	*R*	*p*
CDR-SB	0.01	0.948	-0.13	0.125	-0.03	0.893	0.10	0.606

The table shows the R Pearson correlation coefficients and respective *P*-values of the correlation analysis between the CDR Sum of Boxes (CDR-SB) and the Fazekas scores (periventricular and deep) among 2 groups of patients, distributed according to the absence (ie PART) or presence (ie AD) of neocortical neuritic plaques after neuropsychological evaluation. There are no significant correlations, nor differences between groups. $p < 0.05$ considered as statistically significant.

Table S2. Correlation analysis between relative regional brain atrophy and the Fazekas scores corrected for age in patients with Alzheimer's disease and primary age-related tauopathy.

Corrected age	AD				PART			
	Fazekas perivent		Fazekas deep		Fazekas perivent		Fazekas deep	
	R	*p*	*R*	*p*	*R*	*p*	*R*	*p*
AC	**0.21**	**0.016**	0.13	0.140	0.20	0.293	0.28	0.148
OF	**0.19**	**0.024**	0.15	0.078	0.22	0.248	0.37	0.051
AT	**0.19**	**0.026**	**0.20**	**0.021**	0.07	0.724	0.22	0.246
FI	**0.27**	**0.002**	**0.18***	**0.031**	**0.53**	**0.003**	**0.62***	**<0.001**
MTA	**0.30**	**<0.001**	**0.30**	**<0.001**	**0.39**	**0.037**	**0.47**	**0.010**
Post	-0.16	0.07	-0.18	0.053	-0.21	0.973	0.04	0.840

The analyses presented here are relating to figure 2. The table shows the *R* Pearson correlation coefficients and respective *P*-values of the correlation analysis between relative regional brain atrophy and the Fazekas scores (periventricular and deep) among 2 groups of patients, distributed according to the absence (ie PART) or presence (ie AD) of neocortical neuritic plaques after neuropsychological evaluation. As described in the manuscript, in AD patients, there are significant correlations (represented in **bold**) between the Fazekas scores (periventricular and deep) and atrophy in the medial temporal and orbitofrontal regions, and between the periventricular Fazekas and the fronto- insular region, while in PART patients, significant positive correlations were found between the Fazekas scores (periventricular and deep) and atrophy in the medial temporal and fronto-insular regions, and between the deep Fazekas and atrophy in the orbitofrontal region. Moreover, a statistically significant difference between the regression lines assessing atrophy in the frontoinsular region and the deep Fazekas score in AD versus PART patients (represented by *). $p < 0.05$ considered as statistically significant.

Table S3. Intraclass correlation coefficients (ICC) between raters.

	ICC	*p*
Anterior Cingulate	0.808	<0.001
Orbito-Frontal	0.862	
Anterior Temporal	0.687	
Fronto-Insular	0.768	
Medial Temporal	0.937	
Posterior	0.817	
Periventricular Fazekas	0.894	
Deep Fazekas	0.910	

The table shows significant intraclass correlations between both raters, with values between 0.5 and 0.75, 0.75 and 0.90, and greater than 0.90 indicating, respectively, moderate, good and excellent reliability.

Table S4. Residuals corrected for age of relative regional brain atrophy differences among groups classified according to the density of neocortical neuritic plaques (CERAD score).

Corrected age	PART	AD			
	CERAD 0 (None) (n = 29)	**CERAD 1** (Sparse) (n = 17)	**CERAD 2** (Moderate) (n = 54)	**CERAD 3** (Severe) (n = 67)	*p*
AC	-0.155 (±0.772)	0.355 (±1.130)	-0.193 (±0.717)	0.128 (±0.918)	0.124
OF	0.185 (±0.725)	-0.208 (±1.052)	0.087 (±0.818)	-0.092 (±0.913)	0.268
AT	0.085 (±0.584)	-0.347 (±0.700)	-0.051 (±1.038)	0.0909 (±0.855)	0.320
FI	0.197 (±0.896)	-0.438 (±0.808)	-0.199 (±0.821)	0.187 (±0.857)	**0.022**
MTA	-0.191 (±0.754)	-0.346 (±0.898)	-0.089 (±0.931)	0.236 (±0.815)	**0.044**
Post	0.043 (0.823)	-0.103 (±0.899)	-0.227 (±0.784)	0.188 (±0.922)	0.099

The table shows the assessment of potential differences between the residuals corrected for age of relative regional brain atrophy among groups classified according to the CERAD score, by using Kruskal-Wallis tests. The residuals are represented by mean (standard deviation) for each group, and significant differences with the *p*-value in **bold**. $p < 0.05$ considered as statistically significant.

SUPPLEMENTARY FIGURE

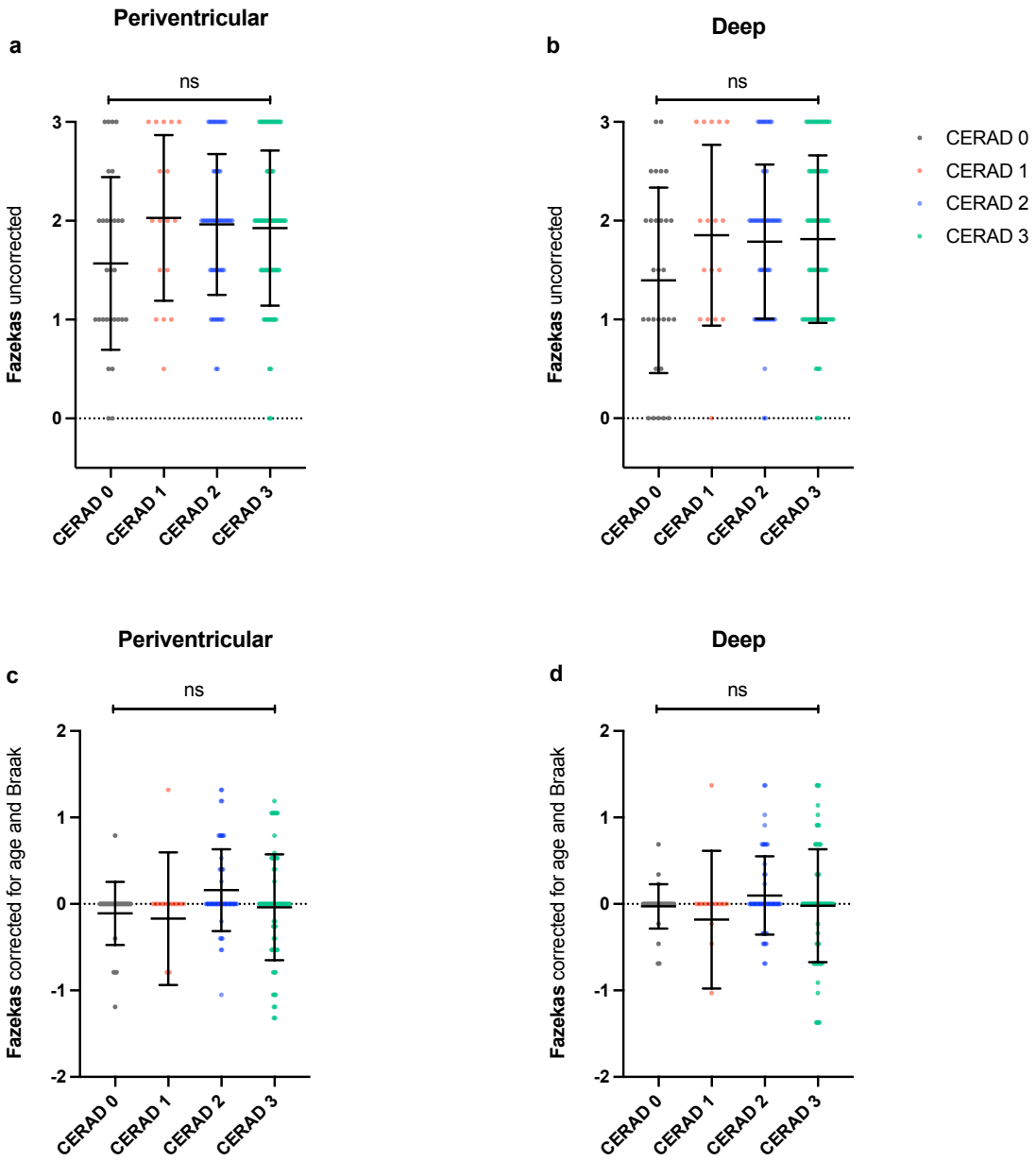


Figure S1. No statistically significant differences were found in the periventricular or deep Fazekas scores between patients from groups with CERAD 0 to 3, without correction for potential confounding factors **(a,b)** and after correction for age and Braak **(c,d)**. 'ns' represents non-significant differences between groups.

Chapter 2.3

Miguel Quintas-Neves, Alexandra Santos, Francisco C. Almeida, Kathryn Gauthreaux, Merilee A. Teylan, Charles N. Mock, Walter A. Kukull, John F. Crary, Tiago Gil Oliveira

ERICA scale magnetic resonance imaging assessment in Alzheimer's disease and primary age-related tauopathy

(In preparation for submission)

ARTICLE TYPE: Original Research.

TITLE: ERICA scale magnetic resonance imaging assessment in Alzheimer's disease and primary age-related tauopathy.

Miguel Quintas-Neves[1,2,3], Francisco C. Almeida[1,2,4], Alexandra Santos[1,2], Kathryn Gauthreaux[5], Charles N. Mock[5], Walter A. Kukull[5], John F. Crary[6], Tiago Gil Oliveira[1,2,3,*]

[1]Life and Health Sciences Research Institute (ICVS), School of Medicine, University of Minho, Braga, Portugal.

[2]ICVS/3B's—PT Government Associate Laboratory, Braga/Guimarães, Portugal.

[3]Department of Neuroradiology, Hospital de Braga, ULS Braga, Braga, Portugal.

[4]Department of Neuroradiology, Centro Hospitalar Universitário do Porto, Porto, Portugal.

[5]Department of Epidemiology, National Alzheimer's Coordinating Center, University of Washington, Seattle, Washington.

[6]Neuropathology Brain Bank & Research Core, Department of Pathology, Nash Family Department of Neuroscience, Department of Artificial Intelligence & Human Health, Friedman Brain Institute, Ronald M. Loeb Center for Alzheimer's Disease, Icahn School of Medicine at Mount Sinai, New York, New York.

(*)Correspondence:

Tiago Gil Oliveira

Life and Health Sciences Research Institute (ICVS), School of Medicine, University of Minho, Campus Gualtar, 4710-057 Braga, Portugal; Tel: +351253604923, tiago@med.uminho.pt.

ABSTRACT

Background: Even though entorhinal cortex atrophy is an early finding in Alzheimer's disease (AD), its characterization in primary age-related tauopathy (PART) and the relationship with AD neuropathologies is understudied.

Purpose: To assess differences in the entorhinal cortex using the MRI visual rating scale for regional atrophy (ERICA), between PART and AD, while assessing its relationship with clinical impairment.

Materials and Methods: Retrospective study based on the National Alzheimer's Coordinating Center database, with participants' last clinical visit and MRI scans ≤ 4 years from death. Two raters assessed the ERICA score and the CDR Sum of Boxes (CDR-SB) was considered for clinical evaluation. Groups were created according to the Consortium to Establish a Registry for Alzheimer's disease (CERAD) score: 0 (PART), 1 (mild AD), 2 (moderate AD), 3 (severe AD). Cross-sectional differences were assessed, followed by evaluation of differences between the ERICA score. Linear regression was used to assess the relationship between ERICA score and CDR-SB.

Results: 305 participants (mean age, 77 years ± 12 [SD]; 185 male) were studied: 70 PART, 37 mild AD, 83 moderate AD, and 114 severe AD. After correcting for age and sex, significant differences were found in the ERICA score between CERAD 0 and 3 ($p < 0.001$), 1 and 3 ($p = 0.002$), and PART and the AD continuum (i.e. CERAD 1-3) ($p < 0.001$), as were also significant correlations found between the ERICA score and the CDR-SB in PART ($p < 0.001$, $R = 0.41$) and in the AD continuum ($p < 0.001$, $R = 0.48$).

Conclusion: These findings support the use of the ERICA score across the AD continuum.

DISCLOSURE OF POTENTIAL CONFLICTS OF INTEREST:

T.G.O. has been a consultant for Sonae and Guidepoint, has received fees as a speaker from Eisai and conference fees covered from Roche and Lilly. The remaining authors have no disclosures to report.

INTRODUCTION

Alzheimer's disease (AD) is a disorder characterized by global cognitive decline, typically involving episodic memory, with progressive functional decline (Tanzi & Bertram, 2005). It can be diagnosed by identification of neurofibrillary tangles and amyloid-β (Aβ) brain deposition, *in vivo* (using the AT(N) biomarkers proposed by the National Institute on Aging and Alzheimer's Association (NIA-AA) 2018 Research Framework) (Jack et al., 2018) or *postmortem* (using the "ABC score", by grading amyloid plaques with Thal phases (A), neurofibrillary tangles with Braak staging (B), and neuritic plaques by the Consortium to Establish a Registry for AD (CERAD) (Hyman et al., 2012).

Primary age-related tauopathy (PART) is a condition characterized by deposition of tau-positive neurofibrillary tangles, in the absence of neuritic plaques (Crary et al., 2014), making this condition essentially a *postmortem* diagnosis. Moreover, patients can be classified as "symptomatic" (dementia or cognitive deterioration present during life) or "asymptomatic" (Crary et al., 2014). Given that AD is diagnosed more than 50% of the time in PART individuals with mild cognitive impairment or dementia (Teylan et al., 2019), there is a need for *in vivo* diagnostic tools to differentiate PART from other neurodegenerative diseases during life, mainly AD, by assessing the cognitive domains involved and several biomarkers, such as nuclear medicine tracer deposition, cerebrospinal fluid parameters and magnetic resonance imaging (MRI) findings. In line with this, studies have shown that the entorhinal cortex and the transentorhinal region are among the first brain structures to show pathologic changes in AD, even before the hippocampus (Braak & Braak, 1991; Delacourte et al., 1999; Khan et al., 2014). Its applicability in PART is, however, unknown, despite this condition being characterized by neurofibrillary tangle deposition in the entorhinal cortex (Crary et al., 2014).

One method of evaluating entorhinal cortex atrophy is by using the entorhinal cortex atrophy score (ERICA) with the aim of detecting AD in an early phase; a score of at least 2 showed an accurate discrimination between subjective cognitive decline and clinically manifest AD (Enkirch et al., 2018).

This study aims to assess potential differences in the entorhinal cortex by *in vivo* brain MRI, using the semiquantitative visual rating scale ERICA (Enkirch et al., 2018), between individuals with "definite" PART and AD, while also assessing the relationship between this score and the degree of clinical impairment, based on Clinical Dementia Rating (CDR) metrics (Morris et al., 1993).

MATERIALS AND METHODS

Study design, participants and selection criteria

This is a retrospective study based on the National Alzheimer's Coordinating Center database, a repository for data collected at the AD Centers located across the US (Beekly et al., 2007; Besser et al., 2018; Morris et al., 2006; Weintraub et al., 2018; Weintraub et al., 2009). All participants provided written informed consent at each local Center, and study protocols were approved by the respective institutional review boards. Participants who contributed to the Neuropathology Data Set gave consent for autopsy.

Our sample was obtained from the March 2024 data freeze, which included 10365 patients with clinical Uniform Data Set data within 2 years from death, and with neuritic plaque and neurofibrillary tangle burden assessed at autopsy. All visits from patients with MRI scans performed no more than 4 years before the date of death and who had neuropathology data available were collected (n = 442); only the last visit and respective brain MRI scan were considered for the analysis. Patients with no 3D T1-weighted sequence (n = 119) and those with images severely affected by artifacts (n = 18) were excluded; a final sample of 305 participants was obtained (Figure 1).

This article follows the STROBE guidelines.

Neuropathology

Participants were categorized according to the Braak stage for neurofibrillary degeneration and CERAD stage. Details on brain tissue preparation and staining within the Neuropathology dataset have been previously described (Besser et al., 2018).

Brain MRI data and imaging analysis

MRI examinations were performed on 1.5T or 3T scanners, both from Philips®, Siemens® or GE® manufacturers. For our analysis, we used 3D T1-weighted sequences, on which we applied the previously validated visual rating scale ERICA (Enkirch et al., 2018). This was performed on a coronal reformat, perpendicular to the hippocampus and at the level of the mammillary bodies, with a score of 0 (normal volume of the entorhinal cortex/parahippocampal gyrus), 1 (mild atrophy with widening of the collateral sulcus), 2 (moderate atrophy with detachment of the entorhinal cortex from the cerebellar tentorium – "tentorial cleft sign") or 3 (pronounced atrophy of the parahippocampal gyrus and a wide cleft between the entorhinal cortex and the cerebellar tentorium). To increase the acuity of the rating process, reference imagens were provided to both classifiers based on Enkirch et al (Enkirch et al., 2018).

Two independent classifiers with 8 and 4 years of experience in clinical neuroradiology were responsible for rating the images, while being unaware of the diagnosis or neuropathological associated changes. In all cases, an average of both classifiers was used. Figure 2 depicts an example of a patient in which this rating method was performed.

Neuropsychological assessment

We used CDR metrics performed at the last Uniform Data Set visit prior to death. The CDR score (Morris et al., 1993) used with the purpose of staging the severity of AD takes into consideration six cognitive categories: orientation, memory, judgment and problem solving, community affairs, home and hobbies, and personal care. It is based on a five-point scale in which none = 0, questionable = 0.5, mild = 1, moderate = 2, and severe = 3. The CDR Sum of Boxes (CDR-SB) is calculated by summing the ratings of these cognitive domains and reflects a quantitative global measure, that ranges from 0 (normal) to 18 (severe dementia) (O'Bryant et al., 2008).

Statistical analysis and bias control

Part of our analysis was based on the division into four groups according to the CERAD score (i.e. density of neocortical neuritic plaques): CERAD 0 (none – "definite" PART); CERAD 1 (sparse – mild AD); CERAD 2 (moderate – moderate AD); CERAD 3 (severe – severe AD). χ^2 test or one-way ANOVA were performed to assess potential baseline differences between groups, followed by appropriate post hoc analyses whenever they were significantly different ($p < 0.05$). Intraclass correlation coefficients were calculated for assessing the acuity of the rating process between classifiers, with a significant correlation obtained between raters ($p < 0.05$), and good reliability (~ 0.80). One-way or Brown-Forsythe/Welch ANOVA tests, as well as Kruskal-Wallis test, were also performed in order to check for significant differences between the ERICA score in the 4 groups of CERAD, followed by appropriate post hoc analysis whenever significant results were obtained ($p < 0.05$), after correcting for Braak, age and sex. A Mann-Whitney test was applied to check differences between groups with absence (i.e. "definite" PART) and presence (i.e. AD neuropathological change) of neuritic plaques.

Linear regression models and Pearson correlation coefficients were used to assess the relation between the ERICA score and the CDR-SB, after correction for age and sex, in "definite" PART versus AD. Values were expressed as (R) and considered statistically significant when $p < 0.05$. ANCOVA was then performed in order to compare the slopes of the regression lines. All statistical analysis and graphics were performed on SPSS Statistics version 30 and GraphPad version 10.4.0.

RESULTS

A final sample of 305 patients were included: 70 with no ("definite" PART – CERAD 0), 37 with sparse (CERAD 1), 83 with moderate (CERAD 2), and 114 with severe (CERAD 3) neuritic plaques density. Significant differences were found between groups regarding sex, with a male predominance in CERAD 3 (approximately 71%), a female predominance in CERAD 1 (approximately 85%), and a 50:50 distribution in CERAD 0 and CERAD 2 (Table 1). Statistically significant differences between groups were also found in the mean age at death and in the mean age at last MRI, with lower values in CERAD 0 (74.5 ± 15.1 and 72.3 ± 14.9, respectively) and 3 (76.4 ± 10.6 and 74.0 ± 10.7, respectively), and higher values in CERAD 1 (88.3 ± 7.2 and 85.8 ± 7.3, respectively) and 2 (83.7 ± 8.4 and 81.5 ± 8.2, respectively) (Table 1). The global CDR and CDR-SB were lower for CERAD 0 (1.1 ± 1.1 and 6.4 ± 6.3, respectively), 1 (0.9 ± 1.0 and 5.0 ± 6.0, respectively) and 2 (1.4 ± 1.0 and 7.9 ± 6.0, respectively), and higher for CERAD 3 (2.2 ± 0.9 and 12.6 ± 5.1, respectively). Moreover, CERAD 0 presented values of CDR between those of CERAD 1 and 2, with no differences between them. Braak staging was also significantly different between groups, with a predominance of lower grades (Braak I and II) in CERAD 0 (i.e. "definite" PART) and higher grades (Braak V and VI) in the more advanced AD spectrum CERAD 2 and 3 cases (Table 1). After correcting for age and sex, statistically significant differences were found in ERICA scores between CERAD 0 and 3 ($p < 0.001$), and CERAD 1 and 3 ($p = 0.002$) (Figure 3A). Moreover, significant differences were also found in the ERICA score between "definite" PART (i.e. CERAD 0) and AD neuropathological change (i.e. CERAD 1-3) after correcting for age and sex ($p < 0.001$; Figure 3B). When also correcting for Braak (i.e. Braak, sex and age), no significant differences were found between the four CERAD groups ($p = 0.25$; Figure 4A) or between PART (i.e. CERAD 0) and AD neuropathological change (i.e. CERAD 1-3) ($p = 0.67$; Figure 4B).

Significant positive correlations were found between the ERICA score and the CDR-SB, in the PART group ($p < 0.001$, $R = 0.41$) and in the AD neuropathological change group ($p < 0.001$, $R = 0.48$), after

correcting for sex and age (Figure 5). No significant differences were found between PART compared to AD regarding ERICA and CDR-SB correlations (Figure 5).

DISCUSSION

This study aimed to assess potential differences in the entorhinal cortex by *in vivo* brain MRI, using the semiquantitative visual rating scale ERICA (Enkirch et al., 2018), between individuals with "definite" PART and in the AD spectrum, while also assessing the relationship between this score and the degree of clinical impairment, based on CDR metrics (Morris et al., 1993). Upon taking into account age and sex as potential confounding factors, we found significant differences in the ERICA score between CERAD 0 (i.e. "definite" PART) and CERAD 3 (i.e. severe AD), and between CERAD 1 (i.e. mild AD) and CERAD 3. Moreover, significant differences were also found between CERAD 0 (i.e. "definite" PART) and the AD neuropathological change group (i.e. CERAD 1-3). These findings are in line with the known evidence that the entorhinal cortex is a starting point of atrophy in AD, even before the hippocampus, with the first stage of the disease (i.e. CERAD 1) being typically characterized by neuronal pathology in the entorhinal region in the form of neurofibrillary tangles and neuropil threads (Braak & Braak, 1991). This could also explain the lack of differences among groups after correcting for Braak, as it is known that atrophy patterns are directly correlated with neurofibrillary tangle deposition, while not as much impacted by Aβ deposition (Nelson et al., 2012; Quintas-Neves et al., 2022). Moreover, our findings indicate that the ERICA score presents a stepwise increase from CERAD 1 to CERAD 3, with CERAD 0 (i.e. PART patients) being positioned between CERAD 1 and 2, which suggests that this score can successfully distinguish patients with PART or mild AD from those with severe AD, much like the well-established medial temporal atrophy (Scheltens et al., 1992). Moreover, the ERICA score is known to have high specificity for AD diagnosis and to correlate well with cerebrospinal fluid AD biomarkers, with abnormal levels for a score of 2, which supports the use of the tentorial cleft sign as a pathologic cutoff (Enkirch et al., 2018). Globally, our results further support this concept, due to the significant differences between mild AD and PART and severe AD, which were nullified after correcting for Braak. Importantly, the differences found in the ERICA score between PART and AD are mainly at the expense of severe AD stages (i.e. CERAD 3). Our results

showing similar entorhinal cortex atrophy for PART and mild AD (i.e. CERAD 1) are in line with the known entorhinal cortex deposition of neurofibrillary tangle on both conditions (Braak & Braak, 1991; Crary et al., 2014). It has been previously observed that PART had intermediate levels of medial temporal atrophy, not following the step-wise increase in atrophy in the AD continuum, from CERAD 1 to 3 (Quintas-Neves et al., 2022), indicating that other co-pathologies such as TDP-43 (Josephs et al., 2017; Quintas-Neves et al., 2022), Lewy bodies (Almeida et al., 2025) or vascular changes (Quintas-Neves et al., 2024) could be relevant drivers of neurodegeneration. When comparing medial temporal atrophy with ERICA scores, ERICA depicts more specifically the early stages of AD pathology and PART, with neurofibrillary tangles confined to the entorhinal cortex and adjacent regions, distinguishing them from more advanced cases of AD.

Another important remark is the correlation found between the ERICA score and CDR-SB, not only in AD but also in PART patients. These results are in line with the well-known role of the entorhinal cortex in learning and memory formation (Squire & Zola-Morgan, 1991), as well as in semantic memory/semantic fluency (Davies et al., 2004; Enkirch et al., 2018). Moreover, these findings support the known correlation between temporal atrophy and semantic memory/language deficits in PART patients (Quintas-Neves et al., 2019). Therefore, since a higher ERICA score correlates well with worse cognitive performance across the entire CERAD spectrum, our results further support its clinical use.

Within the limitations of this study, it was based on a convenience, autopsy-focused sample, which limits its extrapolation. The National Alzheimer's Coordinating Center database has inherent limitations of generalizability, given the tendency of the participants to be more often Caucasian and more affluent than the general population (Besser et al., 2019). Secondly, the use of a visual rating scale is invariably associated with some level of subjectivity. However, this scale has been shown to be accurate for entorhinal cortex atrophy assessment (Enkirch et al., 2018), as long as applied by trained neuroradiologists. Thirdly, another potential source of variability was the heterogeneity in MRI scanners

and field strengths, which was mitigated by taking only into account 3D T1-weighted acquisitions. Additionally, since Braak staging is an incomplete measure of tau burden, accounting for neurofibrillary tangles regional progression and not regional density and tau accumulation levels, it would be beneficial to have other quantitative measures, such as tau PET. Finally, the retrospective nature of the study is a potential source of bias.

In conclusion, our findings support the clinical use of the ERICA score to grade entorhinal cortex atrophy in patients across the entire CERAD spectrum, with significant differences between those with PART or mild AD and those with severe AD.

REFERENCES

Almeida, F. C., Santos, A., Jesus, T., Coelho, A., Quintas-Neves, M., Gauthreaux, K., Mock, C. N., Kukull, W. A., Crary, J. F., & Oliveira, T. G. (2025). Lewy body co-pathology in Alzheimer's disease and primary age-related tauopathy contributes to differential neuropathological, cognitive, and brain atrophy patterns. *Alzheimers Dement*, *21*(1), e14191. https://doi.org/10.1002/alz.14191

Beekly, D. L., Ramos, E. M., Lee, W. W., Deitrich, W. D., Jacka, M. E., Wu, J., Hubbard, J. L., Koepsell, T. D., Morris, J. C., Kukull, W. A., & Centers, N. I. A. A. s. D. (2007). The National Alzheimer's Coordinating Center (NACC) database: the Uniform Data Set. *Alzheimer Dis Assoc Disord*, *21*(3), 249-258. https://doi.org/10.1097/WAD.0b013e318142774e

Besser, L. M., Kukull, W. A., Teylan, M. A., Bigio, E. H., Cairns, N. J., Kofler, J. K., Montine, T. J., Schneider, J. A., & Nelson, P. T. (2018). The Revised National Alzheimer's Coordinating Center's Neuropathology Form-Available Data and New Analyses. *J Neuropathol Exp Neurol*, *77*(8), 717-726. https://doi.org/10.1093/jnen/nly049

Besser, L. M., Mock, C., Teylan, M. A., Hassenstab, J., Kukull, W. A., & Crary, J. F. (2019). Differences in Cognitive Impairment in Primary Age-Related Tauopathy Versus Alzheimer Disease. *J Neuropathol Exp Neurol*, *78*(3), 219-228. https://doi.org/10.1093/jnen/nly132

Braak, H., & Braak, E. (1991). Neuropathological stageing of Alzheimer-related changes. *Acta Neuropathol*, *82*(4), 239-259. https://doi.org/10.1007/BF00308809

Crary, J. F., Trojanowski, J. Q., Schneider, J. A., Abisambra, J. F., Abner, E. L., Alafuzoff, I., Arnold, S. E., Attems, J., Beach, T. G., Bigio, E. H., Cairns, N. J., Dickson, D. W., Gearing, M., Grinberg, L. T., Hof, P. R., Hyman, B. T., Jellinger, K., Jicha, G. A., Kovacs, G. G.,...Nelson, P. T. (2014). Primary age-related tauopathy (PART): a common pathology associated with human aging. *Acta Neuropathol*, *128*(6), 755-766. https://doi.org/10.1007/s00401-014-1349-0

Davies, R. R., Graham, K. S., Xuereb, J. H., Williams, G. B., & Hodges, J. R. (2004). The human perirhinal cortex and semantic memory. *Eur J Neurosci*, *20*(9), 2441-2446. https://doi.org/10.1111/j.1460-9568.2004.03710.x

Delacourte, A., David, J. P., Sergeant, N., Buee, L., Wattez, A., Vermersch, P., Ghozali, F., Fallet-Bianco, C., Pasquier, F., Lebert, F., Petit, H., & Di Menza, C. (1999). The biochemical pathway of neurofibrillary degeneration in aging and Alzheimer's disease. *Neurology*, *52*(6), 1158-1165. https://doi.org/10.1212/wnl.52.6.1158

Enkirch, S. J., Traschutz, A., Muller, A., Widmann, C. N., Gielen, G. H., Heneka, M. T., Jurcoane, A., Schild, H. H., & Hattingen, E. (2018). The ERICA Score: An MR Imaging-based Visual Scoring System for the Assessment of Entorhinal Cortex Atrophy in Alzheimer Disease. *Radiology*, *288*(1), 226-333. https://doi.org/10.1148/radiol.2018171888

Hyman, B. T., Phelps, C. H., Beach, T. G., Bigio, E. H., Cairns, N. J., Carrillo, M. C., Dickson, D. W., Duyckaerts, C., Frosch, M. P., Masliah, E., Mirra, S. S., Nelson, P. T., Schneider, J. A., Thal, D. R., Thies, B., Trojanowski, J. Q., Vinters, H. V., & Montine, T. J. (2012). National Institute on Aging-Alzheimer's Association guidelines for the neuropathologic assessment of Alzheimer's disease. *Alzheimers Dement*, *8*(1), 1-13. https://doi.org/10.1016/j.jalz.2011.10.007

Jack, C. R., Jr., Bennett, D. A., Blennow, K., Carrillo, M. C., Dunn, B., Haeberlein, S. B., Holtzman, D. M., Jagust, W., Jessen, F., Karlawish, J., Liu, E., Molinuevo, J. L., Montine, T., Phelps, C., Rankin, K. P., Rowe, C. C., Scheltens, P., Siemers, E., Snyder, H. M.,...Contributors. (2018). NIA-AA Research Framework: Toward a biological definition of Alzheimer's disease. *Alzheimers Dement*, *14*(4), 535-562. https://doi.org/10.1016/j.jalz.2018.02.018

Josephs, K. A., Dickson, D. W., Tosakulwong, N., Weigand, S. D., Murray, M. E., Petrucelli, L., Liesinger, A. M., Senjem, M. L., Spychalla, A. J., Knopman, D. S., Parisi, J. E., Petersen, R. C., Jack, C. R., Jr., & Whitwell, J. L. (2017). Rates of hippocampal atrophy and presence of post-mortem TDP-43 in patients with Alzheimer's disease: a longitudinal retrospective study. *Lancet Neurol*, *16*(11), 917-924. https://doi.org/10.1016/S1474-4422(17)30284-3

Khan, U. A., Liu, L., Provenzano, F. A., Berman, D. E., Profaci, C. P., Sloan, R., Mayeux, R., Duff, K. E., & Small, S. A. (2014). Molecular drivers and cortical spread of lateral entorhinal cortex dysfunction in preclinical Alzheimer's disease. *Nat Neurosci*, *17*(2), 304-311. https://doi.org/10.1038/nn.3606

Morris, J. C., Edland, S., Clark, C., Galasko, D., Koss, E., Mohs, R., van Belle, G., Fillenbaum, G., & Heyman, A. (1993). The consortium to establish a registry for Alzheimer's disease (CERAD). Part IV. Rates of cognitive change in the longitudinal assessment of probable Alzheimer's disease. *Neurology*, *43*(12), 2457-2465. https://doi.org/10.1212/wnl.43.12.2457

Morris, J. C., Weintraub, S., Chui, H. C., Cummings, J., Decarli, C., Ferris, S., Foster, N. L., Galasko, D., Graff-Radford, N., Peskind, E. R., Beekly, D., Ramos, E. M., & Kukull, W. A. (2006). The Uniform Data Set (UDS): clinical and cognitive variables and descriptive data from Alzheimer Disease Centers. *Alzheimer Dis Assoc Disord*, *20*(4), 210-216. https://doi.org/10.1097/01.wad.0000213865.09806.92

Nelson, P. T., Alafuzoff, I., Bigio, E. H., Bouras, C., Braak, H., Cairns, N. J., Castellani, R. J., Crain, B. J., Davies, P., Del Tredici, K., Duyckaerts, C., Frosch, M. P., Haroutunian, V., Hof, P. R., Hulette, C. M., Hyman, B. T., Iwatsubo, T., Jellinger, K. A., Jicha, G. A.,...Beach, T. G. (2012). Correlation of Alzheimer disease neuropathologic changes with cognitive status: a review of the literature. *J Neuropathol Exp Neurol*, *71*(5), 362-381. https://doi.org/10.1097/NEN.0b013e31825018f7

O'Bryant, S. E., Waring, S. C., Cullum, C. M., Hall, J., Lacritz, L., Massman, P. J., Lupo, P. J., Reisch, J. S., Doody, R., & Texas Alzheimer's Research, C. (2008). Staging dementia using Clinical Dementia Rating Scale Sum of Boxes scores: a Texas Alzheimer's research consortium study. *Arch Neurol*, *65*(8), 1091-1095. https://doi.org/10.1001/archneur.65.8.1091

Quintas-Neves, M., Almeida, F. C., Gauthreaux, K., Teylan, M. A., Mock, C. N., Kukull, W. A., Crary, J. F., & Oliveira, T. G. (2024). Fazekas scale magnetic resonance imaging assessment in Alzheimer's disease and primary age-related tauopathy. *Neuroradiology*, *66*(12), 2185-2193. https://doi.org/10.1007/s00234-024-03464-2

Quintas-Neves, M., Teylan, M. A., Besser, L., Soares-Fernandes, J., Mock, C. N., Kukull, W. A., Crary, J. F., & Oliveira, T. G. (2019). Magnetic resonance imaging brain atrophy assessment in primary age-related tauopathy (PART). *Acta Neuropathol Commun*, *7*(1), 204. https://doi.org/10.1186/s40478-019-0842-z

Quintas-Neves, M., Teylan, M. A., Morais-Ribeiro, R., Almeida, F., Mock, C. N., Kukull, W. A., Crary, J. F., & Oliveira, T. G. (2022). Divergent magnetic resonance imaging atrophy patterns in Alzheimer's disease and primary age-related tauopathy. *Neurobiol Aging*, *117*, 1-11. https://doi.org/10.1016/j.neurobiolaging.2022.04.013

Scheltens, P., Leys, D., Barkhof, F., Huglo, D., Weinstein, H. C., Vermersch, P., Kuiper, M., Steinling, M., Wolters, E. C., & Valk, J. (1992). Atrophy of medial temporal lobes on MRI in "probable" Alzheimer's disease and normal ageing: diagnostic value and neuropsychological correlates. *J Neurol Neurosurg Psychiatry*, *55*(10), 967-972. https://doi.org/10.1136/jnnp.55.10.967

Squire, L. R., & Zola-Morgan, S. (1991). The medial temporal lobe memory system. *Science*, *253*(5026), 1380-1386. https://doi.org/10.1126/science.1896849

Tanzi, R. E., & Bertram, L. (2005). Twenty years of the Alzheimer's disease amyloid hypothesis: a genetic perspective. *Cell*, *120*(4), 545-555. https://doi.org/10.1016/j.cell.2005.02.008

Teylan, M., Besser, L. M., Crary, J. F., Mock, C., Gauthreaux, K., Thomas, N. M., Chen, Y. C., & Kukull, W. A. (2019). Clinical diagnoses among individuals with primary age-related tauopathy versus

Alzheimer's neuropathology. *Lab Invest*; *99*(7), 1049-1055. https://doi.org/10.1038/s41374-019-0186-0

Weintraub, S., Besser, L., Dodge, H. H., Teylan, M., Ferris, S., Goldstein, F. C., Giordani, B., Kramer, J., Loewenstein, D., Marson, D., Mungas, D., Salmon, D., Welsh-Bohmer, K., Zhou, X. H., Shirk, S. D., Atri, A., Kukull, W. A., Phelps, C., & Morris, J. C. (2018). Version 3 of the Alzheimer Disease Centers' Neuropsychological Test Battery in the Uniform Data Set (UDS). *Alzheimer Dis Assoc Disord*; *32*(1), 10-17. https://doi.org/10.1097/WAD.0000000000000223

Weintraub, S., Salmon, D., Mercaldo, N., Ferris, S., Graff-Radford, N. R., Chui, H., Cummings, J., DeCarli, C., Foster, N. L., Galasko, D., Peskind, E., Dietrich, W., Beekly, D. L., Kukull, W. A., & Morris, J. C. (2009). The Alzheimer's Disease Centers' Uniform Data Set (UDS): the neuropsychologic test battery. *Alzheimer Dis Assoc Disord*; *23*(2), 91-101. https://doi.org/10.1097/WAD.0b013e318191c7dd

TABLES

Table 1 Characterization of patients according to the density of neocortical neuritic plaques (CERAD score).

	CERAD 0 (None) (n=70)	**CERAD 1 (Sparse) (n=37)**	**CERAD 2 (Moderate) (n=83)**	**CERAD 3 (Severe) (n=114)**	***p***
Male sex, n (%)[a]	50 (71.4)	15 (40.5)	50 (60.2)	71 (62.3)	0.021
Age at death, mean (SD)[b]	74.5 (±15.1)	88.3 (±7.2)	83.7 (±8.4)	76.4 (±10.6)	<0.001
Age at last MRI, mean (SD)[c]	72.3 (±14.9)	85.8 (±7.3)	81.5 (±8.2)	74.0 (±10.7)	<0.001
Age MRI-Death, mean (SD)[d]	2.2 (±1.2)	2.5 (±1.3)	2.2 (±1.3)	2.5 (±1.2)	0.310
CDR-SB[d]	6.4 (±6.3)	5.0 (±6.0)	7.9 (±6.0)	12.6 (±5.1)	<0.001
Global CDR[e]	1.1 (±1.1)	0.9 (±1.0)	1.4 (±1.0)	2.2 (±0.9)	<0.001
Braak stage, n (%)[f]					
None	21 (30.0)	0 (0.0)	1 (1.2)	0 (0.0)	
I	17 (24.3)	3 (8.1)	2 (2.4)	2 (1.8)	
II	17 (24.3)	11 (29.7)	11 (13.3)	0 (0.0)	
III	6 (8.6)	8 (21.6)	15 (18.1)	4 (3.5)	
IV	7 (10.0)	11 (29.7)	20 (24.1)	8 (7.0)	
V	1 (1.4)	4 (10.8)	16 (19.3)	29 (25.4)	
VI	1 (1.4)	0 (0.0)	18 (21.7)	71 (62.3)	
Braak stage, mean (SD)	1.5 (±1.5)	3.1 (±1.2)	4.1 (±1.5)	5.4 (±1.0)	<0.001

[a]Male sex refers to the absolute mean and relative percentage of male patients in a given group, represented as n (%).

[b]Age at death is the subject age at the time of death.

[c]Age at last MRI is the subject age at the time the last MRI was performed.

[d]Age MRI-Death is the difference between the subject age at the last performed MRI and time of death. These three variables are reported in years as a continuous variable with mean and standard deviation (SD).

[e]CDR-SB refers to the sum of boxes score from the CDR® Dementia Staging Instrument and global CDR refers to the global Clinical Dementia Rating score; they are both attributed to the subject in the last clinical visit and are also reported as continuous variables with mean and standard deviation.

[f]For each Braak stage (from none to VI) values are represented as number of cases and percentage of total. Data presented as n (%) and mean (±SD).

[*]*p* value for One-way or Brown-Forsythe/Welch Analysis of Variance (ANOVA) or chi-square test, as appropriate. $p < 0.05$ considered as significant.

FIGURES

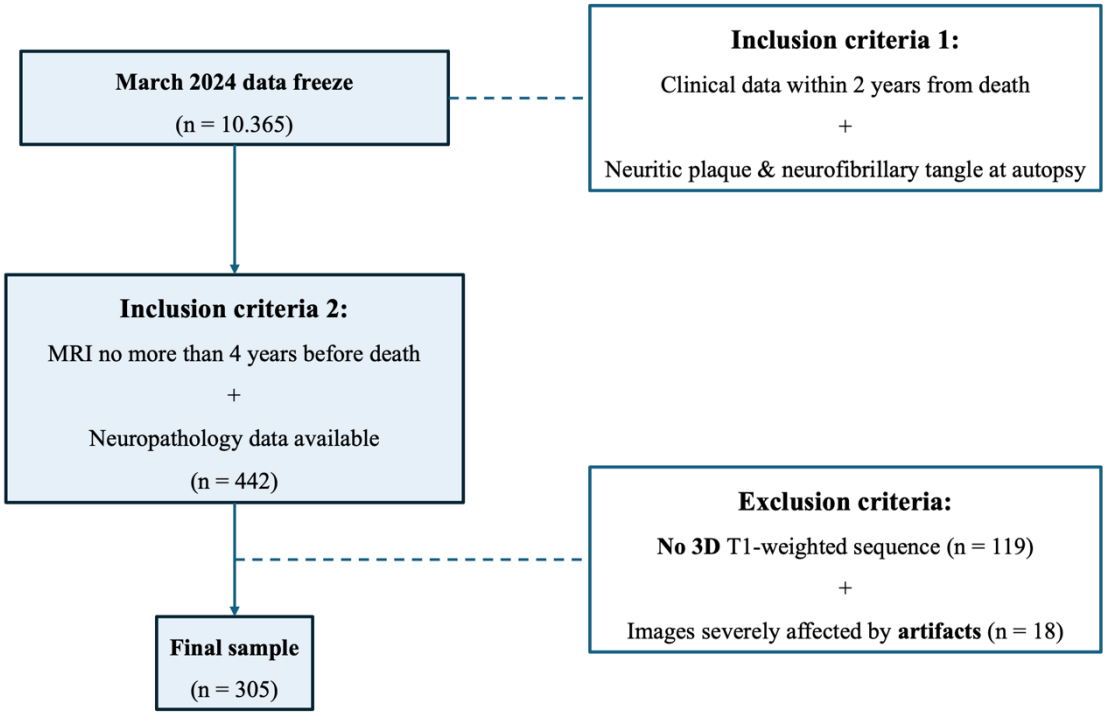


Figure 1. Flow diagram resuming the inclusion and exclusion criteria used to obtain the final sample of patients.

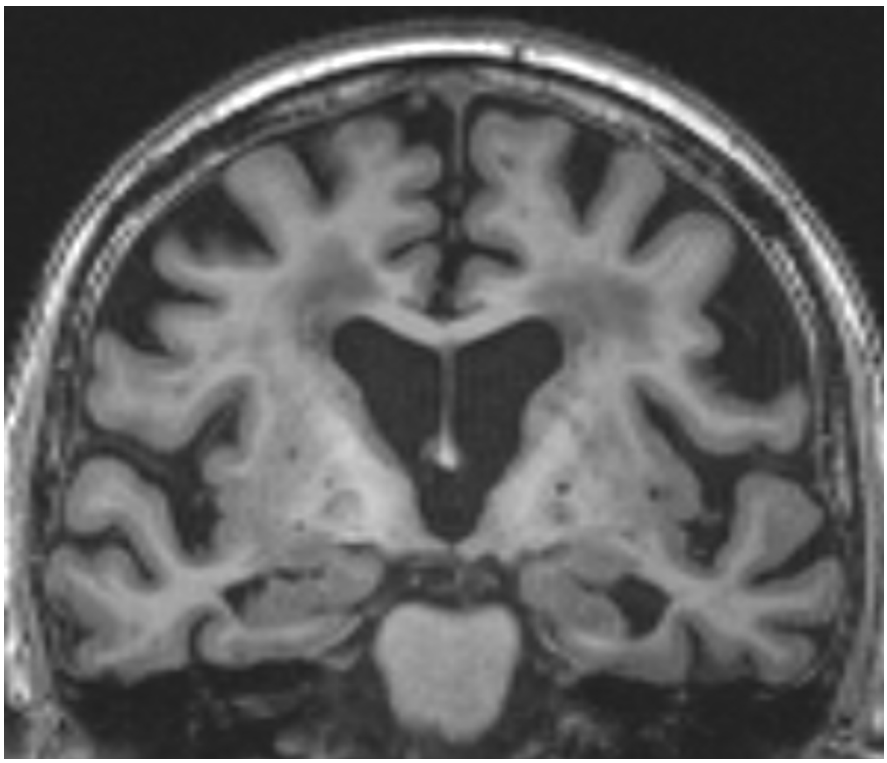


Figure 2. Representative case of a 95-year old male patient with primary age-related tauopathy (PART). Coronal reformat of a 3D T1-weighted sequence shows widening of the right collateral sulcus, in keeping with mild atrophy of the entorhinal cortex and parahippocampal gyrus (ERICA score of 1), and the tentorial cleft sign on the left, in keeping with moderate atrophy of the same structures (ERICA score of 2); therefore, the average score was considered to be 1.5.

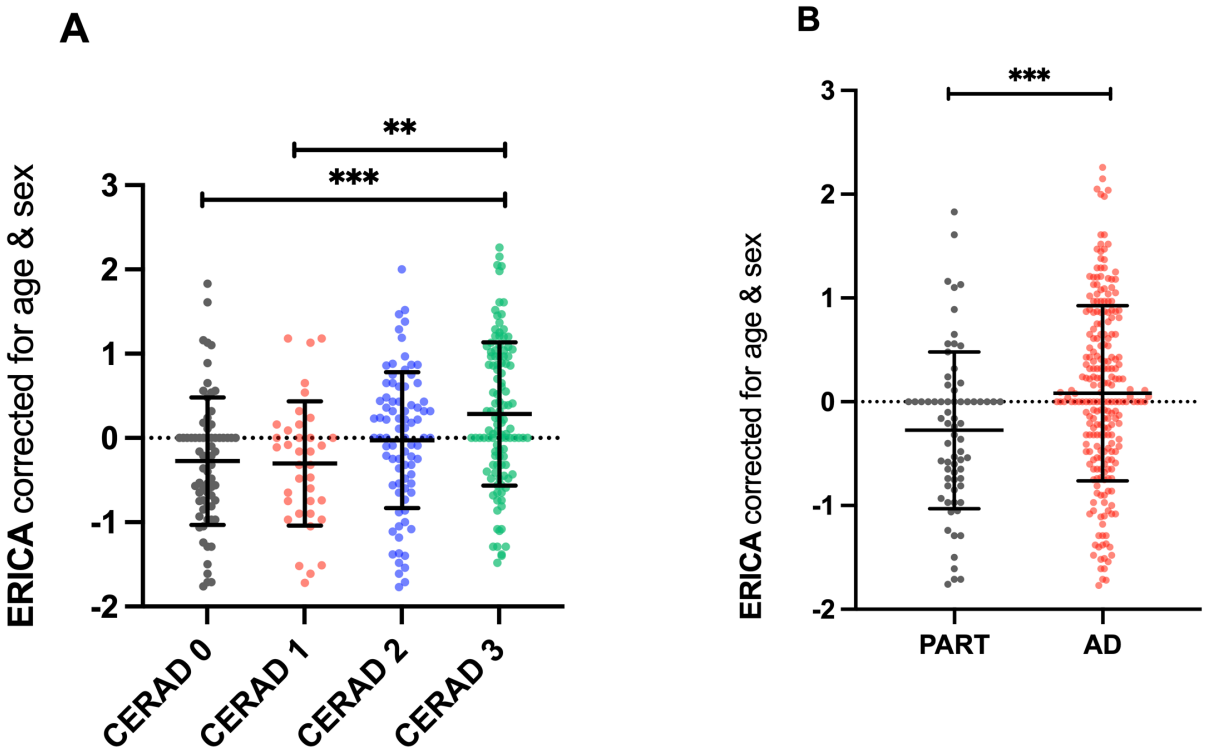


Figure 3. After correcting for age and sex, the entorhinal cortex atrophy (ERICA) score is significantly different **(A)** between CERAD 0 and CERAD 3, and between CERAD 1 and CERAD 3. **(B)** Significant differences are also found between PART and AD neuropathologic change (i.e. CERAD 1-3), after correcting for age and sex. * $p < 0.05$, ** $p < 0.01$ and *** $p < 0.001$.

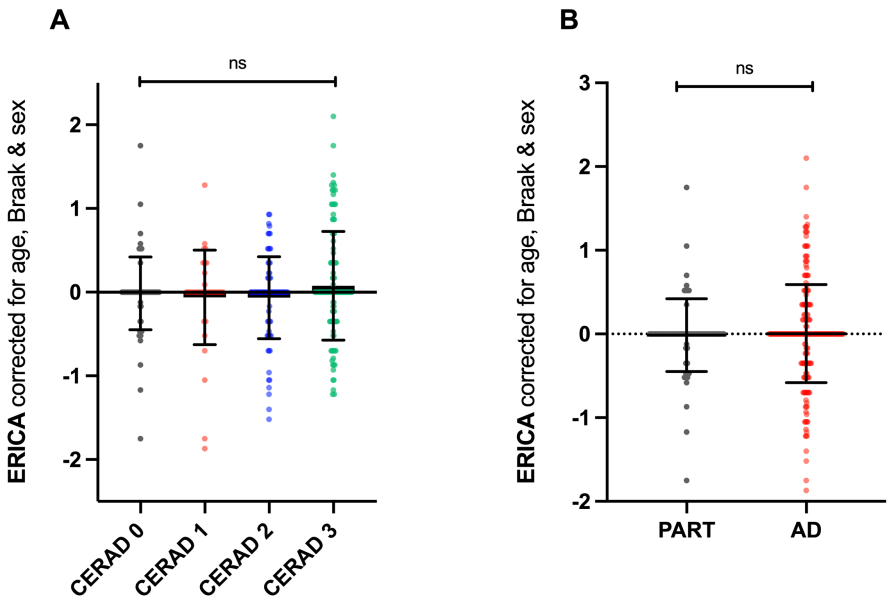


Figure 4. After adjusting for Braak, age and sex, no significant differences are found between the entorhinal cortex atrophy (ERICA) score among the 4 groups of CERAD **(A)** and **(B)** between PART (i.e. CERAD 0) and AD neuropathologic change (i.e. CERAD 1-3). 'ns' represents non-significant differences between groups.

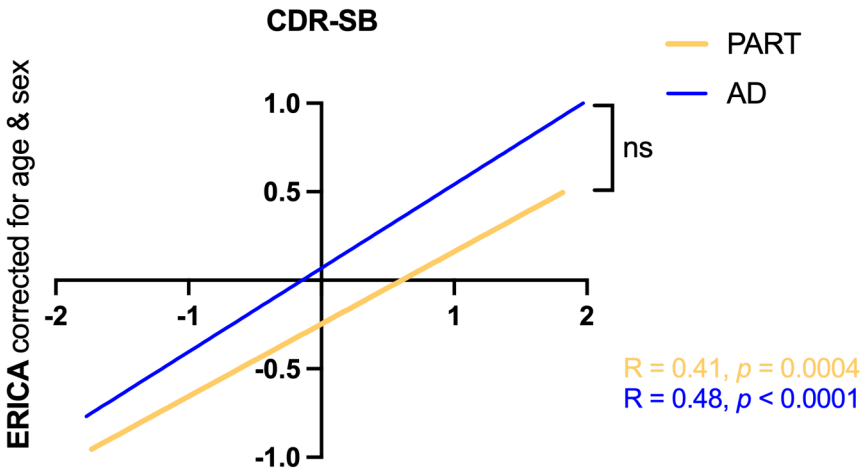


Figure 5. Significant correlations are found between the entorhinal cortex atrophy (ERICA) score and the CDR® Sum of Boxes (CDR-SB), for patients with PART (i.e. CERAD 0) and for patients with AD neuropathologic change (i.e. CERAD 1-3), after controlling for age and sex. There are no significant differences between the regression lines of both groups (i.e. PART vs AD neuropathologic change). Correlation coefficients are represented by *R*. *p*-values < 0.05 considered statistically significant. 'ns' represents non-significant differences between the regression lines of both groups.

The first main aim of this project was to compare the *in vivo* brain MRI findings of individuals with PART and AD, by using previously validated and clinically-applicable visual rating scales (Harper et al., 2016). Moreover, it was assessed the relationship between brain atrophy and the degree of clinical impairment, based on the CDR-SB (Morris, 1993) and neuropsychological tests performance (Weintraub et al., 2018). The obtained results suggest that while AD patients show a stepwise increase in relative age-corrected atrophy in the medial temporal lobe region with increasing CERAD scores, PART individuals present intermediate relative atrophy levels, a finding that further supports PART as an independent pathologic process from AD. Specifically, "definite" PART participants (i.e. CERAD 0) showed higher mean relative age-corrected atrophy than the CERAD 1 cases (i.e. mild AD / "possible" PART) in all the evaluated brain regions, and lower mean relative age-corrected atrophy than the CERAD 3 group (i.e. severe AD) in the medial temporal region, findings that support PART as milder than severe AD but more severe than mild AD. Moreover, it was found that CERAD 1 cases were older at death, had a slight female predominance and had lower levels of age-corrected relative atrophy when compared to the other groups, which is in accordance with more recent observations showing that disease onset at a younger age seems to be associated with more advanced pathology (Jack et al., 2020; Vogel et al., 2021; Whitwell et al., 2019). This finding also supports CERAD 1 (i.e. mild AD / "possible" PART) as a possible state of AD resistance, with CERAD 0 (i.e. PART) representing a completely different condition.

Other co-pathologic factors might be responsible for these differences between groups, such as TDP-43 (Josephs et al., 2020; Josephs et al., 2019; Josephs et al., 2014) and Lewy bodies (Almeida et al., 2023) deposition. Despite only being able to analyze the impact of TDP-43 in a small subset of cases, our results support the notion that this protein contributes to atrophy in PART, but to a lesser extent in AD, most likely due to a ceiling effect (**supplementary figure, chapter 2.2**). Still, these observations suggest that tau (i.e. Braak stage) and TDP-43 contribute differentially to the rate of brain atrophy over time in participants with PART and AD. Moreover, we found evidence that atrophy patterns are mainly Braak-dependent (i.e. dependent on the NFT deposition) and nondependent of the Aβ deposition, further supporting the notion of the widely known correlation between tau NFTs deposition, regional brain atrophy and cognitive deficits, when compared to amyloid-beta plaque distribution (Nelson et al., 2012). Interestingly, PART participants showed a level of atrophy compared to higher CERAD levels, which suggests tau can exert neurodegenerative effects by itself in PART (i.e. independently of neuritic plaques).

The different atrophy patterns found between PART and AD participants is potentially important, as it has been found that clinical AD still is diagnosed more than 50% of the time in PART

patients with mild cognitive impairment or dementia (Teylan et al., 2019), although clinical evidence supports a distinction in the clinical presentation between AD and PART. This observation highlights the potential role of brain MRI as an important tool to differentiate PART from AD, or to follow up patients with PART identified by other biomarkers, such as PET or cerebrospinal fluid. However, due to the fact that our sample of PART participants presented a scarcity of patients with Braak stages of III or IV, this is something future studies should assess.

One of the main objectives of this thesis was to use practical, previously validated and clinically-applicable visual rating scales (Enkirch et al., 2018; Fazekas et al., 1987; Harper et al., 2016) that potentially further validate brain MRI as a clinical routine tool to use in PART participants. The fact that our results are globally in accordance with what other authors and our own team observed with volumetric approaches (F. C. Almeida et al., 2024; Almeida et al., 2025; Josephs, Murray, et al., 2017) further validates our methodologies.

These results are also supported by PET studies assessing *in vivo* Aβ and tau deposition that show synergistic Aβ and tau pathology that lead to higher levels of brain atrophy and worse clinical outcomes (Jack et al., 2019; Weigand et al., 2020). However, it is important to keep in mind that these studies do not segregate Aβ deposition, as performed by the CERAD staging.

We also found overall cognition deficits (given by the CDR-SB) to be directly correlated with regional atrophy in patients with AD, but not in patients with PART. Moreover, we obtained significant differences between the regression lines of both groups (i.e. PART vs AD) for the anterior temporal and posterior regions. These findings indicate that PART and AD show different atrophy patterns, which, in the case of PART, correlate poorly with global cognitive deficits. These are potentially important observations to the clinical routine, as we clearly show different presentations between both conditions, which are in accordance with the previously described steeper decline in cognitive performance shown by AD patients after becoming clinically symptomatic, when compared to PART participants (Teylan et al., 2020). There is now data that shows that this dissociation between atrophy and cognitive performance might be due to other co-pathology known to contribute to cognitive impairment in patients with PART, such as Lewy bodies deposition (Almeida et al., 2023) and cerebrovascular disease (Iida et al., 2021).

Another key finding regarding the first aim was the significant correlation obtained between anterior temporal atrophy and a focal deficit of language in PART participants, while in AD, as expected (Savola et al., 2021; Teylan et al., 2020; Weigand et al., 2020), widespread significant correlations were found between regional atrophy and cognitive deficits. These findings are in accordance with our previous study (Quintas-Neves et al., 2019) that showed a significant correlation between anterior temporal atrophy

and worse performance on semantic memory/language tests in PART participants, and with other reports that showed longitudinal semantic cognitive decline (Jefferson-George et al., 2017) and higher deficits in PART compared to neuropathology negative controls (Weigand et al., 2020).

The second aim of this project was to assess how PART and AD are differentially impacted by brain microangiopathic burden, evaluated by *in vivo* MRI. Using the Fazekas score as an MRI-based surrogate for leukoaraiosis, with the deep white matter hyperintensities predominantly reflecting small vessel disease, we found no major statistically significant differences between groups across the CERAD spectrum nor between "definite PART" and AD participants. However, significant correlations were found between the Fazekas score and regional atrophy patterns on both groups, with PART showing overall stronger positive correlations than in AD, particularly in the medial temporal and in the fronto-insular regions. Conversely, despite small vessel disease not being substantially different between PART and AD at brain MRI, it seems to be differentially contributing to regional brain atrophy, something that further supports the notion of these being two different pathological conditions.

Significant cerebrovascular disease (partially defined as a Fazekas score ≥ 2) was found to be a potential neurodegeneration driver in patients with no significant altered amyloid-beta pathology in PET (i.e. the so-called suspected non-AD pathology or SNAP) (Saridin et al., 2022), and the levels of amyloid deposition, as well as ratings in the Fazekas score (deep and periventricular), have been found to discriminate between cognitively normal and demented individuals (Gordon et al., 2015). Several pathophysiological mechanisms have been described to potentially explain these associations, such as disruption of cholinergic projections from the basal forebrain to the cortex (Alber et al., 2019) and the correlation between the volume of subcortical/deep white matter hyperintensities and lipid peroxidation in the blood, in the setting of hypertension, supporting the hypothesis of a vascular etiology in this location (Swardfager et al., 2017). However, recent studies (Garnier-Crussard et al., 2023; Shirzadi et al., 2023) evaluated the possible etiology of white matter hyperintensities in AD patients, and found that it can be due not only to vascular disease but also secondary to AD pathology itself, from which the term "AD-related white matter hyperintensities" was proposed. Moreover, other studies (Brickman et al., 2015; Weaver et al., 2019) found an association between AD and a posterior predominance of white matter hyperintensities (i.e. parieto-occipital and posterior periventricular areas), with the splenium of the corpus callosum being described as a potentially core feature of AD associated with worse cognition (Garnier-Crussard et al., 2023).

Despite not being able to find significant correlations between the Fazekas score and the CDR-SB, we found significant correlations between the Fazekas scores and the degree of atrophy in several

brain regions, further supporting cerebrovascular co-pathology, represented by predominant small vessel disease, as a key player in the pathophysiology of both PART and AD. Moreover, the magnitude of correlations between microangiopathy and atrophy in the medial temporal and fronto-insular regions was more pronounced in PART than in AD, which might suggest that, in PART, atrophy patterns rely less on neuropathological changes than in AD, something in accordance with the strong role of cerebrovascular disease in PART found in a relatively recent study (Iida et al., 2021).

Finally, the third aim of this thesis was to assess potential differences in the entorhinal cortex by *in vivo* brain MRI, using the semiquantitative visual rating scale ERICA (Enkirch et al., 2018), between individuals with "definite" PART and in the AD spectrum, while also assessing the relationship between this score and the degree of clinical impairment, based on CDR metrics (Morris, 1993). After nullifying the effect of age and sex, we found significant differences in the ERICA score between "definite" PART (i.e., CERAD 0) and severe AD (i.e., CERAD 3), and between mild (i.e., CERAD 1) and severe (i.e., CERAD 3) AD. Furthermore, we also found significant differences between "definite" PART and the AD neuropathological change group (i.e., CERAD 1 to 3). These findings are aligned with the known fact that the entorhinal cortex is the starting point of atrophy in AD, even before the hippocampus, with the first stage of the disease (i.e., mild AD or CERAD 1) being typically characterized by neuronal pathology in the entorhinal region in the form of neurofibrillary tangles and neuropil threads (Braak & Braak, 1991). This could also explain the lack of differences between groups after correcting for Braak, given that regional atrophy is typically correlated with neurofibrillary tangle deposition, and not Aβ (Nelson et al., 2012). Interestingly, the lack of significant differences in the ERICA score between "definite" PART and mild AD is also in line with the known entorhinal cortex deposition of neurofibrillary tangle on both conditions (Braak & Braak, 1991; Crary et al., 2014). Therefore, these results indicate that ERICA might be a valuable clinical tool to distinguish "definite" PART or mild AD from severe AD, but not "definite" PART from mild AD.

Another interesting finding is the correlation found between the ERICA score and the CDR-SB across the entire CERAD spectrum, which is in line with the known role of the entorhinal cortex in learning and memory formation (Squire & Zola-Morgan, 1991), and in semantic memory/semantic fluency (Davies et al., 2004; Enkirch et al., 2018). Conversely, since a higher ERICA score correlate well with worse cognitive performance in PART and AD, our results further support its clinical use.

In conclusion, we found that, while AD patients present a stepwise increase in relative age-corrected atrophy in the medial temporal lobe with increasing CERAD scores, PART cases present intermediate atrophy levels. We also showed that overall cognition deficits are directly correlated with

regional atrophy in patients with AD, but not in PART cases, with the latter presenting a correlation between anterior temporal atrophy and a focal deficit of language, whereas in AD widespread correlations between regional atrophy and cognitive deficits were found. Moreover, significant correlations were found between the Fazekas score and regional atrophy patterns on both groups, with PART showing overall stronger positive correlations than in AD, particularly in the medial temporal and fronto-insular regions. Finally, the ERICA score seems to be a good discriminating tool between PART or mild AD and severe AD, but not between PART and mild AD. Moreover, it correlates well with cognitive performance across the entire CERAD spectrum, which favors its clinical use.

Future Perspectives

Important points that could be tackled by future studies are:

(a) the independent and cumulative impact of Aβ, tau and other co-pathology, such as TDP-43, on brain regional atrophy, using cases of AD, PART and, eventually, of limbic-predominant age-related TDP-43 encephalopathy (LATE) (Nelson et al., 2019);

(b) the characterization of PET and cerebrospinal fluid biomarkers in symptomatic and asymptomatic PART participants, preferably with participants equally distributed across Braak stages I-IV, as a way of clinically diagnosing and longitudinally evaluating this population;

(c) given the recently described concept of "AD-related white matter hyperintensities", which not always seem to correlate with the presence of mixed vascular and AD pathologies (Shirzadi et al., 2023), it would be extremely important to correlate the imaging findings (i.e. Fazekas scores) with the neuropathological findings at autopsy to better ascertain the associated pathophysiological mechanisms;

(d) better assess the described posterior predominance of white matter hyperintensities in AD, specifically by comparing the Fazekas score (periventricular and deep) with the neuropathological findings;

(e) to correlate the number and type of basal ganglia lesions, as defined by the European Task Force on Age-Related White Matter Changes (Wahlund et al., 2001), as well as other markers of small vessel disease, such as cerebral microbleeds, with the Fazekas score and neuropathological findings in PART and AD.

Globally, the results from this thesis further support the notion that PART and AD might be two different neuropathological processes, with different interconnections between regional brain atrophy, microangiopathic burden, and neuropsychological tests performance.

a. References

Alber, J., Alladi, S., Bae, H. J., Barton, D. A., Beckett, L. A., Bell, J. M., Berman, S. E., Biessels, G. J., Black, S. E., Bos, I., Bowman, G. L., Brai, E., Brickman, A. M., Callahan, B. L., Corriveau, R. A., Fossati, S., Gottesman, R. F., Gustafson, D. R., Hachinski, V.,...Hainsworth, A. H. (2019). White matter hyperintensities in vascular contributions to cognitive impairment and dementia (VCID): Knowledge gaps and opportunities. *Alzheimers Dement (N Y)*, *5*, 107-117. https://doi.org/10.1016/j.trci.2019.02.001

Almeida, F., Oliveira, T. G., Jesus, T., Coelho, A., Quintas-Neves, M., Gauthreaux, K., Mock, C., Kukull, W. A., & Crary, J. F. (2023). Lewy body co-pathology contributes to frontal lobe atrophy in Alzheimer's disease and primary age-related tauopathy. *Alzheimer's & Dementia*, *19*(S10), e081877. https://doi.org/https://doi.org/10.1002/alz.081877

Almeida, F. C., Jesus, T., Coelho, A., Quintas-Neves, M., Gauthreaux, K., Teylan, M. A., Mock, C. N., Kukull, W. A., Crary, J. F., & Oliveira, T. G. (2024). Psychosis in Alzheimer's disease is associated with specific changes in brain MRI volume, cognition and neuropathology. *Neurobiol Aging*, *138*, 10-18. https://doi.org/10.1016/j.neurobiolaging.2024.02.013

Almeida, F. C., Santos, A., Jesus, T., Coelho, A., Quintas-Neves, M., Gauthreaux, K., Mock, C. N., Kukull, W. A., Crary, J. F., & Oliveira, T. G. (2025). Lewy body co-pathology in Alzheimer's disease and primary age-related tauopathy contributes to differential neuropathological, cognitive, and brain atrophy patterns. *Alzheimers Dement*, *21*(1), e14191. https://doi.org/10.1002/alz.14191

Braak, H., & Braak, E. (1991). Neuropathological stageing of Alzheimer-related changes. *Acta Neuropathol*, *82*(4), 239-259. https://doi.org/10.1007/BF00308809

Brickman, A. M., Zahodne, L. B., Guzman, V. A., Narkhede, A., Meier, I. B., Griffith, E. Y., Provenzano, F. A., Schupf, N., Manly, J. J., Stern, Y., Luchsinger, J. A., & Mayeux, R. (2015). Reconsidering harbingers of dementia: progression of parietal lobe white matter hyperintensities predicts Alzheimer's disease incidence. *Neurobiol Aging*, *36*(1), 27-32. https://doi.org/10.1016/j.neurobiolaging.2014.07.019

Crary, J. F., Trojanowski, J. Q., Schneider, J. A., Abisambra, J. F., Abner, E. L., Alafuzoff, I., Arnold, S. E., Attems, J., Beach, T. G., Bigio, E. H., Cairns, N. J., Dickson, D. W., Gearing, M., Grinberg, L. T., Hof, P. R., Hyman, B. T., Jellinger, K., Jicha, G. A., Kovacs, G. G.,...Nelson, P. T. (2014). Primary age-related tauopathy (PART): a common pathology associated with human aging. *Acta Neuropathol*, *128*(6), 755-766. https://doi.org/10.1007/s00401-014-1349-0

Davies, R. R., Graham, K. S., Xuereb, J. H., Williams, G. B., & Hodges, J. R. (2004). The human perirhinal cortex and semantic memory. *Eur J Neurosci*, *20*(9), 2441-2446. https://doi.org/10.1111/j.1460-9568.2004.03710.x

Enkirch, S. J., Traschutz, A., Muller, A., Widmann, C. N., Gielen, G. H., Heneka, M. T., Jurcoane, A., Schild, H. H., & Hattingen, E. (2018). The ERICA Score: An MR Imaging-based Visual Scoring System for the Assessment of Entorhinal Cortex Atrophy in Alzheimer Disease. *Radiology*, *288*(1), 226-333. https://doi.org/10.1148/radiol.2018171888

Fazekas, F., Chawluk, J. B., Alavi, A., Hurtig, H. I., & Zimmerman, R. A. (1987). MR signal abnormalities at 1.5 T in Alzheimer's dementia and normal aging. *AJR Am J Roentgenol*, *149*(2), 351-356. https://doi.org/10.2214/ajr.149.2.351

Garnier-Crussard, A., Cotton, F., Krolak-Salmon, P., & Chetelat, G. (2023). White matter hyperintensities in Alzheimer's disease: Beyond vascular contribution. *Alzheimers Dement*, *19*(8), 3738-3748. https://doi.org/10.1002/alz.13057

Gordon, B. A., Najmi, S., Hsu, P., Roe, C. M., Morris, J. C., & Benzinger, T. L. (2015). The effects of white matter hyperintensities and amyloid deposition on Alzheimer dementia. *Neuroimage Clin*, *8*, 246-252. https://doi.org/10.1016/j.nicl.2015.04.017

Harper, L., Fumagalli, G. G., Barkhof, F., Scheltens, P., O'Brien, J. T., Bouwman, F., Burton, E. J., Rohrer, J. D., Fox, N. C., Ridgway, G. R., & Schott, J. M. (2016). MRI visual rating scales in the diagnosis of dementia: evaluation in 184 post-mortem confirmed cases. *Brain*, *139*(Pt 4), 1211-1225. https://doi.org/10.1093/brain/aww005

Iida, M. A., Farrell, K., Walker, J. M., Richardson, T. E., Marx, G. A., Bryce, C. H., Purohit, D., Ayalon, G., Beach, T. G., Bigio, E. H., Cortes, E. P., Gearing, M., Haroutunian, V., McMillan, C. T., Lee, E. B., Dickson, D. W., McKee, A. C., Stein, T. D., Trojanowski, J. Q.,...Crary, J. F. (2021). Predictors of cognitive impairment in primary age-related tauopathy: an autopsy study. *Acta Neuropathol Commun*, *9*(1), 134. https://doi.org/10.1186/s40478-021-01233-3

Jack, C. R., Jr., Wiste, H. J., Therneau, T. M., Weigand, S. D., Knopman, D. S., Mielke, M. M., Lowe, V. J., Vemuri, P., Machulda, M. M., Schwarz, C. G., Gunter, J. L., Senjem, M. L., Graff-Radford, J., Jones, D. T., Roberts, R. O., Rocca, W. A., & Petersen, R. C. (2019). Associations of Amyloid, Tau, and Neurodegeneration Biomarker Profiles With Rates of Memory Decline Among Individuals Without Dementia. *JAMA*, *321*(23), 2316-2325. https://doi.org/10.1001/jama.2019.7437

Jack, C. R., Wiste, H. J., Weigand, S. D., Therneau, T. M., Lowe, V. J., Knopman, D. S., Botha, H., Graff-Radford, J., Jones, D. T., Ferman, T. J., Boeve, B. F., Kantarci, K., Vemuri, P., Mielke, M. M., Whitwell, J., Josephs, K., Schwarz, C. G., Senjem, M. L., Gunter, J. L., & Petersen, R. C. (2020). Predicting future rates of tau accumulation on PET. *Brain*, *143*(10), 3136-3150. https://doi.org/10.1093/brain/awaa248

Jefferson-George, K. S., Wolk, D. A., Lee, E. B., & McMillan, C. T. (2017). Cognitive decline associated with pathological burden in primary age-related tauopathy. *Alzheimers Dement*, *13*(9), 1048-1053. https://doi.org/10.1016/j.jalz.2017.01.028

Josephs, K. A., Martin, P. R., Weigand, S. D., Tosakulwong, N., Buciuc, M., Murray, M. E., Petrucelli, L., Senjem, M. L., Spychalla, A. J., Knopman, D. S., Boeve, B. F., Petersen, R. C., Parisi, J. E., Dickson, D. W., Jack, C. R., & Whitwell, J. L. (2020). Protein contributions to brain atrophy acceleration in Alzheimer's disease and primary age-related tauopathy. *Brain*, *143*(11), 3463-3476. https://doi.org/10.1093/brain/awaa299

Josephs, K. A., Murray, M. E., Tosakulwong, N., Weigand, S. D., Knopman, D. S., Petersen, R. C., Jack, C. R., Jr., Whitwell, J. L., & Dickson, D. W. (2019). Brain atrophy in primary age-related tauopathy is linked to transactive response DNA-binding protein of 43 kDa. *Alzheimers Dement*, *15*(6), 799-806. https://doi.org/10.1016/j.jalz.2019.03.003

Josephs, K. A., Murray, M. E., Tosakulwong, N., Whitwell, J. L., Knopman, D. S., Machulda, M. M., Weigand, S. D., Boeve, B. F., Kantarci, K., Petrucelli, L., Lowe, V. J., Jack, C. R., Jr., Petersen, R. C., Parisi, J. E., & Dickson, D. W. (2017). Tau aggregation influences cognition and hippocampal atrophy in the absence of beta-amyloid: a clinico-imaging-pathological study of primary age-related tauopathy (PART). *Acta Neuropathol*, *133*(5), 705-715. https://doi.org/10.1007/s00401-017-1681-2

Josephs, K. A., Whitwell, J. L., Weigand, S. D., Murray, M. E., Tosakulwong, N., Liesinger, A. M., Petrucelli, L., Senjem, M. L., Knopman, D. S., Boeve, B. F., Ivnik, R. J., Smith, G. E., Jack, C. R., Jr., Parisi, J. E., Petersen, R. C., & Dickson, D. W. (2014). TDP-43 is a key player in the clinical features associated with Alzheimer's disease. *Acta Neuropathol*, *127*(6), 811-824. https://doi.org/10.1007/s00401-014-1269-z

Morris, J. C. (1993). The Clinical Dementia Rating (CDR): current version and scoring rules. *Neurology*, *43*(11), 2412-2414. https://doi.org/10.1212/wnl.43.11.2412-a

Nelson, P. T., Alafuzoff, I., Bigio, E. H., Bouras, C., Braak, H., Cairns, N. J., Castellani, R. J., Crain, B. J., Davies, P., Del Tredici, K., Duyckaerts, C., Frosch, M. P., Haroutunian, V., Hof, P. R.,

Hulette, C. M., Hyman, B. T., Iwatsubo, T., Jellinger, K. A., Jicha, G. A.,...Beach, T. G. (2012). Correlation of Alzheimer disease neuropathologic changes with cognitive status: a review of the literature. *J Neuropathol Exp Neurol*, *71*(5), 362-381. https://doi.org/10.1097/NEN.0b013e31825018f7

Nelson, P. T., Dickson, D. W., Trojanowski, J. Q., Jack, C. R., Boyle, P. A., Arfanakis, K., Rademakers, R., Alafuzoff, I., Attems, J., Brayne, C., Coyle-Gilchrist, I. T. S., Chui, H. C., Fardo, D. W., Flanagan, M. E., Halliday, G., Hokkanen, S. R. K., Hunter, S., Jicha, G. A., Katsumata, Y.,...Schneider, J. A. (2019). Limbic-predominant age-related TDP-43 encephalopathy (LATE): consensus working group report. *Brain*, *142*(6), 1503-1527. https://doi.org/10.1093/brain/awz099

Quintas-Neves, M., Teylan, M. A., Besser, L., Soares-Fernandes, J., Mock, C. N., Kukull, W. A., Crary, J. F., & Oliveira, T. G. (2019). Magnetic resonance imaging brain atrophy assessment in primary age-related tauopathy (PART). *Acta Neuropathol Commun*, *7*(1), 204. https://doi.org/10.1186/s40478-019-0842-z

Saridin, F. N., Chew, K. A., Reilhac, A., Gyanwali, B., Villaraza, S. G., Tanaka, T., Scheltens, P., van der Flier, W. M., Chen, C. L. H., & Hilal, S. (2022). Cerebrovascular disease in suspected non-Alzheimer's pathophysiology and cognitive decline over time. *Eur J Neurol*, *29*(7), 1922-1929. https://doi.org/10.1111/ene.15337

Savola, S., Kaivola, K., Raunio, A., Kero, M., Makela, M., Parn, K., Palta, P., Tanskanen, M., Tuimala, J., Polvikoski, T., Tienari, P. J., Paetau, A., & Myllykangas, L. (2021). Primary age-related tauopathy in a Finnish population-based study of the oldest old (Vantaa 85+). *Neuropathol Appl Neurobiol*, e12788. https://doi.org/10.1111/nan.12788

Shirzadi, Z., Schultz, S. A., Yau, W. W., Joseph-Mathurin, N., Fitzpatrick, C. D., Levin, R., Kantarci, K., Preboske, G. M., Jack, C. R., Jr., Farlow, M. R., Hassenstab, J., Jucker, M., Morris, J. C., Xiong, C., Karch, C. M., Levey, A. I., Gordon, B. A., Schofield, P. R., Salloway, S. P.,...the Alzheimer's Disease Neuroimaging, I. (2023). Etiology of White Matter Hyperintensities in Autosomal Dominant and Sporadic Alzheimer Disease. *JAMA Neurol*, *80*(12), 1353-1363. https://doi.org/10.1001/jamaneurol.2023.3618

Squire, L. R., & Zola-Morgan, S. (1991). The medial temporal lobe memory system. *Science*, *253*(5026), 1380-1386. https://doi.org/10.1126/science.1896849

Swardfager, W., Yu, D., Scola, G., Cogo-Moreira, H., Chan, P., Zou, Y., Herrmann, N., Lanctot, K. L., Ramirez, J., Gao, F., Masellis, M., Swartz, R. H., Sahlas, D. J., Chan, P. C., Ojeda-Lopez, C.,

Milan-Tomas, A., Pettersen, J. A., Andreazza, A. C., & Black, S. E. (2017). Peripheral lipid oxidative stress markers are related to vascular risk factors and subcortical small vessel disease. *Neurobiol Aging*, *59*, 91-97. https://doi.org/10.1016/j.neurobiolaging.2017.06.029

Teylan, M., Besser, L. M., Crary, J. F., Mock, C., Gauthreaux, K., Thomas, N. M., Chen, Y. C., & Kukull, W. A. (2019). Clinical diagnoses among individuals with primary age-related tauopathy versus Alzheimer's neuropathology. *Lab Invest*, *99*(7), 1049-1055. https://doi.org/10.1038/s41374-019-0186-0

Teylan, M., Mock, C., Gauthreaux, K., Chen, Y. C., Chan, K. C. G., Hassenstab, J., Besser, L. M., Kukull, W. A., & Crary, J. F. (2020). Cognitive trajectory in mild cognitive impairment due to primary age-related tauopathy. *Brain*, *143*(2), 611-621. https://doi.org/10.1093/brain/awz403

Vogel, J. W., Young, A. L., Oxtoby, N. P., Smith, R., Ossenkoppele, R., Strandberg, O. T., La Joie, R., Aksman, L. M., Grothe, M. J., Iturria-Medina, Y., Alzheimer's Disease Neuroimaging, I., Pontecorvo, M. J., Devous, M. D., Rabinovici, G. D., Alexander, D. C., Lyoo, C. H., Evans, A. C., & Hansson, O. (2021). Four distinct trajectories of tau deposition identified in Alzheimer's disease. *Nat Med*. https://doi.org/10.1038/s41591-021-01309-6

Wahlund, L. O., Barkhof, F., Fazekas, F., Bronge, L., Augustin, M., Sjogren, M., Wallin, A., Ader, H., Leys, D., Pantoni, L., Pasquier, F., Erkinjuntti, T., Scheltens, P., & European Task Force on Age-Related White Matter, C. (2001). A new rating scale for age-related white matter changes applicable to MRI and CT. *Stroke*, *32*(6), 1318-1322. https://doi.org/10.1161/01.str.32.6.1318

Weaver, N. A., Doeven, T., Barkhof, F., Biesbroek, J. M., Groeneveld, O. N., Kuijf, H. J., Prins, N. D., Scheltens, P., Teunissen, C. E., van der Flier, W. M., Biessels, G. J., & group, T.-V. s. (2019). Cerebral amyloid burden is associated with white matter hyperintensity location in specific posterior white matter regions. *Neurobiol Aging*, *84*, 225-234. https://doi.org/10.1016/j.neurobiolaging.2019.08.001

Weigand, A. J., Bangen, K. J., Thomas, K. R., Delano-Wood, L., Gilbert, P. E., Brickman, A. M., Bondi, M. W., & Alzheimer's Disease Neuroimaging, I. (2020). Is tau in the absence of amyloid on the Alzheimer's continuum?: A study of discordant PET positivity. *Brain Commun*, *2*(1), fcz046. https://doi.org/10.1093/braincomms/fcz046

Weintraub, S., Besser, L., Dodge, H. H., Teylan, M., Ferris, S., Goldstein, F. C., Giordani, B., Kramer, J., Loewenstein, D., Marson, D., Mungas, D., Salmon, D., Welsh-Bohmer, K., Zhou, X. H., Shirk, S.

D., Atri, A., Kukull, W. A., Phelps, C., & Morris, J. C. (2018). Version 3 of the Alzheimer Disease Centers' Neuropsychological Test Battery in the Uniform Data Set (UDS). *Alzheimer Dis Assoc Disord*, *32*(1), 10-17. https://doi.org/10.1097/WAD.0000000000000223

Whitwell, J. L., Martin, P., Graff-Radford, J., Machulda, M. M., Senjem, M. L., Schwarz, C. G., Weigand, S. D., Spychalla, A. J., Drubach, D. A., Jack, C. R., Jr., Lowe, V. J., & Josephs, K. A. (2019). The role of age on tau PET uptake and gray matter atrophy in atypical Alzheimer's disease. *Alzheimers Dement*, *15*(5), 675-685. https://doi.org/10.1016/j.jalz.2018.12.016